UNIVERSITY OF NAIROBI

CLIMATE VARIABILITY AND CHANGE AS STRESSORS IN A HIGH POTENTIAL AGRICULTURE ZONE IN KENYA

By

OUMA ANTONY

I56/83009/2015

DEPARTMENT OF METEOROLOGY

A Dissertation Submitted for Examination in Partial Fulfillment of the Requirement for Award of the Degree of Master of Science in Meteorology of the University of Nairobi

2017

DECLARATION

This dissertation is my original work and has not been submitted elsewhere for examination, award of a degree or publication. Where other people's work, or my own work has been used, this has properly been acknowledged and referenced in accordance with the University of Nairobi's requirements.

---------- ----------

SIGNATURE DATE

OUMA ANTONY

I56/83009/2015

Department of Meteorology

University of Nairobi

This thesis is submitted for examination with our approval as research supervisors:

	SIGNATURE	DATE
Dr. Fred Karanja	……	……

Department of Meteorology

University of Nairobi

PO BOX 30197-00100

Nairobi, Kenya.

fkaranja@uonbi.ac.ke

Dr. Gilbert Ouma	……	…….

Department of Meteorology & Institute of Climate Change and Adaptation

University of Nairobi

PO BOX 30197-00100

Nairobi, Kenya.

DEDICATION

This dissertation is dedicated to my late son, Liam O'Neil, my family, and to God for His unwavering grace, love, and care.

ACKNOWLEDGEMENTS

I first thank my supervisors, Dr. Karanja and Dr. Ouma, of the Department of Meteorology, School of Physical Sciences at the University of Nairobi for their guidance on critical aspects of conducting this research. Also, I appreciate all the lecturers and colleagues who were involved in the verification and advice during the preparation of this dissertation. Without their passionate participation and input, the dissertation could not have been completed.

More so, I acknowledge and appreciate DAAD for financial support and the Department of Meteorology for academic and logistic support. Milestones and objectives achieved this far are because of your support.

ABSTRACT

Climate variability and change are intensifying extreme weather events, making developing countries more vulnerable to the consequences of climate change because of overdependence on natural resources for livelihood. The effects of climate change and variability will probably affect the potential of a high potential agro-ecological area in Kenya.

The main objective of this study was to evaluate the effects of climate change on moisture and thermal resources of Kenya's high potential agriculture zone and account for climate change induced stress for crop suitability assessment. Daily minimum, maximum, dew point and mean temperatures, rainfall, and wind speed data for the period 1985-2014 from Kitale, Kericho, Kakamega, Kisii, and Eldoret stations were used.

Seasonal and Trend decomposition using Loess method, Mann-Kendall trend test, Penman-Monteith Model, ClimPACT, and Simple Water Balance model, and climate diagrams were used to investigate spatial and temporal differentiation of thermal and moisture regimes over the study area.

The study established that mean, maximum, and minimum temperatures are increasing over the five stations. Moreover, rainfall is significantly increasing over Kitale and Eldoret but decreasing over Kakamega and Kericho and non-significant trends over Kisii. The long rains LGPs are shortening over Kericho (2 days/year), Kakamega (2 days/year), and Eldoret (1 day/year) but lengthening over Kitale (2 days/year) and invariant over Kisii. The short rains LGP over Eldoret were shorter but persistent at 95% confidence level. Growing degree days also increased by over 5, 10, 10, and 11 units of cumulated heat per year over Eldoret, Kakamega, Kericho, and Kitale respectively.

In was concluded that variability and change affect moisture and thermal resources leading to constrained soil moisture, in case of shortening length of growing periods, and higher pest and disease development rates due to high heat units. These constraints affect the potential of agricultural production and hence act as stress production factors. From these findings, there is a need for farm level technical adjustments, a financial derivative targeting crop-product prices and a natural resource management domain.

TABLE OF CONTENTS

LIST OF TABLES

LIST OF FIGURES

LIST OF ABBREVIATIONS

AEC-Agro-Ecological Cell

AEZM: Agro-ecological zoning method

AEZs- Agro-ecological zones

AMS: Agrometshell

BA-Bayesian Approaches

CC- Climate Change

CDD- Consecutive Dry Days

DEM-Digital Elevation Map

DRT- Diurnal Temperature Range

EBA- Ecology-based Approach

FAO- Food Agriculture Organization

GCM- General Circulation Models

GDD-Growing Degree Days

GDP-Gross Domestic Product

GHCND-Global Historical Climatological Network Daily

GIS- Geographical Information System

GSL -Growing Season Length

IPCC- Intergovernmental Panel on Climate Change

LGP-Length of Growing Period

LGP_t – Length of Growing Season at temperature, T.

LULC-Land Use Land Cover

MI-Moisture Index

MI MCMC- Multiple Imputations Markov Chain Monte Carlo

MTT-Moving t-test

NCEI-National Center for Environmental Information

PET- Potential Evapotranspiration

RDA-Research Data Archive

SST- Sea Surface Temperature

STL-Seasonal and Trend decomposition using Loess

CHAPTER ONE: INTRODUCTION

1.1 Background

There is enough evidence showing that global climate is gradually changing, and not only due to anthropogenic forcing, but also other external factors (Karl & Trenberth, 2003). Seo (2014) asserts that current and projected climate changes and variations will modify agriculture potentials in different production systems in the world. Results from economic models also suggest that agricultural potentials will shift and affect agro-ecological zones (AEZs) differently (Kala *et al.*, 2012). Kabubo-Mariara and Kabara (2015) posit that developing countries are more susceptible to climate change crisis and hazards for three reasons. Firstly, they depend on the natural resource as their source of livelihood. Secondly, they have limited resources to counter the effects of the projected climate change. Finally, there are few or no measures put in place by governments to mitigate the projected effects. These factors would derail recovery from climate crisis and hazards, and they would then result in severe social and economic damages.

Laswai (2010) suggests that the rampant food crisis among African countries show the continent's vulnerability to the impacts of climate change on agriculture. As of February 2016, over 40 million people faced food insecurity and some, outright famine, and the continent needed over $4.5 billion for food relief support (Fan & Rosegrant, 2016). Even though finance and policy aspects significantly affect food security, the dominant driver is weather and its variation because droughts precede failed harvest. Several cases of food crises have since 1980 been reported in Africa. Specifically, the Ethiopian, Malawian, Horn of Africa, Niger, and Sahel Drought food crises turned out to be some of the severe ones. The Ethiopian food crisis lasted two years (1983 to1985) and claimed thousands of lives. The crisis was attributed to droughts though some researchers have postulated that climate change contributed to what has been referred to as the worst food crisis of the 20th century (Verpoorten *et al*., 2013). Further, droughts contributed to failed harvests in Malawi, Niger, and Horn of Africa between 2005 and 2006 affecting 5 million, 3.5 million, and 11 million people respectively. The Horn of Africa again endured another crisis in 2010 during which thousands of Ethiopians, Somalians, and Kenyans died from starvation while millions suffered from malnutrition (Pretty & Bharucha, 2015). The frequency of failed harvests due to droughts keep increasing with most countries becoming more

susceptible to food inaccessibility and unavailability. The fourth assessment report of the Inter-Governmental Panel on Climate Change's (IPCC) concluded that climate change had increased the frequency of natural disasters in the last century. It follows that the increasing frequency of failed harvest due to droughts can be ascribed to climate change, especially its effects on agro-ecological zones (IPCC, 2014).

The inventory and characterization of an agro-ecological zone use information on climate, landforms and soils, crop nutrient supply system and physical support to crops. These elements interact, and changes in the climate system can alter their interactions resulting in imbalances in the production system. For instance, an increase in carbon dioxide concentration can consequently boost photosynthesis rates; an ideal condition for *C_3-plants* at considerably high temperatures and in limited water environments (Kirschbaum, 2004). Moreover, increase in temperature also distresses photosynthesis, but plants can acclimatize to prevailing growth conditions and can perform even at extreme temperatures, provided that water requirements are met (Adler *et al.*, 2009). Notably, the optimum temperature for crop growth is dependent on species and growth conditions and tends to be higher in atmospheric conditions with higher carbon dioxide concentration (Kirschbaum, 2004). Körner and Basler (2010) theorize that increasing temperature will also increase vapor pressure deficits in the atmosphere resulting in a proportional acceleration in the rates of transpiration. However, an increase in concentration of CO_2 or a drop in diurnal temperature range (DRT), can suppress transpiration rates because it induces closure of the stomata (Kirschbaum, 2004). Further, higher near surface temperatures accelerate decomposition of soil organic materials and, as a result, plant nutrients are mineralized easily and availed for plant use. Under optimal conditions, both high temperatures and CO_2 concentrations can improve photosynthesis in nutrient-limited ecologies. However, the interactions of these factors are complex, and they induce different water and nutrient constraints in various agronomic systems. Consequently, plants have adoptive mechanisms suitable for each climate systems and the accumulative effects of these interactions cause agroclimatic variations and modify the production potential of the land.

Conversely, Fischer *et al.* (1996) suggest that the increase in the concentration of CO_2 can enhance potential agricultural productivity and improve crop water efficiency. However, the suggested potential depends on atmospheric characteristics such as temperature, rainfall distribution and amount, evapotranspiration regimes, incident insolation regimes, and other

ancillary consequences of changing the climate on production capacity such as increased pest invasions and effects of diseases and weeds (Pretty & Bharucha, 2015). These atmospheric conditions constitute the primary elements of agroecological zones, and their variations induce constraints on production. In general, agricultural productivity is expected to extend poleward into higher latitudes, suggesting a shift in agro-ecological zones. According to Fisher (2007), few aspects of changing the potential of agricultural areas have been considered globally, and only a few countries have systematically mapped the possibility of the shifts diverse crops and evaluated the planning consequences for national development. The shifts in agricultural potentials and the changes in the characteristics of the AEZs will affect agricultural production. According to IPCC (2014) projection, Sub-Saharan Africa's agricultural productivity will reduce immensely by 2050, and if no mitigation measures are put in place, then the reduction will increase the proportion of the poor population relying on subsistence agriculture. The effects of climate change will push this portion of the population into deeper poverty and make them more vulnerable to food insecurity. Additionally, the projection forecasts a 21% decline in food availability per individual and a new upsurge in the population of undernourished families by more than ten million; an aggregate of fifty-two million children in Africa by 2050. Most of these projections suggest that the impacts will be dire in Sub-Saharan countries including Kenya.

Kenya depends on agriculture for its economic growth and rainfed agriculture is the leading contributor to the real gross domestic product (GDP). Kabubo-Mariara and Karanja (2007), established that Kenya's production system is very unstable and susceptible to climate change due to poor planning, overdependence on a rainfed production system, and poor allocation of resources. Kenya's agriculture system has sub-systems based on spatial differentiation of weather quantities. Sombroek *et al*. (1982) categorized Kenya's agroecological system into seven zones using rainfall, moisture index, vegetation, and farming systems attributes. The first three areas are hyper-humid since they have over 50 percent moisture index. The first zone (Zone I) is agro-alpine and consists of protected forest areas and account for 0.1% (800 km^2) of Kenya's total landmass. The second zone (Zone II) has high potential for agricultural production and is 9.2% (53,000 km^2) of total landmass. The third one is the medium potential area which is 9.2% of Kenya's total land. This study focused on the high potential zone (Zone II). This zone lies at altitudes above 1200 meters (Sombroek *et al*.,1982) and it has a mean annual temperature of 18°C. Due to its attributes, it supports a wide range of commercial and subsistence agriculture.

The agroclimatic characteristics of Zone II consist of cool and wet, and warm and wet regions in medium altitudes. The cool and wet agro-climate conditions are found at altitudes ranging from 1,800m to 2,400m and has a 4-5 year mean annual rainfall tendency of 1,000mm. Counties such as Trans Nzoia, Nandi, Kericho, Narok, and Kisii lie within this zone. Most of Kenya's dairy farming are concentrated in parts of this zone with mixed farming being the leading mode of agriculture (Sombroek *et al*., 1982). Additionally, maize, tea, and coffee legumes, pasture, and fodder are grown in these regions.

1.2 Statement of the Problem

Agricultural productivity is expected to extend into higher altitudes as temperatures continue to rise, suggesting a shift in agro-ecological zones. Besides, a few aspects of the changes in this potential have been considered globally, and only a few countries (China, United States, Germany, and the United Kingdom) have systematically mapped the possibility of the shifts and evaluated the planning options for national development (Leclère *et al*., 2014). African countries, Kenya among them, have not mapped potential shifts in their agriculture systems that will result from climate change. Kenya's high potential agriculture zone accounts for most of its food and cash crop production. The warm and wet conditions are found in Kakamega, Siaya, Kisumu, Kisii, Bungoma, Busia, and Southern Nyanza which also lie within the zone. These regions have a four to five year mean annual rainfall tendency of between 1000 and 2500mm and experiences a high and reliable bimodal rainfall regime. Furthermore, the region has productive soils although some of its parts under produce due to high population density and weather extremes. In addition to maize, some parts of the region support the production of millet, sorghum, cassava, beans among others (Sombroek *et al*., 1982; Jaetzold *et al.*, 1982)., It is likely that climate change is modifying the existing agroecological characteristics and the effects will likely affect its productive capacity in the long run. As it is, there is a high likelihood that when rainfall and temperature change over the zone then both its thermal and moisture characteristics will change in response. The response involves feedbacks that affect physiological and phenological characteristics of crops grown. Hence, climate change induced agricultural stress does not only affect production potential of the zone but also poses a major food insecurity threat. Climate change loads will increase drought frequencies which will stress production cycles and suppress yields. As Kenya's population continues to grow, food availability and food access will worsen because of the probable high frequencies of failed harvest due to droughts. Hence, the changes in

the characteristics of Zone II because of climate change are precursors to food unavailability, inaccessibility, and severe hunger and famine.

1.3 Study Objectives

The main objective of the study was to evaluate the effects of climate variability and change on the moisture and thermal resources of Kenya's high potential agriculture zone. Its specific objectives were:

1. To investigate climate variability and change of Agroclimatic Zone.
2. To evaluate the changes in agro-ecological characteristics of Zone II.
3. To explore the suitability of Zone II to crop farming under the current climatic conditions.

1.4 Justification of the Study

Historically, the country has faced food insecurity due to failed harvest during droughts, which mostly coincides with La Nina. Climate change will intensify such extreme events and without the proper capacity to ensure surplus production during normal rain years or El Nino related rains, the country's vulnerability to food unavailability and inaccessibility may intensify in future.

Moreover, other factors such as the rapidly growing population and urbanization are increasing the pressure on cultivable land further reducing the production capacity of the land. The future action plans notwithstanding, the information on thermal and moisture differentiation that this study may establish can be crucial in spatial planning and resource allocation for surplus and consistent production. Further, the information on moisture and thermal constraints such as shorter growing periods and rainfall variability can assist in decision-making and planning. The changes call for the implementation of adjusted responses without necessarily stopping current agricultural practices but simply switching to ones that fit the new agroecological conditions.

Besides, the sudden changes in rainfall and temperature, as well as the sudden and occasional extreme weather events are increasingly becoming normal. Consequently, agriculture in all areas will face more constraints with a possibility that crops with shorter maturation period will be preferred because of reduced risk of failure. More importantly, Zone II was chosen because it accounts for most of food and cash crops production in Kenya.

1.5 Significance of the Study

Studies that assess the impacts of climate change have paid far less attention to the effects of the change on different individual AEZs. Further, a few of those studies have directly investigated the potential for adaptive strategies to the change. In most cases, researchers encourage impact responses that use a static set of agronomic and economic variables (IPCC, 2014). Conversely, this study sought to establish the necessity of farm level technical adjusted and regional level policy responses for building sustainable agriculture. Specifically, the study aimed at establishing thermal and moisture resource differentiation, including possible crop suitability constraints that affect production. The information can also provide a background for creating a resource management domain for land use planning, which would promote sustainability in agricultural production and ensure food availability. As such, the study is a step towards the zero-hunger sustainable development goal in Kenya. Finally, the study identified an interdisciplinary research opportunity that can contribute to stability in food access in Kenya through modeling of the weather-related financial derivative.

1.6 Study Assumptions

Model related, and general assumptions were used in this study. Firstly, the study assumed that soil and land use land cover (LULC) characteristics were invariant over the study period. Soil and LULC are mandatory aspects of agro-ecological zoning, but since the study did not use Geographical Information System (GIS) applications for spatial analysis due to the few data points, they were assumed not to have changed over the 30-year period and had little influence on the zone's characteristics changes. Additionally, the assumption also narrowed the study to the effects of climate change on the zone. Secondly, the study assumed that data points were in the interior sub-humid areas with light to moderate winds beside using wind speed data. The assumption applied to the estimation of daily evapotranspiration from temperature data. The subhumid conditions facilitated in the estimation of relative humidity and vapor pressure from dew point, minimum and maximum temperatures. Thirdly, the study assumed that the coefficients of Angstrom equation for estimating radiation were $a = 0.25\ and\ b = 0.5$ with a further adjustment for elevation. The Food Agriculture Organization's (FAO) Penman-Monteith Model also required radiation data for the calculation of the reference evapotranspiration but due to lack of such data, Angstrom's equation was used to estimate the radiation using temperature, elevation, and latitude and longitude.

CHAPTER TWO: LITERATURE REVIEW

2.1 Introduction

The contextual analysis presented in this chapter is a concise compendium of studies on climate change and its effects on weather patterns, thermal and moisture regimes of an AEZ, and agricultural productivity and potential. The reviewed articles give a theoretical basis, scientific knowledge, and proven methods for detecting climate change, computing climate indices and conducting multi-criteria suitability analysis for complex decision-making.

2.2 Climate Change (CC) Overview

Climate change is among the major scientific and social challenges in this era, and it is also fast becoming politicized in some parts of the world (Luo & Yu, 2012). Shi *et al.* (2016) define climate change as a deviation from the mean state of prevailing climatic conditions. This definition is mostly used for classification and regionalization purposes despite its failure to meet needs of addressing the changes. Cao *et al*. (2015) assert that stable climate has a significant influence on social development while instability in the climate system is a threat to sustainable development. They ascribe the changes in the climate system to internal and external factors and observe that external forcing induces positive temperature feedback that raises mean global temperatures. Some of the forcing agents include carbon dioxide and solar radiation, and climate change signals related to them have been detected in surface temperature and rainfall fields (Luo & Yu, 2012; Cao *et al*., 2015).

Despite the ongoing debate on human contribution to climate change, Zhang (2016) attributes the 1980-2016 warming hiatus to natural radiative forcing. Specifically, the researcher shows that the drop-down of the global surface temperature in the 1960s was due to natural volcanic forcing while he attributed the 1980-2016 warming to cooling in the Eastern Pacific Ocean (Zhang, 2016). Theoretically, the cooling of the Pacific Ocean enhances trade winds in the open water and redistribute global heat offsetting balance in the system, triggering feedbacks that intensify weather extremes, including warming.

However, most researchers and theorists attribute climate change to anthropogenic forcing, supporting the axiom that CO_2 emission is the leading anthropogenic contributor to climate change. Amaechi and Ekene (2016) assert that oil-producing countries and high rates of fossil fuel consumption are the major sources of CO_2 and concluded that the gas contributes to

environmental degradation, including greenhouse warming that leads to climate change. Conversely, Montzka *et al.* (2011) attribute climate change to non-carbon greenhouse gases. All these arguments confirm that greenhouse gases affect the ability of the atmosphere to absorb incident solar radiation, offsetting the Sun-Earth energy balance. The response to the energy imbalance is warming with higher latitudes more likely to have higher responses registered in surface temperature signals than lower latitudes (Stott & Jones, 2009).

It is imperative to note that the observed warming is not uniform as there was cooling between 1960 and 1970 followed by a subsequent warming from the 1980s (Back *et al.,* 2013; Zhang, 2016). However, natural atmospheric coupling processes seem to complicate the warming rates of surface temperatures. That is, short-term variabilities in the climate system contribute to the warming process. For instance, the 1998 El Nino resulted in the warmest temperatures in South America, Europe (many regions of France, Central Russia, and the UK), Indonesia with severe droughts in Guyana and Papua, and severe floods in Peru, Ecuador, and Kenya (Lean & Rind, 2009). However, the 2008 El Nino had similar but mild effects on these regions (Back et al., 2009). Such factors make short-term climate change forecasts difficult, especially on spatial scales where the variations can easily magnify the observed surface temperature changes.

Globally, there was a temperature increment of 0.7°C during the 20th Century, and projections anticipate 1°C to 4°C increment in the 21st Century (Clavero *et al*., 2011). These projections indicate a high likelihood of extreme weather events in future and as such, impacts of climate change will most likely intensify. Adaptation and mitigation campaigns are on the rise, but climate change perception remains a critical barrier to resilience building. Habtemariam *et al.* (2016) explain that the perception of climate change has a major role in the design and implementation of adaptation and mitigation strategies. Moreover, Milfont *et al.* (2014) associate climate change perception to both belief and concern for it. They argue that people believe that climate change is too uncertain and perceive it as less lethal, which explains the lack of interest in resilience building (Ibrahim *et al*., 2015).

Extreme weather events and other vulnerability sequelae of climate change affect climate-sensitive sectors such as agriculture. Of the many factors that influence vulnerability, Shukla *et al.*, (2017) showed that exposure, sensitivity, and adaptive capacity are the key drivers of the spatial differences. The spatial differential of vulnerability is associated with a spatial differential of the impacts on different regions. In agricultural applications, the regions are the agro-

ecological zones, and their climatic variability and ecological sensitivity show their vulnerability to the consequences of climate change (Shukla et al., 2017; Bunn *et al.,* 2015). Moreover, climate variability alongside ecological sensitivity affects the potential and suitability of arable land. Consequently, climate change and its causes in the context of this paper is critical for apprasing Zone II and establishing its suitability. As Ranjitkar *et al.*, (2016) suggested, climate change will reduce the potential of suitable zones by 2050 and concluded that identification of new potential areas is only possible by understanding the causes and evolution of climate patterns. Hence, the study used a pragmatic approach to identify spatial differentials of the characteristics of the zone based on sensitivity to and negative impacts of progressive climate change.

2.3 Climate Change Detection

Climate change detection is necessary for different applications in various sectors. Climate change detection is a process that characterizes internal variations of the climate system to isolate the change signal in a statistical sense (Imbers *et al.*, 2014). A change in the system can either be abrupt or gradual; an abrupt change is sudden, and the long-term mean shifts at the point of the change, while gradual change is progressive and has a trend (Goossens & Berger, 1987). Liu *et al.* (2016) define an abrupt change as "a shift in the climate system from one steady state to another," and it refers to a significant statistical change of a climate variable over a specified temporal scale. Detection of climate change is still a contentious issue because of hurdles of attributing the change to a forcing factor.

Previous studies such as Dobrynin *et al*. (2015), Min *et al*. (2013), Imbers *et al*. (2014), Lackner *et al*. (2011), and Leroy and Anderson (2010) have used parametric and non-parametric statistical tests to detect changes in climate datasets. These articles explain complex and advanced methods such as optimal fingerprinting and Bayesian Approaches (BA). The statistical detection methods are unique and specific for sudden and progressive changes. Abrupt change detection methods include abrupt variance, mean value, frequency, probability density change and the multivariate analysis (Liu *et al.*, 2016; Guolin *et al.*, 2010; Goossens & Berger, 1987). Accuracy in detecting abrupt changes is a mandatory requirement for developing and designing early-warning systems based on the signals. Many researchers have studied detection under a transitioning climate system. For instance, Min et al. (2013) used an optimal detection analysis to

associate changes in in-situ datasets to model simulations and obtained results that are consistent with trend analysis using percentile climate indices.

The sudden change detection methods include parametric, non-parametric, cumulative sum, BA, sequential, and fingerprinting techniques (Zhou & Tung, 2013). However, climate change detection in operational meteorology mostly uses moving t-test (MTT). He *et al.*, (2013) compared and evaluated five methods of detecting abrupt changes and concluded that MTT, Yamamoto (YAMA) and *LePage* were more accurate than the rest. More specifically, MTT that uses simple computation algorithm, has high operational efficiency, and has clear physical interpretation because of its strong theoretical background. Many studies continue to focus on abrupt climate change because of the development of statistical methods used. For example, Fangfang *et al.*, (2007) used abrupt change to analyze climate data retrieved from stations in Yellow River catchment. In a different study, Kang et al. (2010) investigated change points forrainfall and temperature data over China and established rapid warming in NE China and drastic climate change in Qinghai-Tibet area.

Variability aspects such as nonlinearity and non-stationarity are common features of the climate system, and they introduce complexities in detection processes. The change in the system is multidimensional and combines gradual and abrupt changes against a backdrop of variability. It has proven difficult to detect either abrupt or gradual change from measured variables, and it is also difficult to accurately attribute causes. Some researchers such as, Pingale *et al*. (2015), Paeth and Manning (2013), Ribes *et al.* (2010), Hergel *et al.* (2006), Lee *et al.* (2005), and Hasselmann (1997) used a combination of trend change tests in their studies to detect change in climate variables. Such tests include Man-Kendall, Spearman Rho test, and linear regression. Mayowa *et al.* (2015) used Mann-Kendall test to investigate rainfall trends along East Coast of Malaysia and established a substantial increase in rainfall during the monsoon phase. Liu *et al*. (2011) used Mann-Kendall test along LePage test to investigate inter-decadal rainfall variability in Eastern China and established four interdecadal changes in summer rainfall. Mann-Kendall tests suit dataset of shorter temporal scales, unlike MTT tests.

2.4 Features of Agro-ecological Zones

An agroecological zone (AEZ) or cell is a unit of land with homogeneous climate, soil and production characteristics (Sachs *et al*., 2010). The definition of AEZ and its classification relies on agroclimatic variables, which if changed can affect the soil, climate, land characteristics and

hence modifying the zone. The cells or zones are delineated using agro-ecological zoning method, and the resultant AEZ consists of the unique thermal regime, moisture regime, soil unit, and production potential (Seo, 2014). Agro-ecological Zoning method (AEZM) is a complex multicriteria and ecology-based approach which combines climate, soil and land feature to classify agricultural land into zones based on a set of constraints (Fischer *et al.*, 2001). An example of Agro-climatic data analysis algorithm is shown in Figure 1, and it computes thermal and moisture regimes using meteorological data for each of the zone (Guhathakurta & Saji, 2013; Fischer *et al.*, 2012).

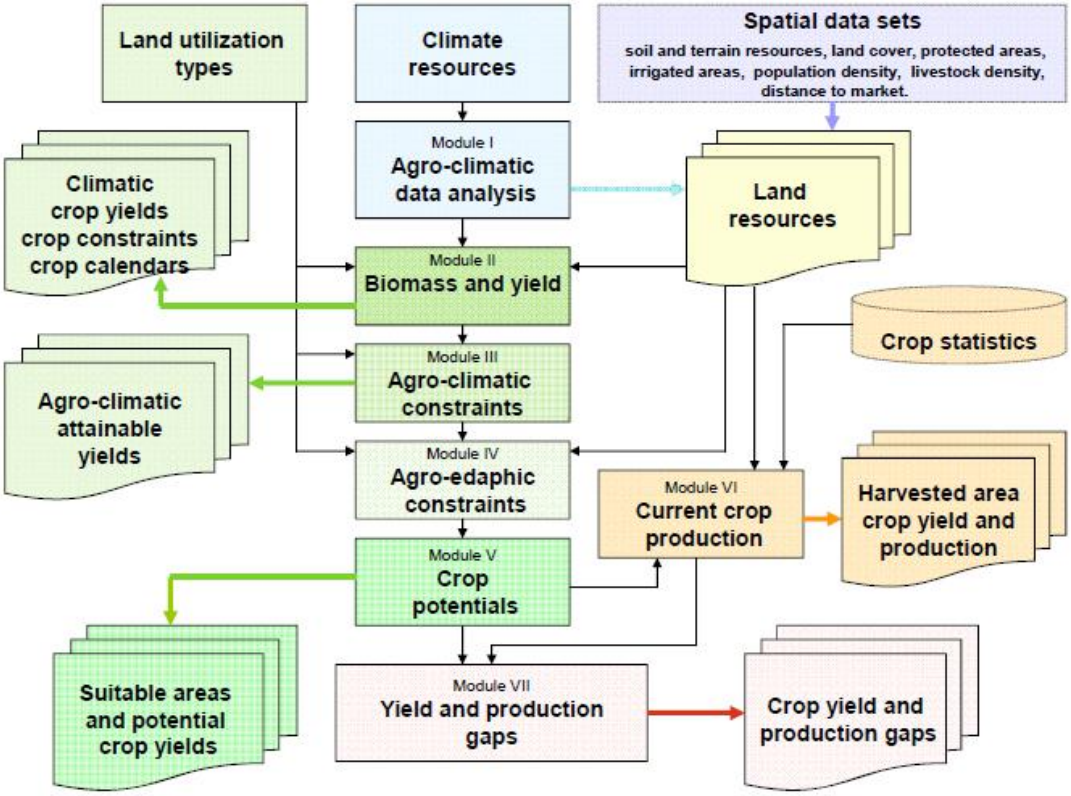

Figure 1: Global Agro-ecological zoning modules developed by IIAT and FAO (1992).

Hulme (2014) reiterates that climate change affects rainfall patterns and increases near-surface temperature. Studies such as Habeeb *et al.*, (2015), Raut *et al.*, (2014), and Ziska (2014) have related the changes in these weather variables to changes in land use types, vegetation, moisture regimes, and thermal regimes through an increased number of extreme weather events. Yu and Li (2012) explain that rainfall responds to air temperature changes in a study that investigated the association between hourly rainfall and temperature over Eastern China. Several scholars have proved direct effects of global warming on air temperatures (Kato *et al.*, 2009; Kerr, 2001; Karl & Easterling, 1999). They argue that, as the globe warms, near-surface temperature increase

through a positive feedback mechanism. The positive temperature response, in turn, induces changes in rainfall patterns, and its confounding effects modulate agro-climatic characteristics of agricultural lands. Specifically, the positive temperature responses affect rainfall intensity and its duration, potential annual evapotranspiration, and inter-annual rainfall amounts (Fisher *et al*., 1996; Fisher *et al*., 2012). These variations affect crop growth cycle and crop productivity although they are projected to vary depending on the latitude location of the arable land. For instance, Tait and Schiel (2013) suggest that rising global temperatures may increase productivity among natural algae although under minimal temperature variations. Such findings support the argument that temperature increments in higher latitudes may alleviate temperature constraints., Kreyling *et al*. (2008) argue that extreme weather events stress both plants and animals and reduce production potential.

A few studies including Seo *et al*. (2009) Yu *et al*. (2009), and Lin *et al*. (2013) have been conducted in different parts of the world to explore the effects of climate change on AEZs. Further, very few studies have been carried out to explore the effects of climate change on Kenya's AEZ system in as much as articles have been published on the impacts of climate change on agriculture (Brayan *et al*., 2013; Herrero *et al*., 2010; Awuor & Ogola, 1997). It is only a study by Boitt and Pellikka (2014) that models the impacts of climate change on Taita Hills using agro-ecological approaches, and it established that the zone is shrinking. Nonetheless, Seo and Mendelsohn (2008) theorize that farms situated in high altitude and moist forest are more valuable than farms in semi-arid lowland areas and that the climate conditions in high potential zones are more temperate, and they rely on rainfall for production. It is the overdependence on rainfall that makes the high potential zone susceptible to the effects of climate change and most of the previous studies used econometric models to project the likelihood of the impacts of the change.

Kurukulasuriya and Mendelsohn (2008) conclude that AEZs are likely to shift, and the changes are mainly due to changes in seasonal patterns of temperature and rainfall. The two variables are necessary inputs for agricultural production and their interdependence define the thermal and moisture features of the zones. Spatially, evidence of a significant correlation between temperature and rainfall has been established. For instance, Aldrian and Susanto (2003) studied the relationship between sea surface temperature (SST) and precipitation and established that rainfall variability over Indonesia is sensitive to SST variability in neighboring Indian and Pacific Oceans. In 2005, Black also examined the relationship between Indian Ocean SST and

rainfall over East Africa and deduced that intense rainfall over the region are associated with warming in both the Western Indian and Pacific Oceans. Further, the study noted a coupling cooling in the Eastern Indian Ocean with East African region. Consequently, as the SST and near-surface temperature increases, rainfall will likely increase between January and May but reduce in July affecting moisture and thermal balance (Rajeevan *et al.,* 1998).

To take climate change into account, econometric models use climatic data in evaluating the productivity of arable land by investigating the probability of occurrence of changes in bioclimatic elements of the zone. Using such likelihoods, Kala *et al.* (2012) and Parry *at al.* (2004) concluded that climate change would cause shifts in AEZs leading to size increments in some of the zones and shrinkage in others. Trnka *et al.* (2009) investigated climate-driven agricultural production changes in Central Europe and concluded that increased temperatures and changes in amount and distribution of annual precipitation would induce further shifts in individual agro-climatic zones.

Some of the econometric models are integrated with crop model modules, and Mendelsohn and Dinar (2009) used such a composite model to examine the interaction between land use and climate change and concluded that yields of main cereals would drastically fall with increasing temperatures.

It is important to note that derivatives of temperature and rainfall such as growing season length (GSL), growing degree days (GDD), and length of growing period (LGP) have been used in some studies to characterize agro-climates for agricultural applications. For example, Potopová *et al.* (2015) used daily temperature to evaluate long-term variations in growing season length and observed that cool and wet decades are associated with delays besides persistent above normal rainfall and lowest temperature deviations. It is also important to note that growing season length is a temperature derivate whereas the length of growing period is a rainfall derivative, but both indicate the number of days a crop takes to mature. Hence, it is the spatial and temporal changes in rainfall and temperature that induce shifts in AEZs and subsequently reduce production potential and contribute to food insecurity in the long run (Rosenzweig & Parry, 1994).

Kenya has seven AEZs based on moisture index (MI) computed from the ratio of annual precipitation to potential evapotranspiration (PET) as outlined by Sombroek *et al*. (1982) and Jätzold and Kutsch (1982). Based on the relationship between climate and agroclimatic variables,

any changes in temperature and precipitation patterns due to climate change will affect moisture regime and impose thermal constraints that will affect the potential of the zone. Kenya's agro-climatic zones based on moisture availability, annual precipitation, and land area is as shown in Table 1.

Table 1: Agroecological Zones and Corresponding Areas of Agricultural Potential Land in Kenya.

ACZ	Classification	MI (Percentage)	Annual Precipita-tion	Area (percentage)
I	Humid	>80	1100-2700	
II	Sub-humid	65-80	1000-1600	12
III	Semi-humid	50-65	800-1400	
IV	Semi-humid to semi-arid	40-50	600-1100	5
V	Semi-arid	25-40	450-900	15
VI	Arid	15-25	300-550	22
VII	Very Arid	<15	150-350	46
Source: Sombroek et al. (1982)				

The zones as shown in Table 1 were based on the initial map that Sombroek *et al*. produced in 1982. The percentage of the areas for humid and semi-humid zones were not shown. Sub-zoning of the seven zones uses mean annual temperatures which forms the basis for major cash and food crops suitability. In general, high-potential lands are found 1200 meters above the sea level, but with an annual mean temperature that is below 18°C. As Boitt and Pellika (2014) noted in their study, there is an ambiguity in demarcating the boundaries among the AEZs as they tend to overlap each other. The overlap introduces a time-dependent spatial variability that complicates the analysis of the direction and magnitude of the shifts in the AEZs. However, the spatial and temporal differentials of the agro-ecological characteristics can suggest the degree of the impacts of climate change.

2.5 Agro-climatic Constraints and Suitability

Weather extremes associated with climate change, especially droughts, offset the balance in moisture and thermal regimes in the high potential zone. As temperature increases, rainfall patterns change leading to either lengthened or shortened growing season length. Despite reporting increased rainfall, some studies concluded that changing patterns is still a challenge to farmers. For example, Huho *et al.* (2012) investigated the impacts of changing rainfall patterns on subsistence farming in Laikipia East and concluded that performance of subsistence farming

was poor despite an increase in annual rainfall over the region between 1976 and 2005. Due to changes in climate state, the number of rainy days in a season are reducing resulting in water stress or shortening of the growing period despite the increase in rainfall intensity. Moreover, an experimental study conducted over three growing seasons in the United States by Fay et al. (2003) on responses of productivity to changes in rainfall patterns established that rainfall variations lower soil water content and make it vary as well. The moisture deficit results in poor root activity, stunted growth due to poor photosynthesis and reduced productivity. Hence, it becomes necessary to find ways of improving agricultural production amidst increasing temperatures and changing rainfall patterns in response to climate change.

Ainsworth and Ort (2010) analyzed crop suitability based on IPPC's projections and suggested that adaptation should target crops that are thermally resistant to compensate for the likely effects of higher temperatures. Other studies such as Fisher et al. (2006) and Kotir (2011) have established that agriculture is sensitive to climate and weather variations, especially short-term rainfall, temperature, and light fluctuations. In general, climate change affects rain patterns, increases drought frequency, and raises the average near-surface temperature thereby stressing crops and suppressing yields (Yu et al., 2009; Kotir, 2011; Mika, 2012). Most studies use 30-year ensembles of precipitation, temperature, the coefficient of variation of rainfall, and diurnal temperature range to establish stable climate conditions (Seo, 2014). As such, normal climate conditions exclude variable weather variations despite their role in changing climate patterns.

The variability imposed on the normal climate conditions imposes climate sensitivity issues besides driving the change. Katz and Brown (1992) examined the importance of variability on extreme events and concluded that agriculture is sensitive to rainfall and temperature deviations. Moreover, Fisher *et al*. (2006) established that a temperature increase of 2°C paired with a 5% increase in rainfall would lead to a 6% decrease in arable land in developing countries. However, if temperatures increase by 3°C paired with a 10% increase in precipitation, then farmland in the developing countries would decrease by 11%. These projections on temperature and rainfall sensitivity suggest that developing countries are more likely to be affected by climate suitability constraints. For example, Matsui *et al*. (1997) demonstrated that high air temperatures induce sterility among Japonica rice at flowering stage thereby reducing yields. From these findings, it is clear that climate change has introduced abiotic and yield suitability challenges including yield gap sterility and stem lodging. These suitability issues arise from high temperatures and its derivatives. However, rainfall amounts, and its variability has also introduced disease and water

stress suitability barriers. Inbar *et al*. (2001) and Mattson and Haack (1987) concluded that percentage of disease attacks and conditions of limited water are more likely to increase with increasing rainfall. Hence, crop success under changing climate conditions depends on factors such as temperature, water availability, stem lodging, and potential of disease events.

Table 2: Characteristics of Agro-ecological Zones and Crop Suitability Based on Jatzold and Kutsch's Classification of 1982 in Kenya.

AEZ	R/ETo	Zone Class	Probable Crops and CS
0	>1.2	Per humid	Forestry
I	0.8-1.2	Humid	Tea/dairy
II	0.65-0.79	Sub-humid	Wheat, maize, beans, Irish potatoes
III	0.5-0.64	Semi-humid	Beans, maize, cotton, wheat, cassava
IV	0.4-0.49	Transitional	Barley, cotton, maize, groundnut, sorghum
V	0.25-0.39	Semi-Arid	Livestock, beans, pigeon peas, sweet potatoes, millet
VI	0.1-0.24	Arid	Ranching and irrigated crops
VII	<0.1	Per Arid	Range land

Source: Jätzold & Kutsch (1982).

Furthermore, Tol (2002) and Waha et al. (2016) established a connection between crop success and land potential under changing climate conditions. Using economic approaches, the researchers concluded that climate change affects productivity although their evaluation was not in the context of agro-ecological systems. Moreover, projections from crop simulation models and general circulation models (GCMs) assert that these impacts will be greater in developing countries (Fisher *et al*., 2006; Seo, 2009).

2.6 Research Gap

A multitude of studies have been conducted to examine the impacts of climate change on agriculture although very few use ecology-based approaches (EBA), especially agro-ecological zoning. Given the social, economic, and environmental consequences of climate change and of the many methods of appraising its impacts, spatial assessments provide an all-encompassing evaluation of the interactions among arable land, prevailing weather, anthropogenic activities, and the environment. Further, very few studies have been conducted to examine the effects of climate change on Kenya's AEZs and as such this is an obscure field that needs further research.

Moreover, Kenya's high potential agriculture zone leads in food, and cash crop production yet it has not been studied for resource management and spatial planning for food production. It is, therefore, necessary to explore the zone and develop knowledge about its characteristics because information available on its moisture index, annual rainfall, temperature, and the ratio of rainfall to potential evapotranspiration do not suffice to conduct a multi-criteria analysis under the current agro-climatic constraints.

2.7 Conceptual Framework

The reviewed literature has established that climate change is increasing global surface temperatures and affecting rainfall cycles. These changes are expected to modify the extent and potential of arable land due to the sensitivity of agroclimatic variables to the changes. Rainfall and temperature sensitivity measured using gradual trends are the proxy for climate change signals in this study. The trends, either monotonic up or down, affect the thermal and moistures derivatives of temperature and rainfall respectively. Suppose the trends do not meet the sensitivity limits that Fisher *et al*. (2006) posit then other temperature and rainfall indices replace them as proxies to climate change signals.

The thermal resources considered include the growing season length (GSL or LGPt) and cumulated growing degree days (GDD sum). GSL refers to the number of days when the daily temperature is above 5°C, and it is expected to increase with increasing air temperatures. On the other hand, GDD sum is a measure of accumulated heat units, and its computation uses base temperatures of 5°C, 8°C, and 10°C;the annual GDD sum should increase with increasing temperatures.

The moisture resources included the length of growing period (LGP), moisture index (ratio of annual rainfall to annual PET), and annual precipitation. The LGP is based on a simple water balance model, and it compares daily rainfall and daily reference evapotranspiration which is a function of air temperature to wind velocity. The LGP should increase with increasing rainfall, but the observation may fail because PET increases linearly with temperature. The moisture index should increase if annual rainfall increases but annual PET decrease or remains constant otherwise it should decrease. The response of CDD, GSL, GDD sum, LGP, and MI lead to spatial and temporal differentials that introduce suitability variations over the zone. Specifically, increasing temperatures cause abiotic suitability and disease challenges while decreasing rainfall introduces water stress. Further, increased rainfall can also cause stem lodging (abiotic suitability)

and introduce workability issues. These suitability issues affect crop performance and reduce the potential of the land. Figure 2 gives a graphical display of the study's conceptual framework.

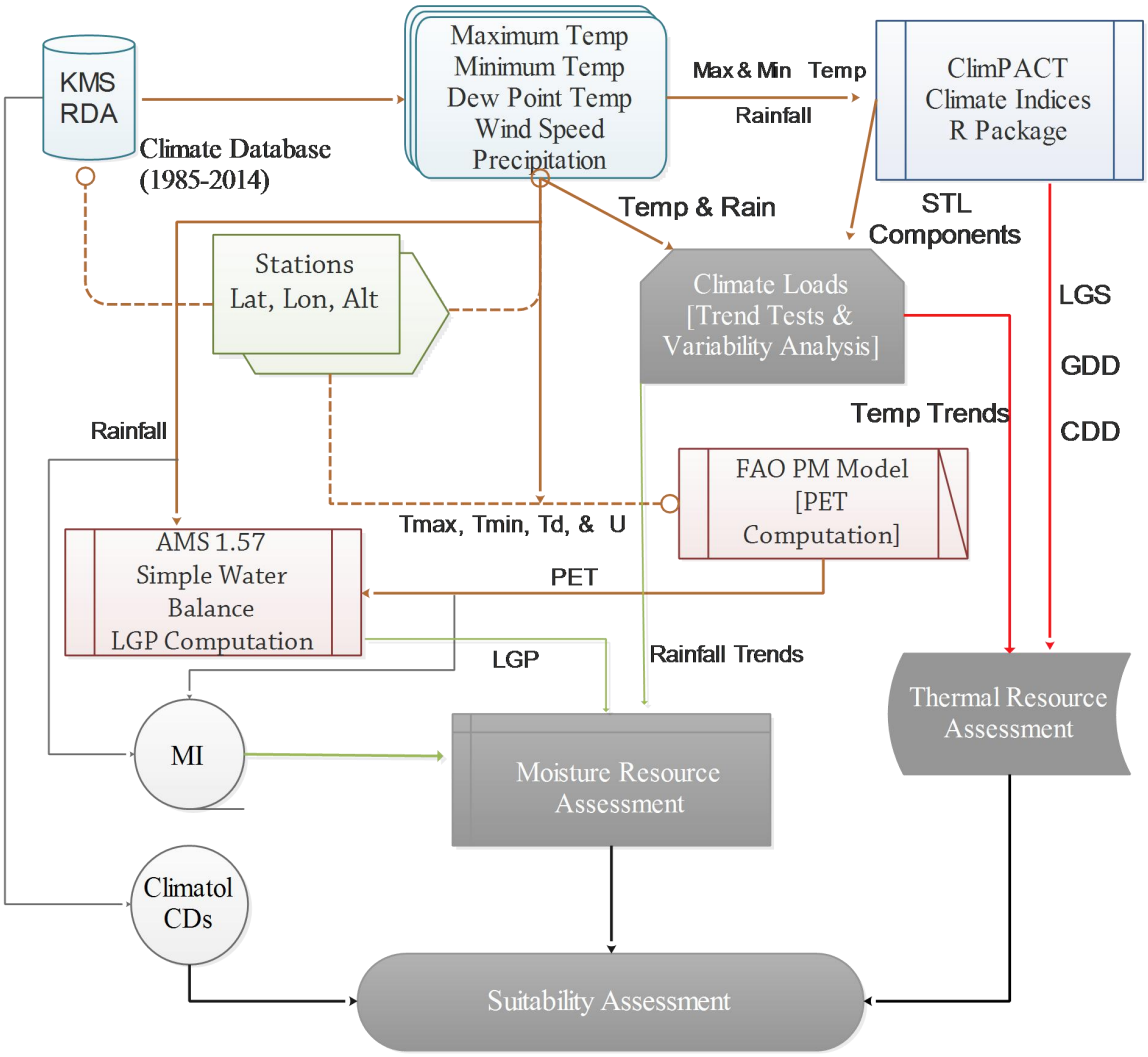

Figure 2: Conceptual Framework: Climate Loads as Stressors in Kenya's High Potential Agriculture Zone.

CHAPTER THREE: MATERIALS AND METHODS

3.1 Introduction

The data sources and types, data management approaches, model specifications, and specific objective methods are detailed in this chapter. The chapter is divided into two subsections namely; materials and methods.

3.2 Materials

3.2.1 Climate Data

Historical daily climate data for the period spanning 1985 to 2014 for minimum temperature, maximum temperature, dew point, rainfall, and wind speed (2m) were used in the study. The data retrieved was for Kisii, Kitale, Kericho, Kakamega, and Eldoret stations. Table 3 summarizes the station specific geo-data used in the models. The data was obtained from Kenya Meteorological Department and Global Historical Climatological Network Daily (GHCND). The National Center for Environmental Information (NCEI) manages the GHCN-daily data set and ensures compliance with climatological limits, removal of duplicate data, and assurance of temporal and spatial persistence (Durre *et al*., 2010). The GCHN-daily data was retrieved from the Research Data Archives' website using a Perl Script (See Appendix 1).

Table 3: Geo-information for the Selected Weather Stations

Station	Latitude	Longitude	Altitude
Kisii	0.68S	34.79E	1640m
Kitale	1.02N	35.01E	1890m
Eldoret	0.51N	35.26E	2120m
Kakamega	0.26N	34.76E	1565m
Kericho	0.41S	35.29E	1970m

3.2.2 The Study Area

The study focused on the high potential zone (Zone II) which lies at altitudes above 1200 meters. The zone has a mean annual temperature of 18°C and supports a wide range of commercial and subsistence agriculture. The agroclimatic characteristics of Zone II consist of cool and wet, and warm and wet regions in medium altitudes. The cool and wet agro-climate conditions are found

from 1,800m to 2,400m altitude range which has a four to five year mean annual rainfall tendency of 1,000mm. Some parts of Trans Nzoia, Nandi, Kericho, Narok, and Kisii experience these cool and wet conditions. Most of Kenya's dairy farming are concentrated in parts of this zone with mixed farming being the leading mode of agriculture (Sombroek *et al*., 1982). Additionally, maize, tea, and coffee are grown in these regions besides legumes, pasture, and fodder. The warm and wet conditions are found in Kakamega, Siaya, Kisumu, Kisii, Bungoma, Busia, and Southern Nyanza. It has a four to five year mean annual rainfall tendency of between 1000 and 2500mm. The region experiences high and reliable bimodal rainfall regime besides the good soils although some of its parts under produce due to high population density and weather extremes. In addition to maize, certain parts of the zone support the production of millet, sorghum, cassava, beans amongothers (Sombroek *et al*., 1982; Jätzold & Kutsch, 1982). This region was chosen because it accounts for most of the food and cash production in Kenya.

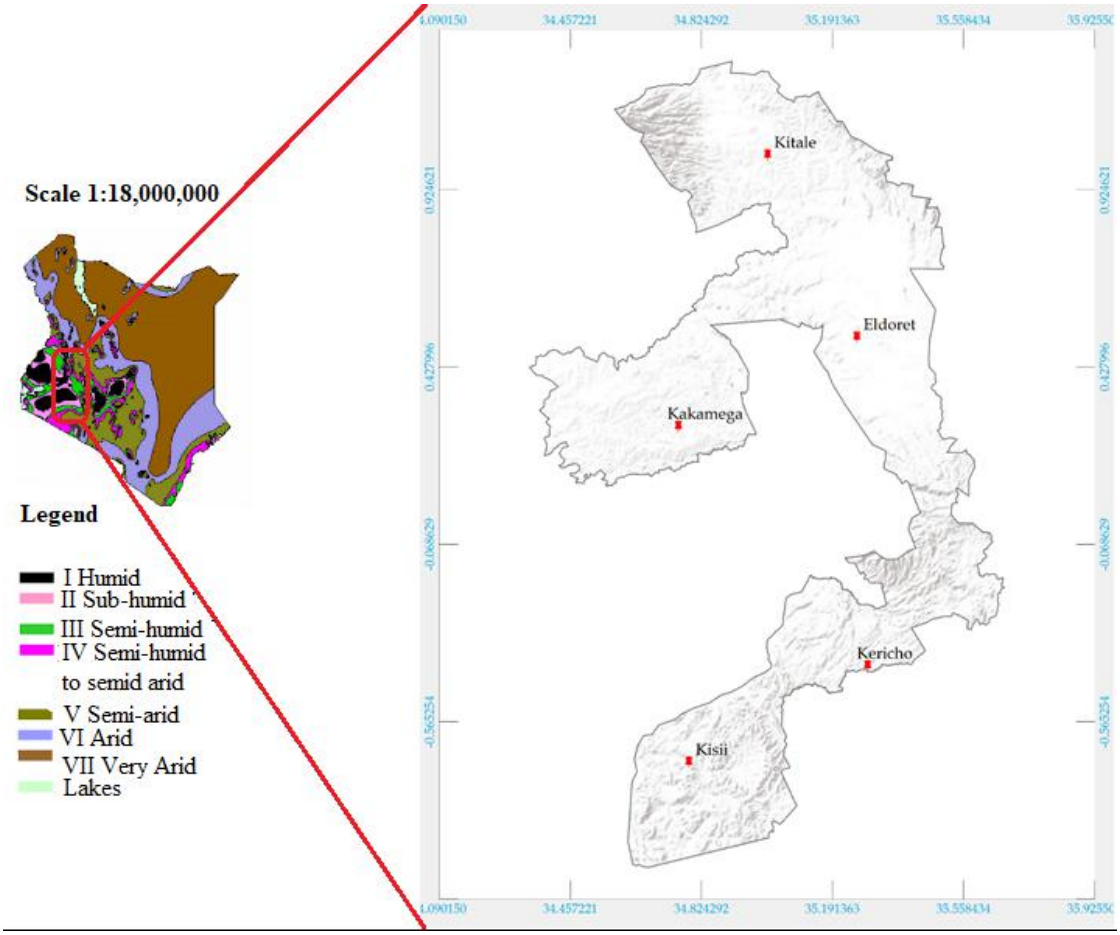

Figure 3: Map of the Study Area showing the Terrain and the Data Stations

3.2.3 Data Management

Data management included estimation of missing values and data quality control. The missing values were ascribed to random environmental and human factors and as such Multiple Imputation, Markov Chain Monte Carlo (MIMCMC) sufficed for the estimation (Pigott, 2001). A Black Box MCMC was used in the research to impute the missing data. The MIMCMC handles missing data without introducing variations, and it suits datasets that require a short time to analyze (Azur et al., 2011; Chavance, 2002; Yuan, 2010). Rainfall, minimum and maximum temperatures, dew point temperatures, and wind speed for Kisii, Kakamega, Kericho, Kitale, and Eldoret that were used in the analysis had missing values (over 15%), which were estimated using MI MCMC before embarking on quality control. However, it is imperative to note that observed data from Kenya Meteorological Headquarters had extensively wider gaps in the periods of 1985-1994 and 1999-2003. Consequently, additional data were obtained from Research Data Archive's (RDA) website; Global Historical Climatological Network Daily (GHCND) (ds564.0). Blending the two sets reduced missing gaps to below 10% for all the five stations. The RDA dataset can be accessed through Globus Transfer Service; a GridFTP service which allows for the transfer of large files. Alternatively, the dataset can be retrieved using a command shell or Perl Scripts in Appendix 1. Moreover, it should be noted that the estimation method imputes different values for every model run and as such, it would be prudent to use the completed dataset in any replicative analysis otherwise the findings may differ.

Data quality control included search and removal of duplicates, outliers as well as homogeneity tests using ClimPACT. The model uses a "penalized maximal *F-test"* that Wang (2008) recommends over Pettit's test, Bushland's test, von Neumann, and SNHT due to its in-built recursive testing functions that overcome the challenges of uneven distribution.

The output of the data quality control consists of box plots, diurnal temperature range (DTR) plots, duplicates summary, outliers, missing values statistics, plots of maximum temperature, minimum temperature and rainfall, variable rounding summary, and flatline and jumps in both maximum and minimum temperatures (Zhang *et al*., 2011). These plots and summary statistics determined whether to proceed to the second step (the calculation of the indices) or not (Alexander et al., 2013).

3.3 Methods

The methods focused on each specific objective and include detailed contextual analysis and initialization of the models used for achieving the objectives although estimation of missing data using MCMC was addressed.

3.3.1 Estimation of Missing Data

The estimation wad done independently for all the variables. The raw data with missing values were first arranged in a matrix-like format shown below.

	1985	1985	...	2014	2014
Days	*Jan*	*Feb*	...	*Nov*	*Dec*
1	...	...	...	...	...
2	...	...	...	...	...
⋮	⋮	⋮	⋮	⋮	⋮
31	31	28 / 29	...	30	31

Assuming that months in the matrix had a multivariate normal distribution, the data was augmented using Bayesian inference for missing data by iterating the imputation I-step and posterior P-step. In the imputation I-step, a mean vector and covariance matrix of the raw data were estimated and used to independently simulate the missing value for each observation. That is, the I-step used the following conditional probability equation to estimate missing values.

$$P(X_{i(miss)} \mid X_{i(obs)}) = \frac{P(X_{i(miss)} \text{and } X_{i(obs)})}{P(X_{i(miss)})}$$

In the equation, $Y_{i(miss)}$ denotes the variable with missing values while $Y_{i(obs)}$ denotes variables with observations. The generated complete set was then used in the posterior P-step in which a posterior population mean vector as well as a covariance matrix were simulated, and the new estimates used in the second I-step. In this step, the missing values for this iteration ($X_{miss}^{(t+1)}$) are drawn from $P(X_{i(miss)} \mid X_{i(obs)}\lambda^{(t)})$ and the P-step subsequently drew $(\lambda^{(t+1)})$ from $P(\lambda \mid X_{i(obs),}X_{i(mis)}^{(t+1)})$ .The iteration between I-step and P-step continues resulting in a Markov chain that converges at $P(X_{i(miss),}\lambda \mid X_{i(obs)})$. At the point of convergences, the iterations stop, and the resultant matrix is a complete data.

To achieve this in R, first load the dataset and covert it to a data frame and append the variables. Secondly, load the multiple imputation package and run the analysis using the *mi()* function and its arguments. A code snippet for conducting multiple imputations is as follows.

3.3.1 Specific Objective 1: Climate Variability and Change Detection

Firstly, the time series of minimum, maximum, and mean temperatures and rainfall were decomposed using 'Seasonal and Trend decomposition using Loess' (STL) method. Each of the variables was assumed to be represented by Equation 1.

$$Y_t = f\left(S_t, T_t, E_t\right)$$

* MERGEFORMAT (1)

Equation 1 expresses each series (Y_t) as a function of seasonal (S), trend (T), and random (E) components at period (t). Such a series can be decomposed using additive or multiplicative models, but STL was preferred because of its robustness against outliers. Additionally, STL algorithm in R provides an option for controlling variation on seasonal component which was assumed to have a natural periodicity. The R-source code used in this study is presented in Appendix 2. Secondly, the trend component was assessed for monotonic upward and downward linear trends using Mann-Kendall test statistic calculated using Equation 2 (Donald *et al.*, 2011).

$$S = \sum_{i=1}^{n-1} \sum_{j=i+1}^{n} \text{sign}(y_j - y_i) \qquad \text{* MERGEFORMAT (2)}$$

In which, S is the sum of the differences between the later- and earlier-measured data values, $Sign(y_j - y_i)$ is either or +1, or 0, or -1 and is the difference between the later-measured and earlier-measured values of the variable under investigation. For a large positive S, the later values tend to be larger than the former ones and a monotonic upward trend is deduced. Similarly, larger negative S suggest smaller latter values and the subsequent monotonic downward trend. The data set does not have a trend when the absolute value of S is small. The significance of S can be tested using a test statistic calculated as (Donald *et al.,* 2011):

$$\tau = \frac{S}{n\left(n-1\right)/2} \qquad \text{* MERGEFORMAT (3)}$$

The test statistic (τ) in Equation 3 is analogous to correlation coefficient in a regression analysis and the significance of the trend is tested using the following hypotheses in Equations 4 and 5. The number of observations used in Kendall's tau (τ) is represented as *n* in Equation 3.

$$H_0 : S = 0 \qquad \text{* MERGEFORMAT (4)}$$

$$H_1 : S \neq 0 \rightarrow S < 0 / S > 0 \qquad \text{* MERGEFORMAT (5)}$$

In Equations 5 and 6, H_0 and H_1 are null and alternative hypotheses respectively. As Pohlert (2016) explains, Mann-Kendall test detects monotonic trends (S) in either climate or environmental, or hydrological time series data. The probability associated with Mann-Kendall statistic is derived from a normal distribution function of the form in Equation 6.

$$f(z) = \frac{1}{\sqrt{2\pi}} e^{z^2/2} \qquad \text{* MERGEFORMAT (6)}$$

The normalization (Z) of the Mann-Kendall test statistic (S) as used in Equation 6 is based on the following condition.

$$Z = \begin{cases} \dfrac{S-1}{[Var(s)]^{1/2}} & \text{if S} > 0 \\ 0 & \text{if S} = 0 \\ \dfrac{S+1}{[Var(s)]1/2} & \text{if S<0} \end{cases} \qquad \text{* MERGEFORMAT (7)}$$

In Equation 7, Var (s) is the variance of the Mann-Kendall statistics S which determines the direction of the monotonic trends in the dataset.

Discerning spatial differentials of the characteristics of the zone depended on detection of linear change in time series of the study variables. Climate change served as the key component in the study and change signals detected using Mann-Kendall trend tests and Sen's slopes were the tenet of evaluating the changes in thermal and moisture resources over the zone. As a result, further analysis was dependent on the significance of the gradual trends detected in temperature and rainfall alongside associated indices. Thirdly, relationship between rainfall and temperatures was established using Pearson's correlation coefficient in a matrix format. The Pearson's Correlation Coefficient is as presented in the equation:

$$\gamma = \frac{N\sum xy - \left(\sum x\right)\left(\sum y\right)}{\sqrt{\left[N\sum x^2 - \left(\sum x\right)^2 N\sum y^2 - \left(\sum y^2\right)\right]}} \qquad \text{* MERGEFORMAT (8)}$$

In Equation 8, N is the number of pairs of scores, $\sum xy$ is the sum of the products of paired scores, $\sum x$ is the sum of x score, $\sum y$ is the sum of y scores, $\sum x^2$ is the sum of squared x

scores, and $\sum y^2$ is the sum of squared y scores. The observed trends and the interaction between weather variables can account for variations in agro-ecological characteristics of the zone.

3.3.2 Specific Objective 2: Agro-ecological Characteristics Evaluation

Firstly, PET was calculated using the ET calculator and the output files exported to AMS for the determination of length of growing period (LGP). There are several models for estimating reference evapotranspiration, but Subedi and Chavez (2015) demonstrated that Penman-Monteith model is consistent over a wide range of climate conditions. ET calculator is based on an FAO customized Penman-Monteith equation with aerodynamics and vegetation resistance features. The model is of the form expressed in Equation 9.

$$ET_0 = \frac{0.408\Delta(R_n - G) + \gamma \frac{900}{T+273} u_2(e_s - e_a)}{\Delta + \gamma(1 + 0.34u_2)}$$

* MERGEFORMAT (9)

In Equation 7, ET_0 (mm/day) refers to crop reference evapotranspiration, R_n (MJ/m^2/day) is the net radiation that the crop intercepts, T is air temperature at two meters height, G (MJ/m^2/day) is soil heat flux density, $u_2(m/s)$ is wind speed, $e_s(kPa)$ is the saturation vapor pressure, $e_a(kPa)$ is the actual vapor pressure, $e_s - e_a(kPa)$ is the saturation pressure deficit, $\Delta(kPa/°C)$ is the slope of the vapor pressure curve, and $\gamma(kPa/°C)$ is the psychometric constant.

The model assumed that crops over the zone were 1 meter tall with a roughness parameter of 70 s/m and a surface albedo of 0.23. Further, due to unavailability of radiation data on a daily time step, the model estimated radiation using Angstrom's equation expressed below.

$$R_s = 0.16 \times \sqrt{(T_{\max} - T_{\min}) \times R_a}$$

* MERGEFORMAT (10)

The model derived the extraterrestrial radiation R_a from mean, altitude, and latitude of the stations. The coefficient of 0.16 was used because of the inland study area's location in. Additionally, it was assumed that the crops of reference are naturally ventilated, and the model used due point temperature to estimate air humidity with a psychometric constant of 0.0008. Sub-humid conditions were also assumed to reflect the moisture conditions of the study area.

The model data input files were organized into meteorology data file and a description data with former having a *.DTA* format and the latter using a *.DSC*. The meteorology data file contained daily maximum, minimum and dew point temperatures, and daily windspeed. The user defined lower and upper limits for temperature and windspeed were -15 to 45 °C and 0 to 15 m/s respectively. The corresponding model defined upper and lower limits were 15 to100% for relative humidity, 0.0286 to 9.8525 kPa for vapor pressure, 0 to 12.6 hours for hours of bright sunshine, and 0 to 27.2 (23rd June) and 31.2 (8th August) MJ/m^2*day for day radiation (Jabloun & Sahli, 2008). The estimated solar radiation had a correction for station altitude with acceptable deviation of ±5%. Angstrom's equation with the correction factor is as shown in Equation 11.

$$R_s = a + b\left(\frac{n}{N}\right) * R_a$$

* MERGEFORMAT (11)

In Equation 9, a and b are the coefficients with values $a = 0.25, b = 0.5$ and the ratio n/N is unity.

Secondly, the legnth of growing period was calculated using the Agrometshel model. Daily rainfall reference evapotranspiration output from the ET Calculator became the variables of the input file for the water balance calculations. The model used a Simple Water Balance model to calculate the LGP by assuming that a crop growth season starts when the ratio of rainfall to potential evapotranspiration exceeds 0.5 (Yildiz *et al.,* 2015).

$$LGP_{start} if : \frac{R}{PET} > 0.5 \qquad \text{* MERGEFORMAT (12)}$$

In Equation 12, LGP_{start} is onset of the length of the growing period, R is daily rainfall, and PET is daily potential evapotranspiration. The model produces a table showing the name of the weather stations, geographical position, altitude, the number of seasons in that year, the length of growing season, the season's onset and cessation dates. The LGP refers to the number of days with adequate moisture and thermal conditions for plant growth.

Thirdly, growing season lengths ($LGP_{t=5,\ 8,\ 10°C}$), and growing degree days (GDD) sum for the three base temperatures were computed. These indices were calculated using the ClimPACT model. ClimPACT is a model that calculates 34 climate indices, and it is based on RClimDex which has variants such as FClimdex (Fortran) and Climdex (Windows NT/95 application). The model computes WMO approved climate indices that are mostly used for agriculture and health

applications (Herold & Alexander, 2017). Its current capabilities restrict calculations of indices related to daily minimum and maximum temperatures and daily precipitation. Koster *et al*. (2015) and Alexander *et al.* (2013) provided detailed documentation of the model including worked examples.

Finally, the spatial and temporal differential analyses of LGP, LGPt, GDD sum, annual rainfall, and MI ensued to establish moisture and thermal regimes over the zone. Further, the frequency of each of the growing season was tabulated and their yearly distribution generated.

3.3.3 Specific Objective 3: Suitability Assessment and Potential Appraisal

Firstly, moisture and thermal constraints were evaluated over the zone by grouping the LGP and LGPt into standard classes and appropriate risks assigned to each thermal and moisture regime. Secondly, annual rainfall trends and moisture indices were assessed over the region and compared to the values in Table 1. Thirdly, the historical trend of the ratio of rainfall to potential evapotranspiration was also obtained and compared to the values in Table 2. In specific, the moisture index (MI) was calculated using the following Equation:

$$MI = \frac{R_{Annual}}{\mathrm{PET}_{Annual}} \qquad \text{* MERGEFORMAT (13)}$$

The moisture index that Equation 13 yields uses annual rainfall (R_{Annual}) and annual potential evapotranspiration (PET_{Annual}).

Tables 1 and 2 constitute the parameters that were used to define the zone of study in 1982 and any differences observed in these attributed to temperature and rainfall changes. Finally, indices for agriculture and food security applications beside Walter and Leith's climate diagrams were calculated and diagrams plotted for further constraint analysis.

Walter and Leith's climate diagrams have been used in both geo- and biosciences to investigate how soils, climate, and vegetation are related. In agriculture, the diagrams are used to assess the suitability range of crops in given ecosystems. These diagrams were plotted using Climatol black box mode in R (Walter & Leith's Diagrams). According to Guijarro and Maintainer (2016), these climatic diagrams are used in vegetation studies, and the optimum temperature values are indicated at the margin of the diagram. They synthesize the climate of a place by plotting monthly temperatures and rainfall for quick identification of wet months. The Climatol model plots Walter & Leith diagrams using the *diagwl* function (Walter & Leith's Diagrams). The data

set for plotting must be passed as a $4x14$ vector in the order of mean rainfall, mean maximum daily temperature, mean minimum daily temperature, and absolute monthly minimum temperature (Table 4), and Appendix 3 presents R-source code used in this study.

Table 4: A sample of Input data for plotting Walter and Leith Diagram

		Months											
		1	2	3	4	5	6	7	8	9	10	11	12
Mean Rainfall	1	123.0	105.7	192.8	264.1	268.5	175.8	114.3	162.6	168.9	173.5	177.4	140.9
Tmax Mean	2	23.5	24.7	24.7	24.4	24.0	23.1	22.4	22.3	22.8	23.0	23.1	23.4
Tmin Mean	3	10.9	10.7	11.7	12.3	11.4	10.5	10.3	10.3	9.7	11.0	11.6	10.8
Abs Tmin Mean	4	10.9	10.7	11.7	12.3	11.4	10.5	10.3	10.3	9.7	11.0	11.6	10.8

The absolute values of minimum temperatures help in identify frost conditions.

It is important to note that when plotting the diagrams, the precipitation scale increases from 2 mm/°C to 20 mm/°C for monthly rainfall amounts that exceed 100 mm. The change in scale help avoids very high diagrams, and the bold black line indicates the change on the diagram. The regions above the line represent very wet conditions, and the models fill it in solid blue (Samways, 1989).

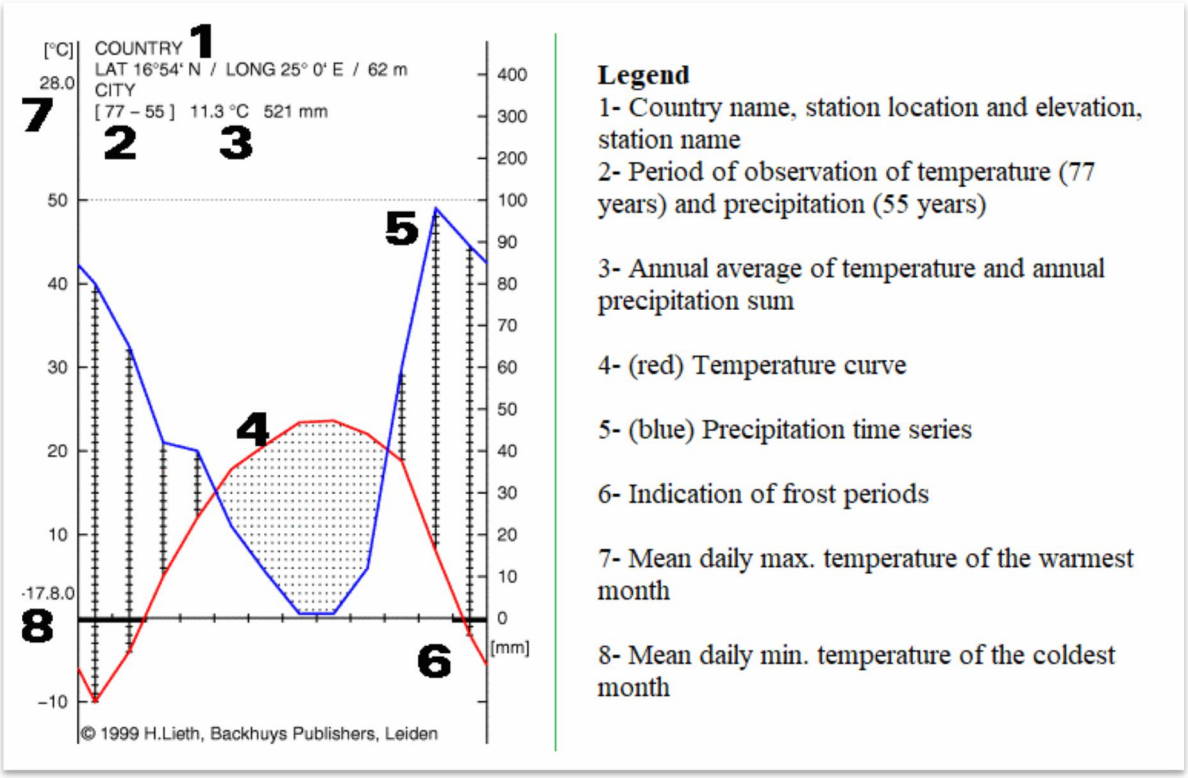

Figure 4: A sample Climate Diagram with Critical Elements

Furthermore, Consecutive Dry Days (CDD) were computed from CLIMPACT model in a two-process black box model procedure; Load and Check Data (Step 1) and Calculate Climate Indices (Step 2). The input data file must be in a text format with six columns ordered in the format year, month, day, rainfall, maximum temperature, and minimum temperature. The record information required for station data processing and quality control include the name of the station, latitude, longitude, and base period. It is important to note that studies that use base periods different from the study period must invoke the bootstrapping function embedded in the model. Nonetheless, the model base period started from 1984-12-31 to 2014-12-31 while the study period ranged from 1985-01-01 to 2014-12-31. The difference between the base and study periods was as a result of the bootstrapping and despite the extra day the model commenced computation from 1985-01-01

CHAPTER FOUR: RESULTS AND DISCUSSION

4.1 Introduction

Information on missing data, quality control, data analysis results, and discussions are presented in this chapter. As a result, the chapter is divided into data handling and management and specific objective sections. The data handling and management section discuss imputations of missing data and quality control, which included search and removal of duplicates and identification of outliers.

4.2 Data Management

4.2.1 Quality Control Report

ClimPACT quality control runs yielded daily time-series plot, potential outliers, duplicated observations, rounding issues, and observations exceeding set optimum values. The investigation of potential outliers was based on the interquartile range. The values that quality control graphs identified were based on upper and lower margins obtained from percentiles. That is, a 'Prec up,' 'TX up,' and 'TX low' indicate precipitation outlier, maximum temperature higher than $p75 + 3 * IQR$, and maximum temperatures lower than $p25 - 3 * IQR$ respectively. IQR refers to interquartile range whereas $p75$ and $p25$ refers to 75th and 25th percentiles respectively.

(a) Kitale.

A simple time series plot of minimum temperature, maximum temperature, DTR and precipitation for Kitale weather station revealed uncharacteristic patterns between 1998 and 1999. Figure 5 shows the deviations, which can be attributed to extreme weather events.

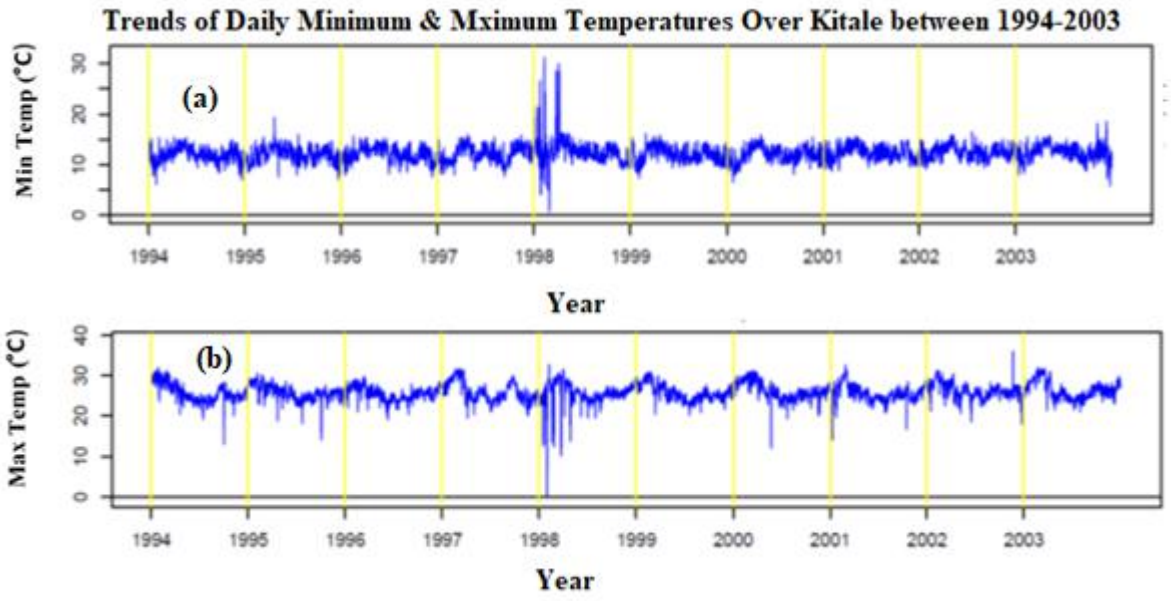

Figure 5: Time series plot of Minimum (a) and Maximum (b) Temperature over Kitale for the years between 1994 and 2003

Kitale boxplots of rainfall and temperature flagged outliers (circles) meeting the IQR definition. However, rainfall outliers used 5IQR bound range instead of 3IQR. The box-series are shown in Figure 6. The station input file did not have duplicates as well as missing values. The outliers were assumed to be due to extreme weather variations and treated as not erroneous.

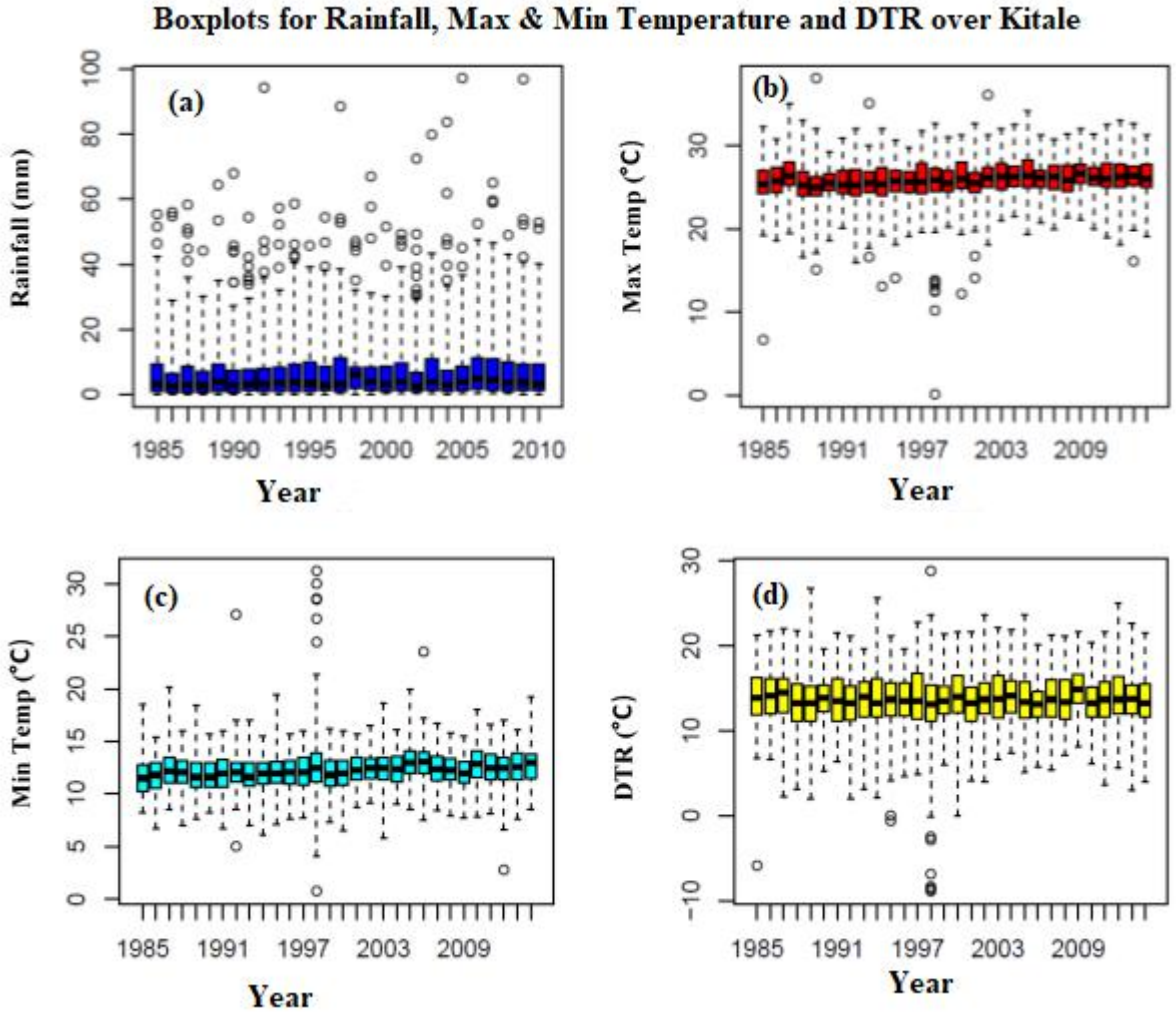

Figure 6: Box-series for Rainfall (a) Maximum Temperature (b), Minimum Temperature (c), DTR (d) over Kitale

(b) Kisii

The quality control result for Kisii weather data indicated that the input file did not have duplicates and missing values but outliers which presumably were due to extreme weather variations. Figure 7 is a box-series summarizing the outliers' information for Kisii station.

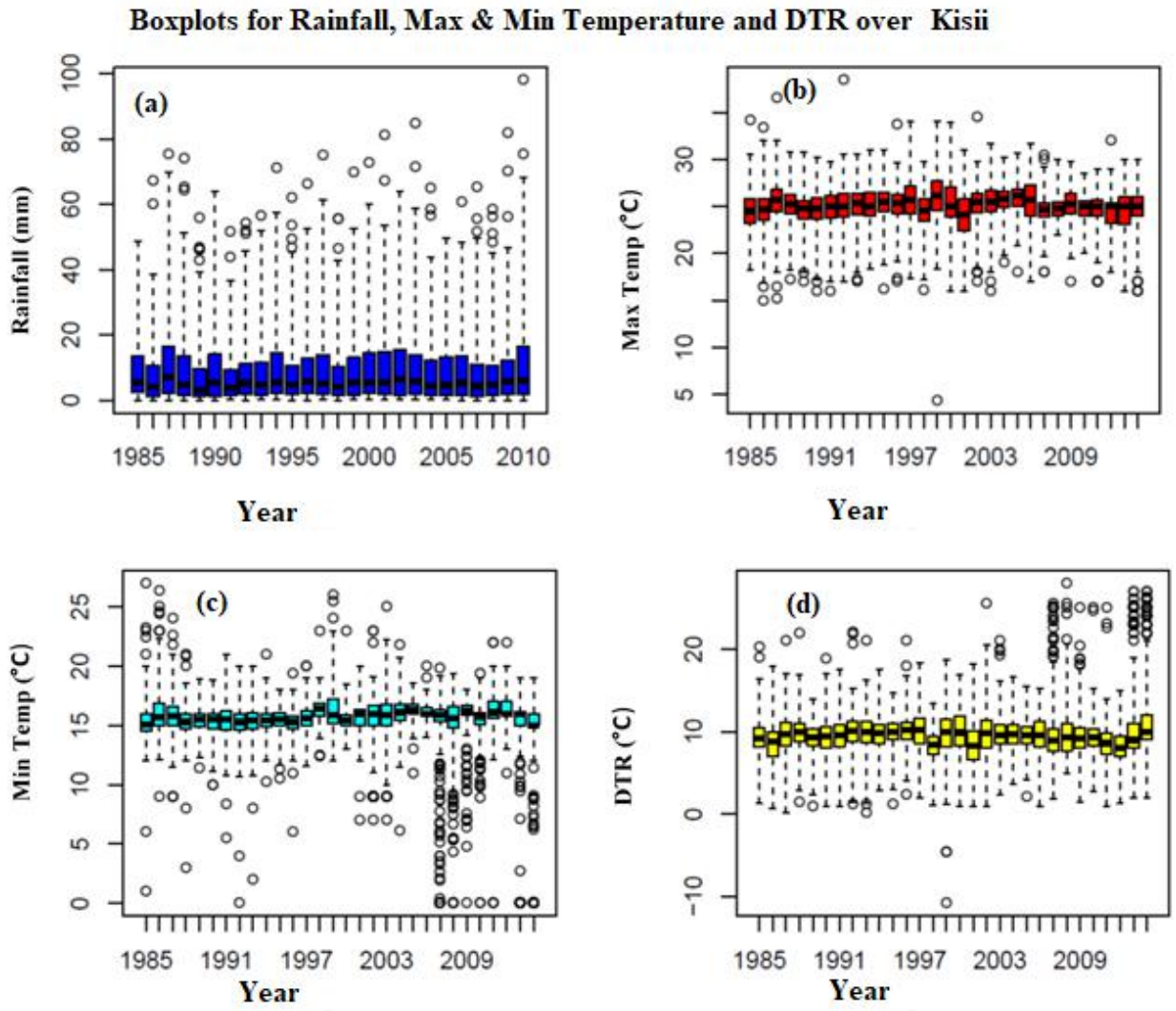

Figure 7: Box plot series for Rainfall (a), Maximum Temperature (b), Minimum Temperature (c) and Diurnal Temperature Range (d) for Kisii Station.

(c) Eldoret, Kakamega, and Kericho

All three stations did not have missing values or duplicates but several cases of outliers. Most of the flagged outliers involved temperatures, especially values of maximum temperature as well as the maximum values of minimum temperatures. Consequently, they were not treated as outliers but responses of temperature to climate change and the input files were used without any modifications.

4.3 Climate Variability and Change Over the Region

Graphical representations of the decomposed times series for each of the stations illustrate climate change (trend) and variability (random) over the study area.

4.3.1 Components of Temperature and Rainfall Series

(a) Eldoret Region

The trend component data indicate that maximum temperatures over Eldoret range from 22.5°C to 24.5°C while minimum temperature ranges between 10.0°C and 12.0°C (Figure 8).

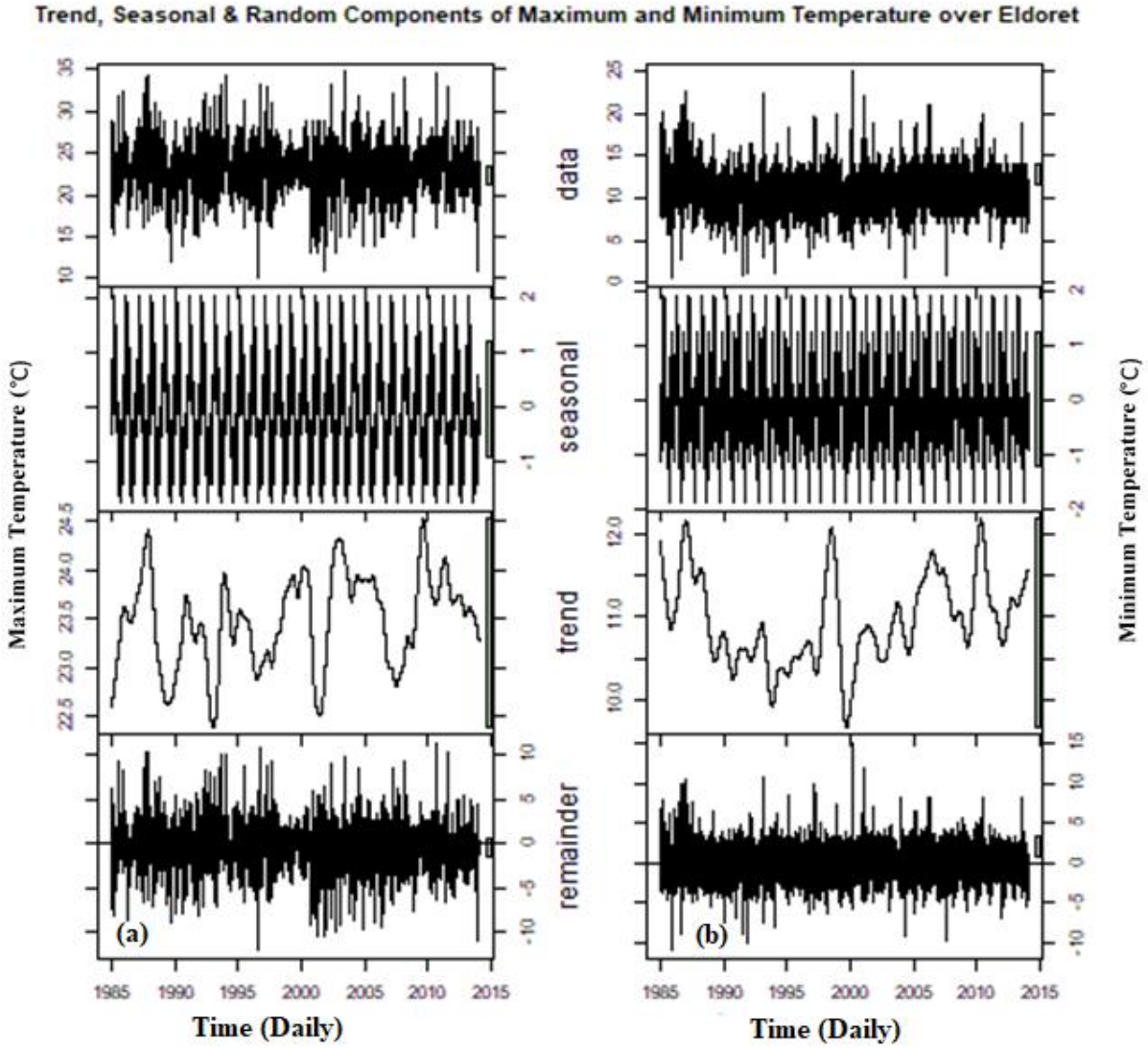

Figure 8: Graphical Display of Trend, Seasonal and Random Components of Maximum (a) and Minimum (b) Temperatures over Eldoret

Mean temperatures over the region ranges from 16.6°C to 17.8°C (Figure 9 (b)). However, the trend component indicates that maximum and minimum temperatures are highly variable with almost a distinct periodicity but not in the sense of seasonality. The decomposed daily mean temperature over Eldoret in Figure 9 (b) illustrates that mean surface temperatures increased over the region from 1985 to early 1990s before declining. However, it further suggests that mean surface temperatures have been increasing over the region since the late 1990s.

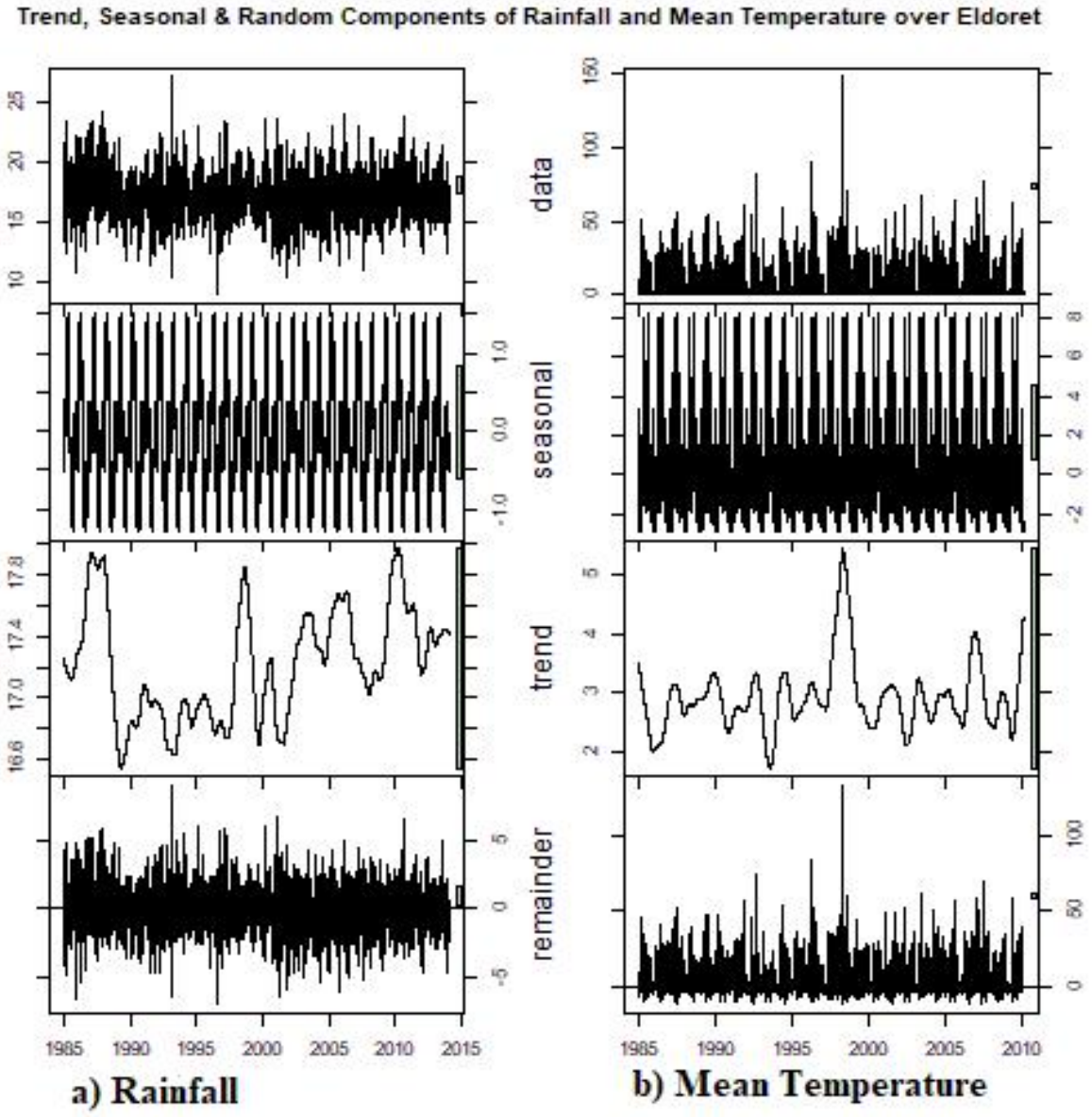

Figure 9: Graphical Representation of Trend, Seasonal and Random Components of (a) Rainfall and (b) Mean Temperatures over Eldoret

The results of the decomposition of rainfall over Eldoret suggest a daily tendency of rainfall that ranges between 2mm and 5 mm. According to the trend and random component graphs, rainfall over Eldoret is highly variable, but the variations tend to depend on the seasons (Figure 6 (a)).

(b) Kitale Region

The result of the decomposition of the series suggests that maximum temperatures tend to range from 24.9°C to 26.5°C while minimum temperatures tend to range from 11.5 °C to 13.1°C. Further, both trend graphs exhibit variability and increasing temperature tendencies as shown in Figure 9.

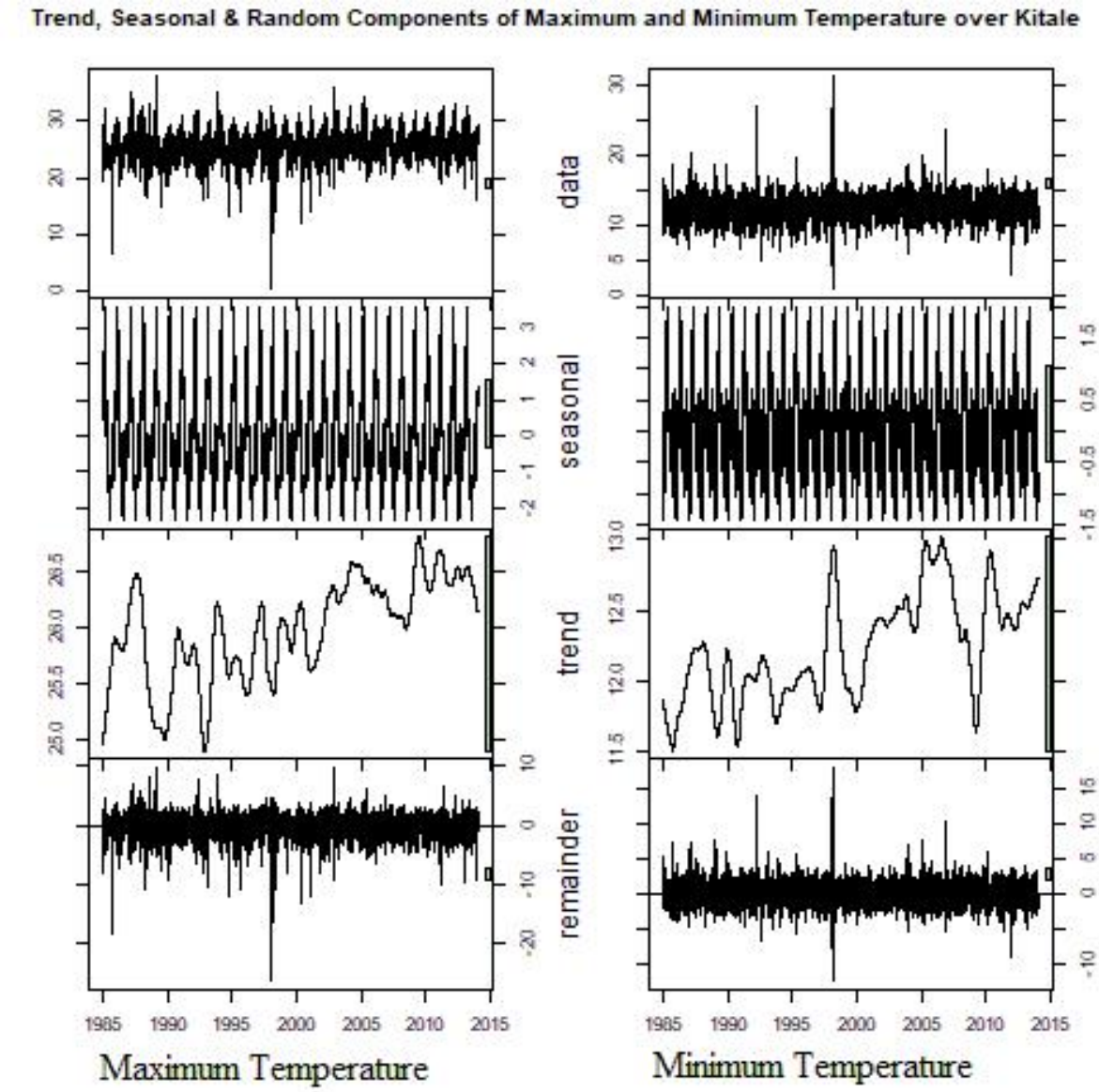

Figure 10: Graphical Representation of Trend, Seasonal and Random Components of Maximum and Minimum Temperatures over Kitale

The mean temperatures tend to range from 18.4 °C to 19.7°C with a distinct upward trend suggested in the trend component graph (Figure 11 (b)). The result of the decomposition of rainfall series for Kitale station indicated that the region receives highly variable rainfall (Figure 11 (a)). However, the seasonal and random components of the rainfall overshadow and affect the trend. The trend of daily rain suggests that Kitale receives between 2.7 mm and 5.5 mm on average per day.

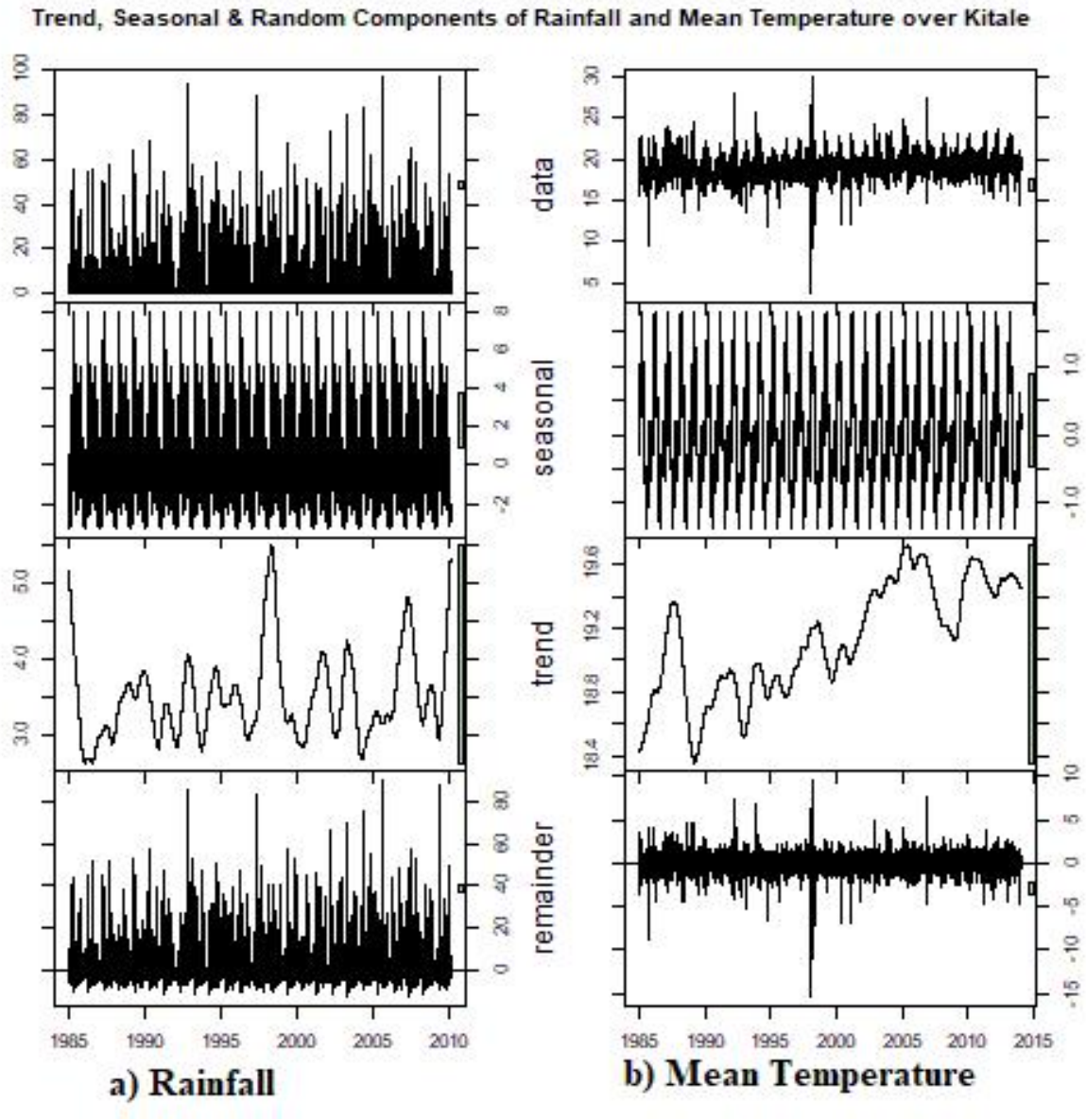

Figure 11: Graphical Representation of Trend, Seasonal and Random Components of Daily (a) Rainfall and (b) Mean Temperature over Kitale

(c) Kakamega Region

The trend graph of the series decomposition results shows that maximum temperatures range from 25.5°C to 28.5°C while minimum temperature ranges from 14°C to 15.5°C. The graph also suggest that maximum temperatures increased over the region from 1985 to around 2010 before declining drastically. Conversely, the minimum temperatures declined from the late 1980s toward 1995 but have been increasing from the mid-2000s (Figure 12).

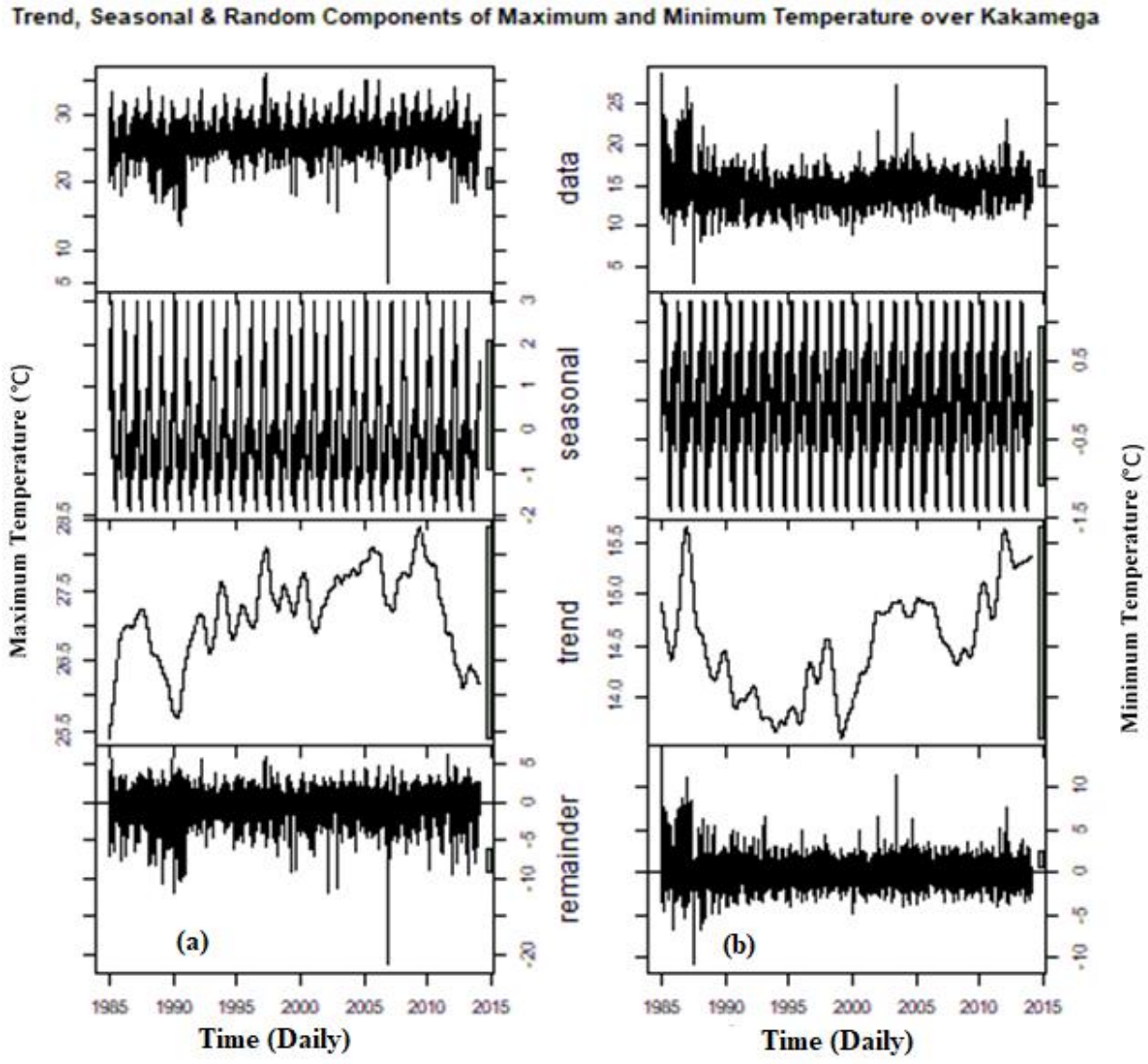

Figure 12: Graphical Display of Trend, Seasonal and Random Components of Maximum (a)and Minimum (b) Temperatures over Kakamega

Moreover, the mean temperatures from the trend component data range from 20.0°C and 22.5°C, and the graphical representation of the trend component data suggest that the mean temperatures have the tendency of increasing over the region (Figure 9 (b)).

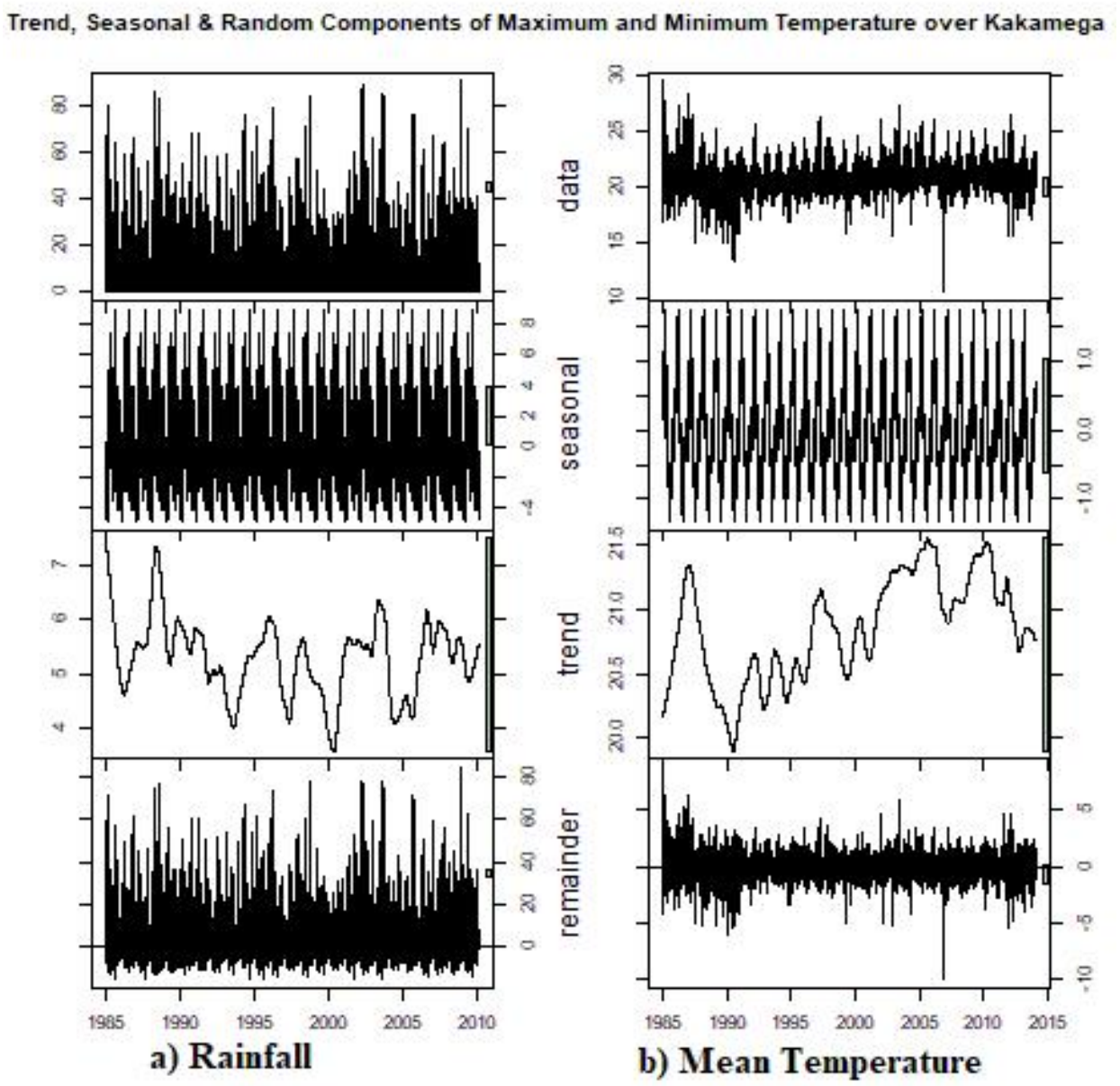

Figure 13: Graphical Representation of Trend, Seasonal and Random Components of Daily (a) Rainfall and (b) Mean Temperature over Kakamega

The Rainfall trend component displays distinct variability although the graph suggests that daily rainfall over the region ranges between 4mm and 7 mm. It was noted that the region tends to receive about 5 mm more frequently from the mid-1990s (Figure 13(b)).

(d) Kisii Region

The trend component data for Kisii indicates that maximum temperatures ranges between 24.0°C and 28.0°C while the minimum temperature ranges between 13°C and 18°C. However, as the graph shows, maximum temperatures are highly variable over Kisii, and it can be partly due to response to the rapid urbanization of the area hence the effects of urban heat island (Figure 14).

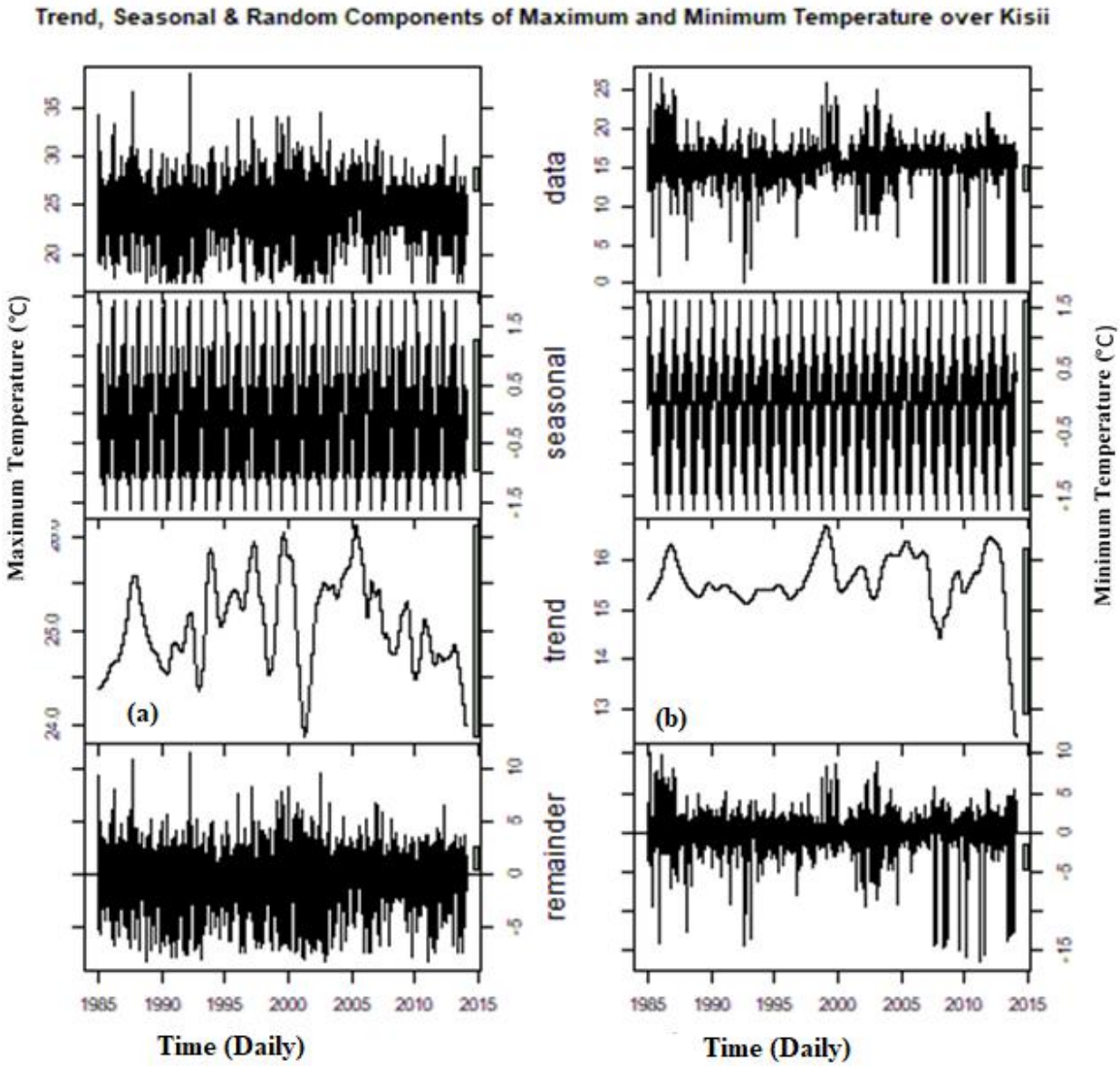

Figure 14:Graphical Display of Trend, Seasonal and Random Components of Maximum and Minimum Temperatures over Kisii

The graph of the trend component also shows that mean temperatures range from 18.5°C to 20.5°C. However, the mean temperature is not highly variable over Kisii, and the graph of the

trend component does not show any tendencies for increasing or decreasing temperatures (Figure 15 (b)).

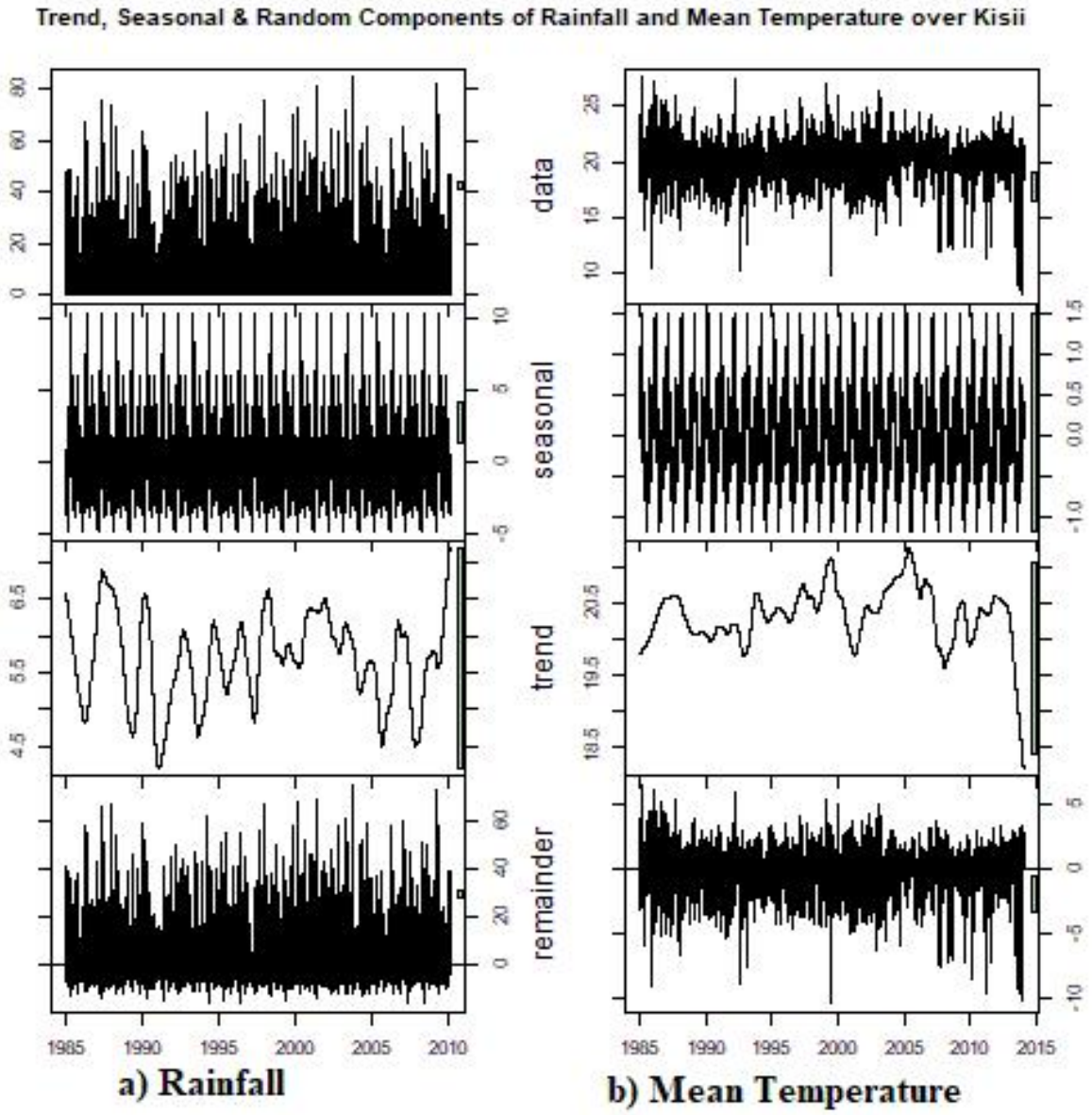

Figure 15: Graphical Representation of Trend, Seasonal and Random Components of Daily (a) Rainfall and (b) Mean Temperature over Kisii

Furthermore, the graph of the trend component for rainfall over the region suggests that the area tends to receive rainfall that averages between 4.5 and 7 mm on a daily basis as illustrated in Figure 15 (a). Despite the rainfall being variable, the graph fails to delineate any clear increment or decrement in rainfall amounts.

(e) Kericho Region

The trend component graph indicates that maximum temperatures range from 21.0°C to 25.0°C while its minimum temperature ranges from 13°C to 16.8°C. Maximum temperatures have stronger variation signals besides increment tendencies (Figure 16).

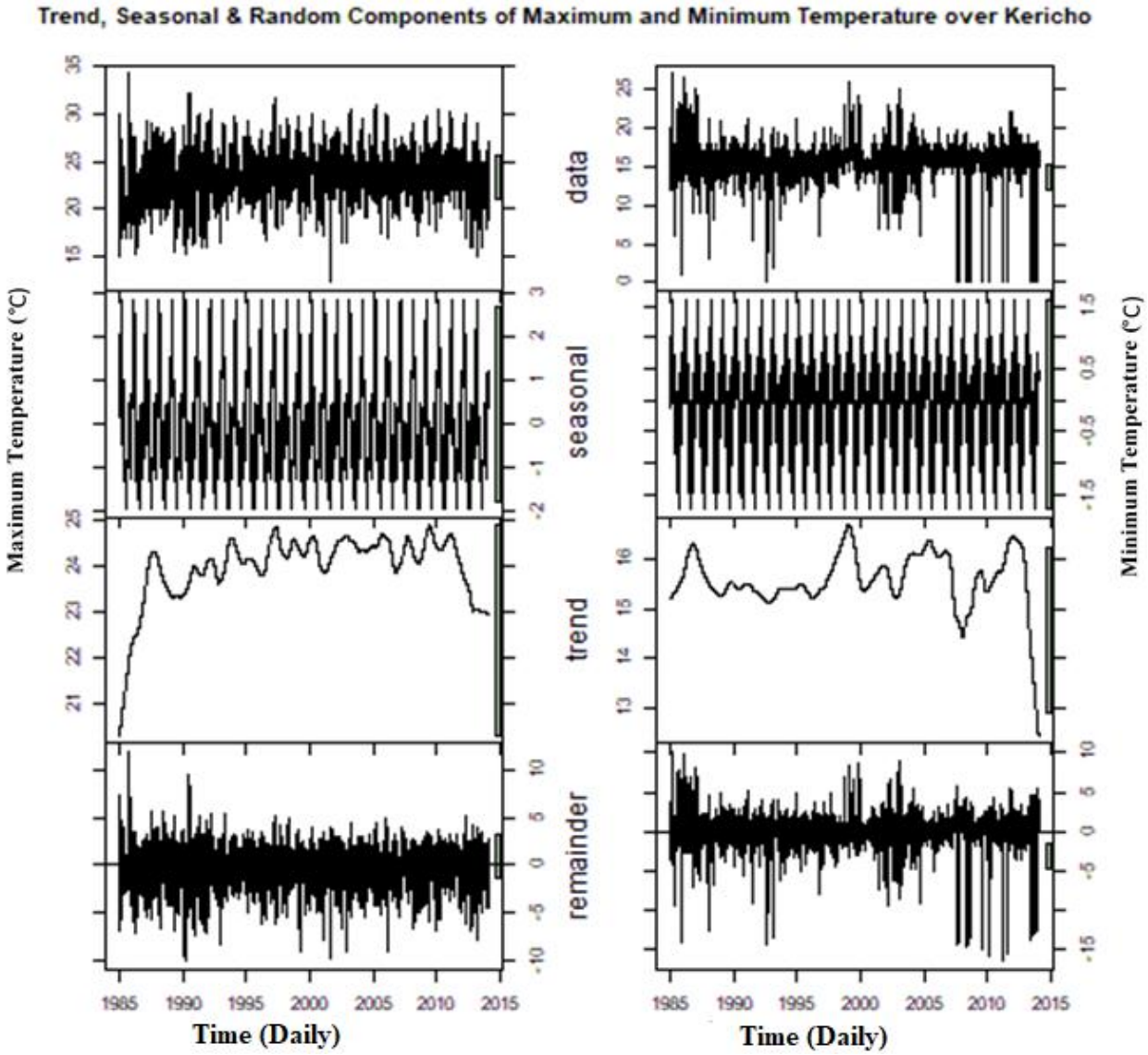

Figure 16:Graphical Display of Trend, Seasonal and Random Components of Maximum and Minimum Temperatures over Kericho

Further, the graph shows that mean temperatures range from 16.5°C and 19°C, with tendencies of increasing mean temperatures over the region (Figure 17 (b)). Kericho is usually wet with daily rainfall ranging from 4.0 mm to 8 mm (Figure 17 (a)). However, the trend graph suggests that the rainfall is highly variable and characterized by intense storm episodes.

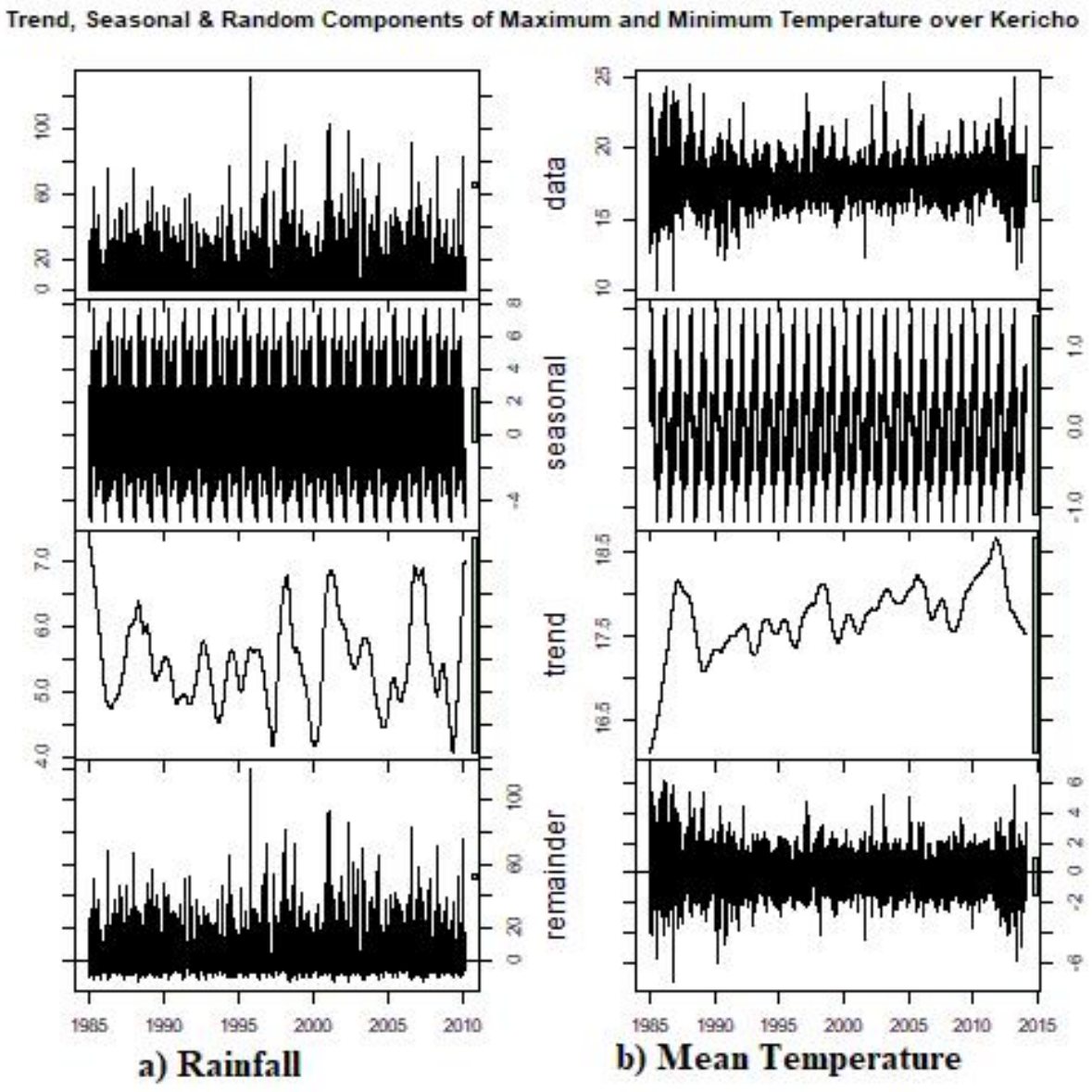

Figure 17: Graphical Representation of Trend, Seasonal and Random Components of Daily (a) Rainfall and (b) Mean Temperature over Kericho

4.3.2 Change Detection (Linear Trend Tests)

Variability is evident on the random and trend component of each of the data series from all the five stations, and suggestive linear trends were deduced from the graphical representation of the trend component for each of the variable. Statistical analysis and hypothesis testing alongside line fitting techniques were employed to ascertain the presence or absence of linear trends in the trend component data. As earlier mentioned, the Mann-Kendall trend test was used to determine

whether each of the variables had a monotonic upward or downward trend or not. Linear trends for all the variables were detected for the five stations.

The Mann-Kendall test results in Table 5 suggest that temperatures (maximum, minimum, and mean) have monotonic upward trends over Kitale, Kisii, Kakamega, Kericho, and Eldoret regions. The monotonic trends suggest that near surface temperatures are increasing over the region. The results also suggest similar monotonic trends in rainfall over Kitale, Kakamega, Eldoret, and Kericho. However, the tests concluded that rainfall over Kisii region does not have any monotonic trends and this could be because the region is normally wet. Further, graphs of linear trends were used to assess the nature of these monotonic trends.

Table 5: Mann-Kendall Test Results for Mean, Maximum and Minimum Temperatures and Rainfall over the Study Area

		Mean Temperature	Maximum Temperature	Minimum Temperature	Rainfall
Kitale	tau	0.6017	0.5002	0.4653	0.1493
	p-vale	<0.0001	<0.0001	<0.0001	<0.0001
Kisii	tau	0.1108	0.3473	0.3232	-0.009
	p-vale	<0.0001	<0.0001	<0.0001	0.1949
Kakamega	tau	0.421	0.3473	0.3232	-0.1085
	p-vale	<0.0001	<0.0001	<0.0001	<0.0001
Kericho	tau	0.4699	0.3187	0.1227	-0.0249
	p-vale	<0.0001	<0.0001	<0.0001	0.0004
Eldoret	tau	0.2463	0.1816	0.1641	0.0576
	p-vale	<0.0001	<0.0001	<0.0001	<0.0001

The graphs representing linear trends of temperatures (mean, maximum, and minimum) and rainfall over Kitale indicate that monotonic temperature trends are upward and hence temperatures are increasing over the region. However, it is inconclusive whether the trend in rainfall is monotonic upward or downward as Figure 18 illustrates.

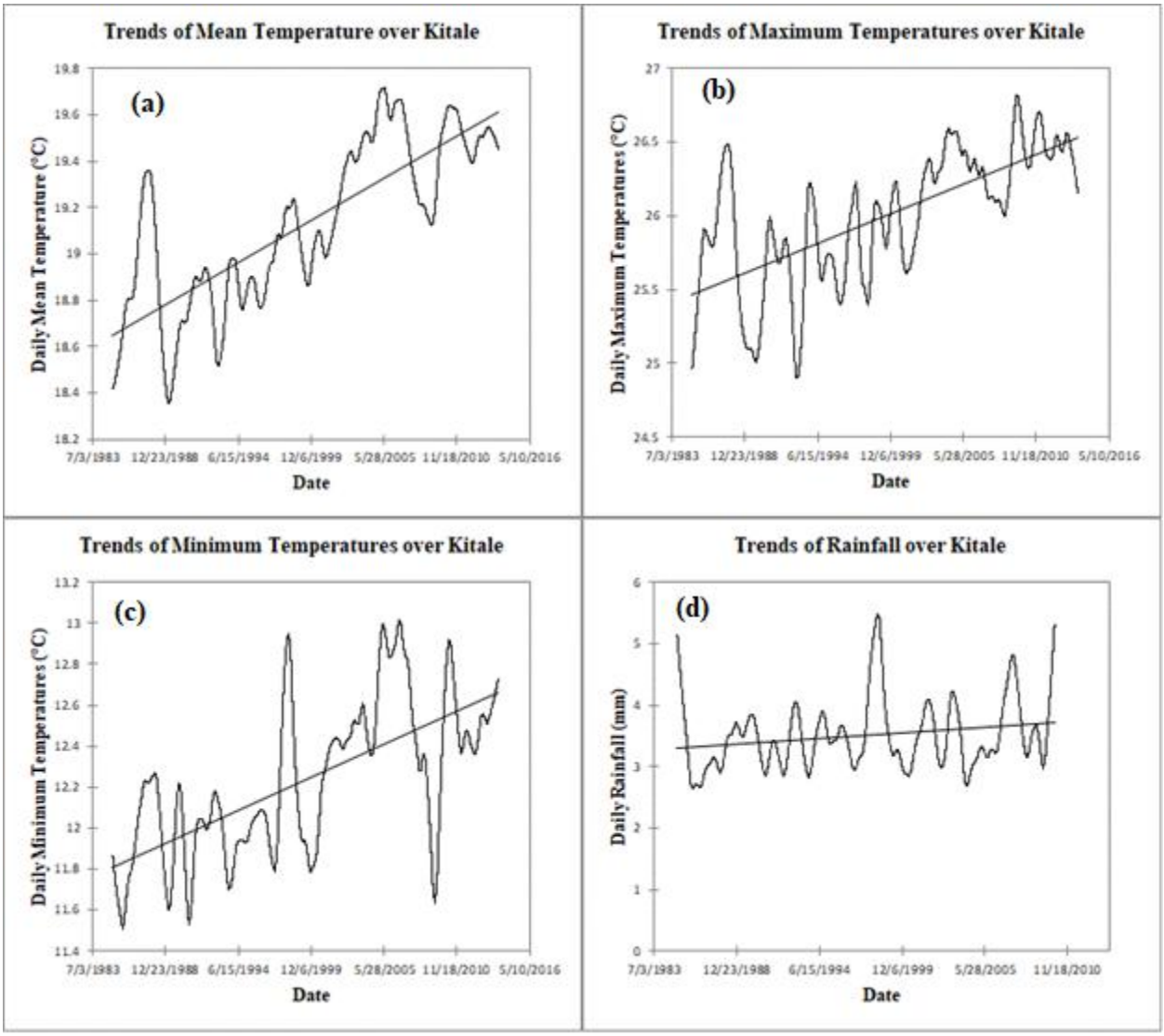

Figure 18: Linear Trends of Mean (b), Maximum (b), and Minimum Temperatures (c) and Rainfall (d) over Kitale

The linear trends over Kakamega that Figure 19 represents suggest upward trends in daily temperatures (mean, maximum, and minimum) and a downward trend in daily rainfall amounts.

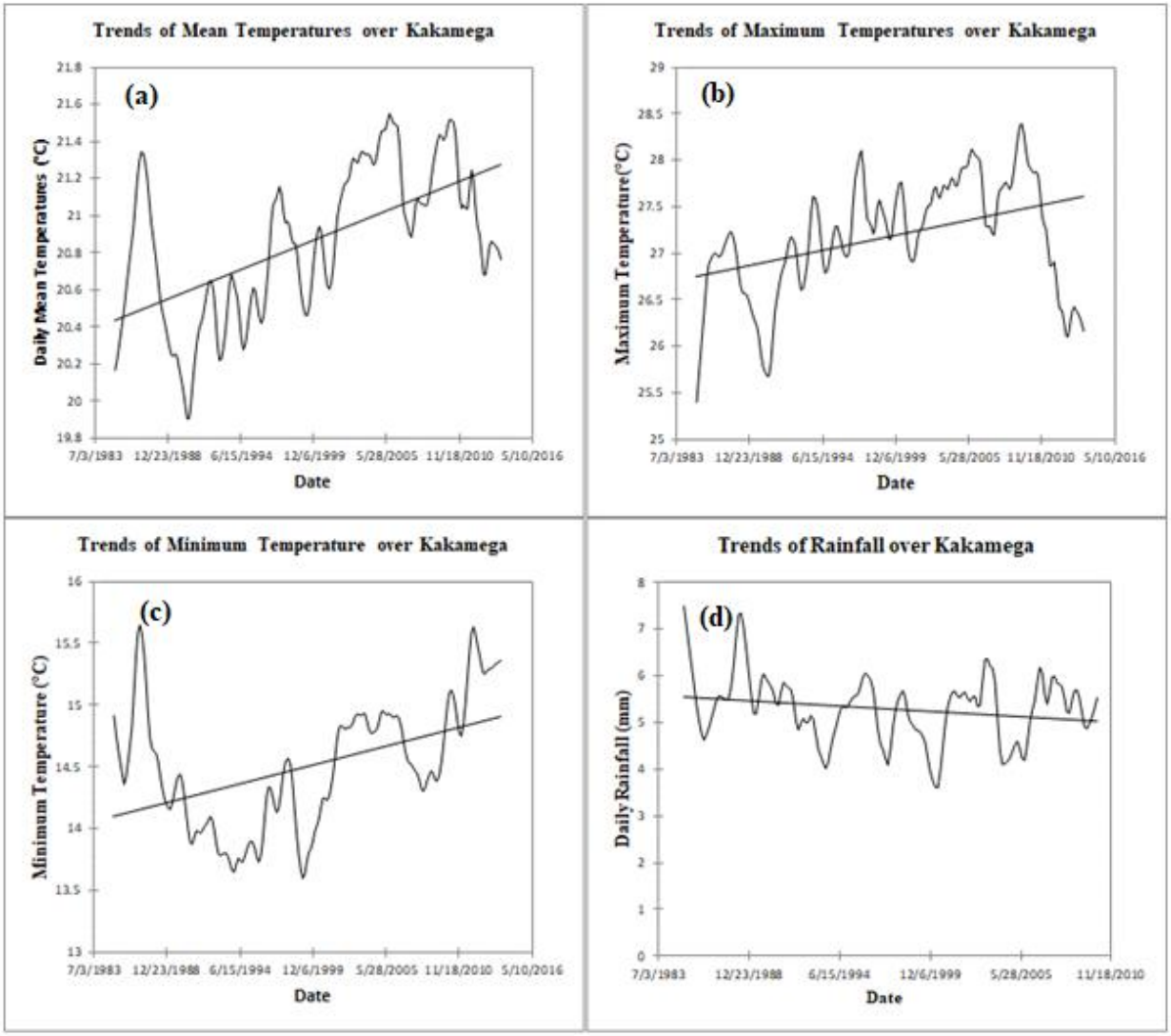

Figure 19:Linear Trends of Mean (a), Maximum (b), and Minimum (c) Temperatures and Rainfall (d) over Kakamega.

Further, Figure 20 only depicts a concise upward trend in mean temperature alongside inconclusive trends in maximum temperatures, minimum temperatures, and rainfall over Kericho.

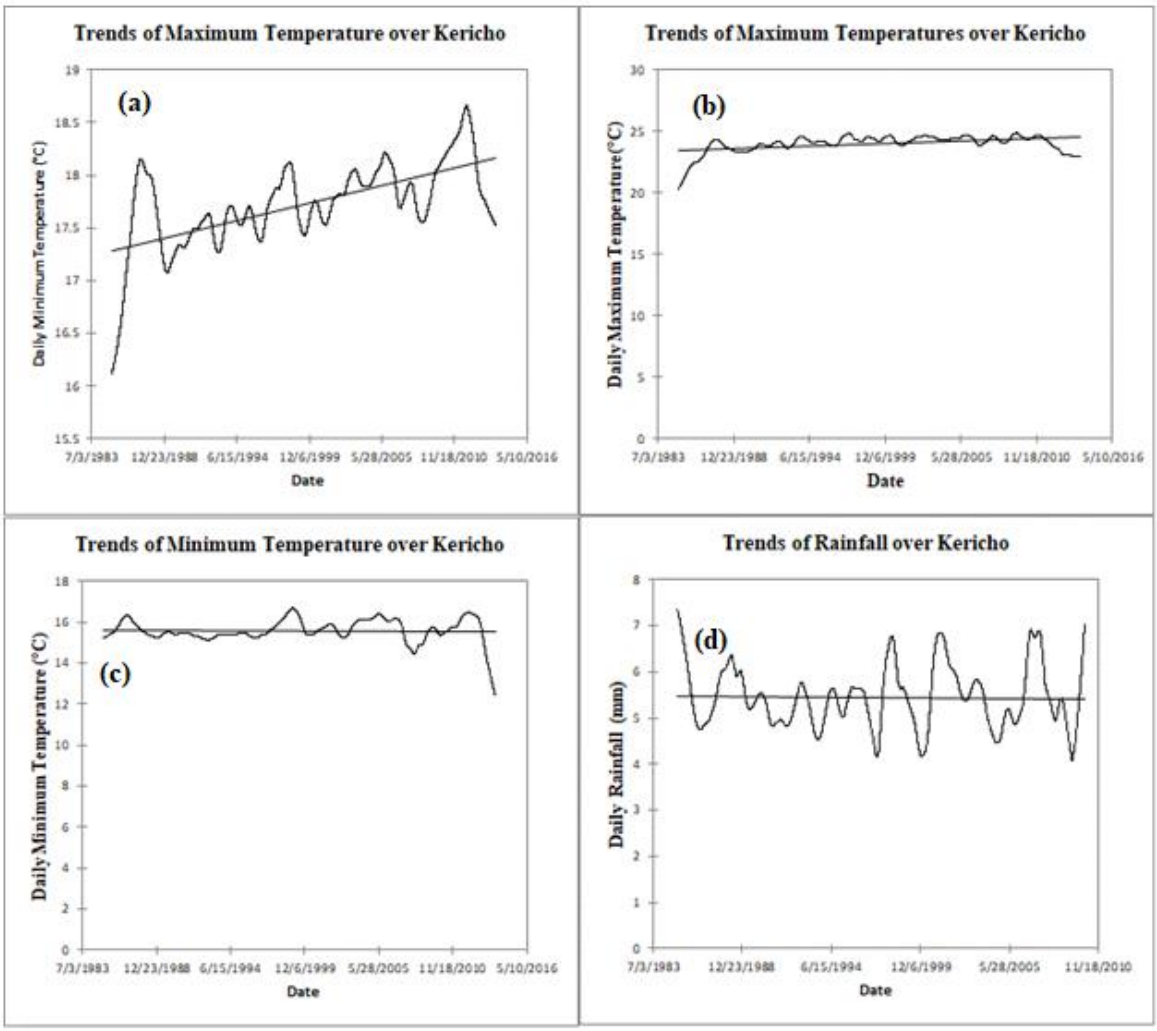

Figure 20: Linear Trends of Mean, Maximum, and Minimum Temperatures and Rainfall over Kericho.

However, over for Kisii, maximum and minimum temperatures have concise upward trends whereas mean temperature graph is inconclusive on the direction of the trend (Figure 21). The rainfall graph is consistent with the Mann-Kendall trend test since it does not indicate a trend in the rainfall data.

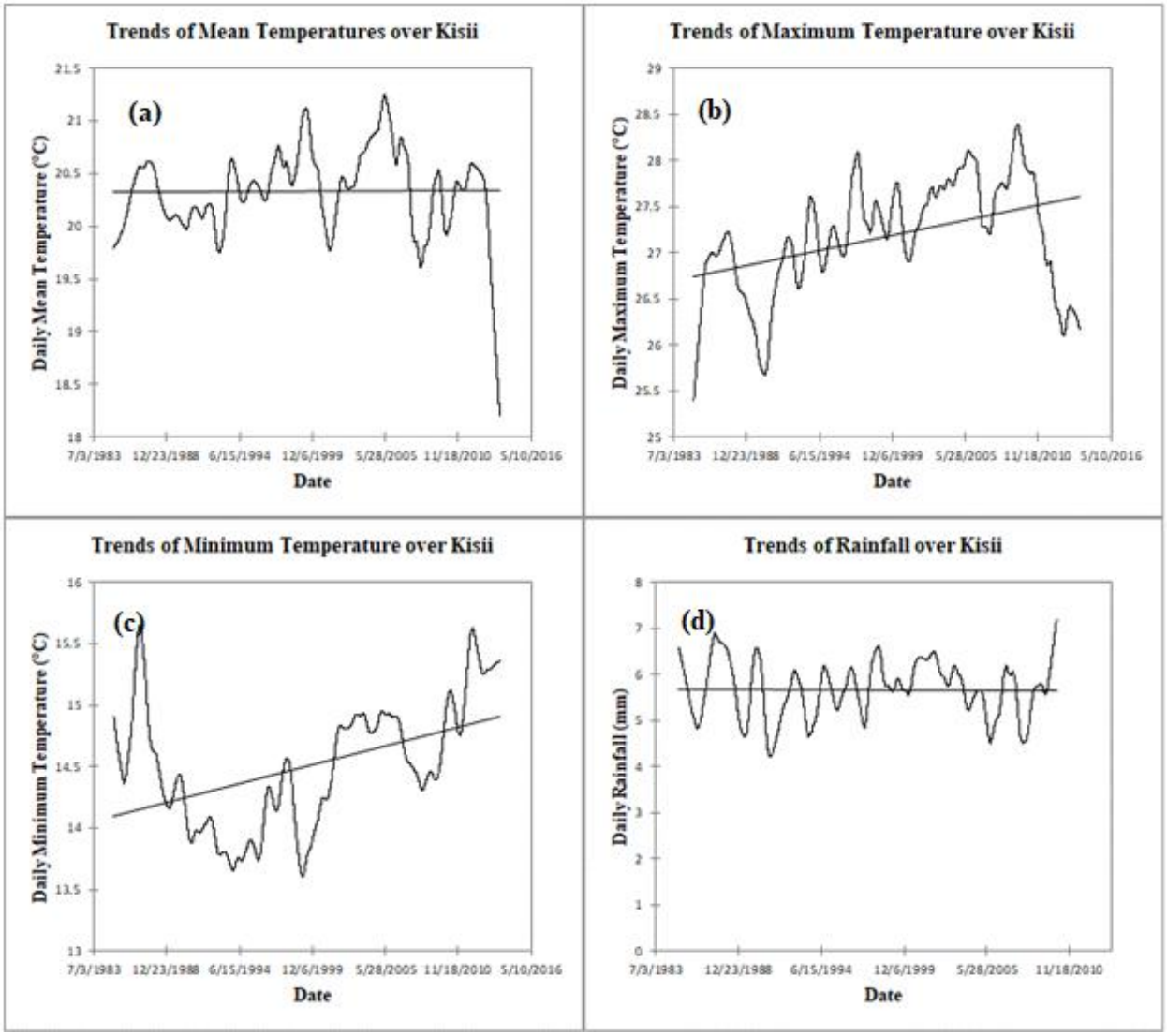

Figure 21: Linear Trends of Mean (a), Maximum (b), and Minimum (c) Temperatures and Rainfall (d) over Kisii

Finally, the linear graphs of mean and maximum temperatures over Eldoret suggest clear upward trends although linear trends of minimum temperature and rainfall are inconclusive (Figure 22).

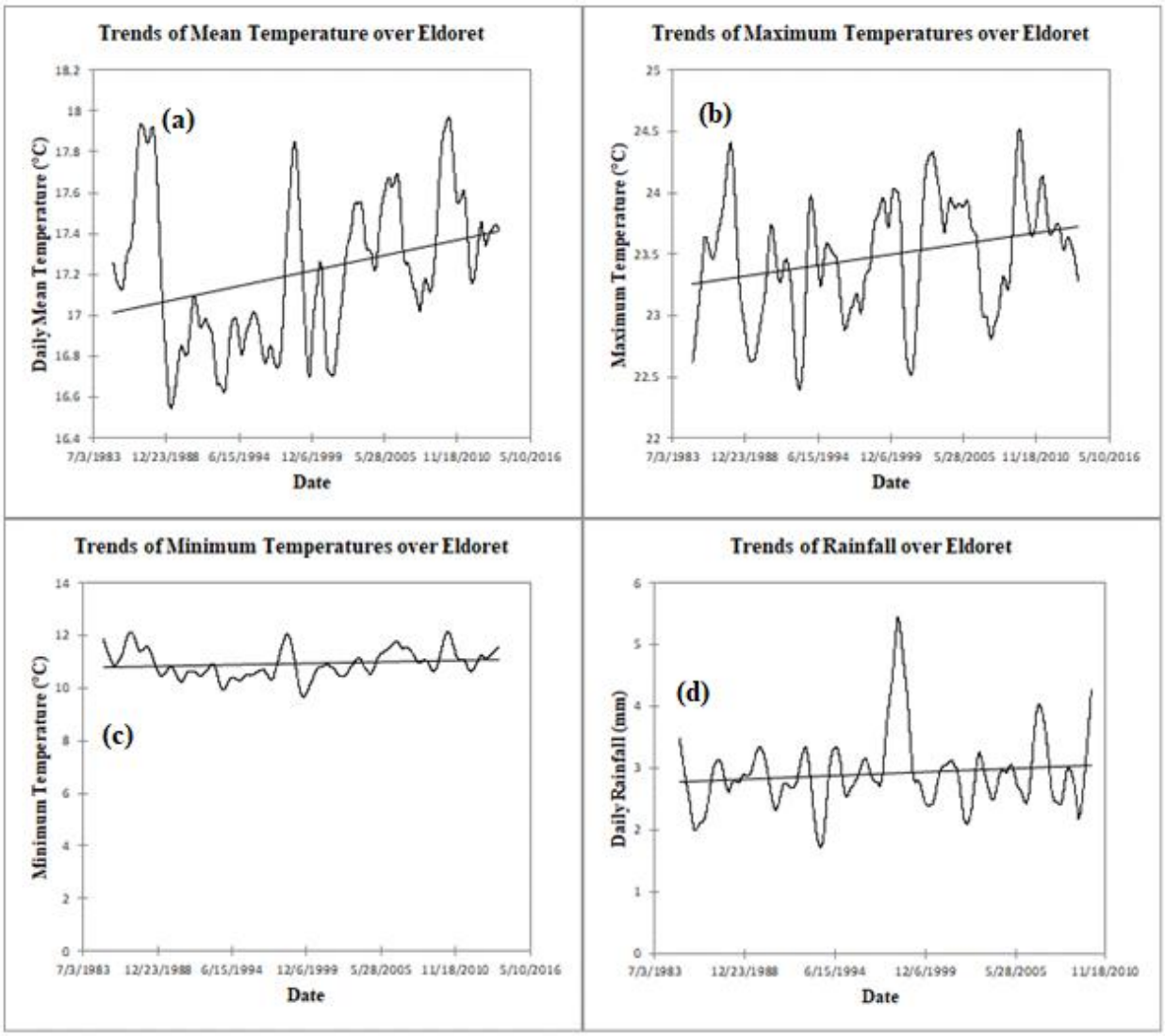

Figure 22: Linear Trends of Mean (a), Maximum (b), and Minimum (c) Temperatures and Rainfall (d) over Eldoret

4.3.3 Rainfall-Temperature Relationships

The linear trends and variabilities identified between temperature and rainfall suggest a likely relationship between these two variables. More importantly, the interaction between the variables affect the characteristics and potential of the study area. From Table 5, rainfall has an inverse relationship with mean temperatures over Kakamega, Kisii, Eldoret, and Kitale while Kakamega has the strongest correlation coefficient. Consequently, it can be deduced that a 1°C increase in mean temperatures over Kakamega region results in a rainfall decrease of about 0. 2 mm. The deduction and the subsequent observation account for the upward trend in mean temperatures and a downward trend in rainfall observed in Figure 19. Notably, mean temperatures and rainfall

have an inverse relationship so that as mean temperature increases then rainfall should decrease, although by a small margin.

Table 6: Kendall's Correlation Coefficients between Rainfall and Mean, Maximum, and Minimum Temperatures over the Study Area

	Rainfall				
	Kakamega	Kericho	Eldoret	Kisii	Kitale
Mean Temperature	**-0.1475**	0.0022	-0.0001	**-0.0261**	-0.0038
Maximum Temperature	**-0.2843**	**-0.1957**	**-0.1847**	**-0.1309**	**-0.2388**
Minimum Temperature	**0.1480**	**-0.0355**	**0.2134**	**0.1733**	**0.2831**
Note: Values in bold are different from 0 with a significance level alpha=0.05					

It is imperative to note that maximum temperatures are inversely related to rainfall over all the five stations and that the strength of correlation as suggested by the coefficient is stronger than those between rainfall and mean temperatures and thus greater influences on precipitation. Specifically, a one-degree increase in maximum temperature results in 0.3 mm, 0.2mm, 0.2 mm, 0.1 mm, and 0.2 mm decrease in daily rainfall over Kakamega, Kericho, Eldoret, Kisii, and Kitale respectively. Finally, minimum temperature has a direct relationship with rainfall over Kakamega, Eldoret, Kisii, and Kitale and an inverse relationship over Kericho.

Conclusively, the graphs in Figures 18, 19, 20, 21, and 22 alongside the coefficients in Table 6 suggest that the magnitude of change in trend is greater in maximum temperatures than both mean and minimum temperatures. Consequently, rainfall will most likely decrease as maximum temperature increases over most of the high potential agriculture zone.

4.4 Agro-Climatic Characteristics of Zone II

In subsection 4.3 (4.3.1, 4.3.2, and 4.3.3), variability and change were established in temperature and rainfall data. Most importantly, it has also been demonstrated that temperatures influence rainfall and the analysis in the following sections build on this relationship.

4.4.1 Rainfall and Evapotranspiration Patterns Over Zone II

The characterization of agro-climatic zones prioritizes the balance between rainfall and potential evapotranspiration (PET). PET is a function of temperatures (minimum, maximum and dew point), wind speed, and altitude and season-adjusted radiation. However, these variables also affect the soil water content and can affect plant and animal performance. From Figure 23, it is evident that the zone has a bimodal rainfall system with the long rain season in March-April-May and the short rain season between July and December depending on the location of the station. For instance, the onset of the short rains over Eldoret is July, and the cessation is in September. Over Kakamega, the onset of the short rains is in August while the cessation is in December, and the same onset and cessation patterns are observed in Kitale, Kisii and Kericho regions.

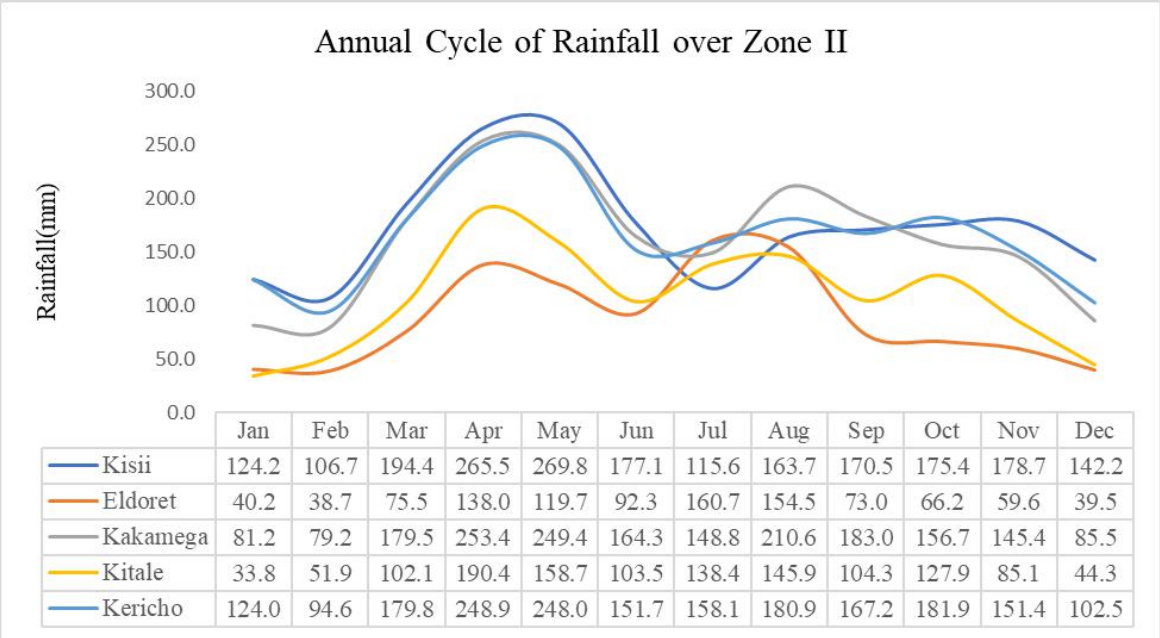

	Jan	Feb	Mar	Apr	May	Jun	Jul	Aug	Sep	Oct	Nov	Dec
Kisii	124.2	106.7	194.4	265.5	269.8	177.1	115.6	163.7	170.5	175.4	178.7	142.2
Eldoret	40.2	38.7	75.5	138.0	119.7	92.3	160.7	154.5	73.0	66.2	59.6	39.5
Kakamega	81.2	79.2	179.5	253.4	249.4	164.3	148.8	210.6	183.0	156.7	145.4	85.5
Kitale	33.8	51.9	102.1	190.4	158.7	103.5	138.4	145.9	104.3	127.9	85.1	44.3
Kericho	124.0	94.6	179.8	248.9	248.0	151.7	158.1	180.9	167.2	181.9	151.4	102.5

Figure 23: Climatology of Rainfall over Zone II

Evapotranspiration peaks in March-April-May (MAM) and September-October-November over Eldoret, Kakamega, Kitale, and Kericho (Figure 24). However, the greatest rates are observed between the MAM season. From Figures 23 and 24, it is deduced that the peak of maximum rainfall lags behind the peak of maximum evapotranspiration in a climatological sense. However, the daily rates of PET and rainfall received over Zone II were used to determine the length of the growing season. In cases where PET exceeds half of the rainfall amounts received, then soil water deficit becomes a production problem. Consequently, the start dates of the growing season

besides considering onset during MAM and OND or SON ought to consider the prevailing PET rates.

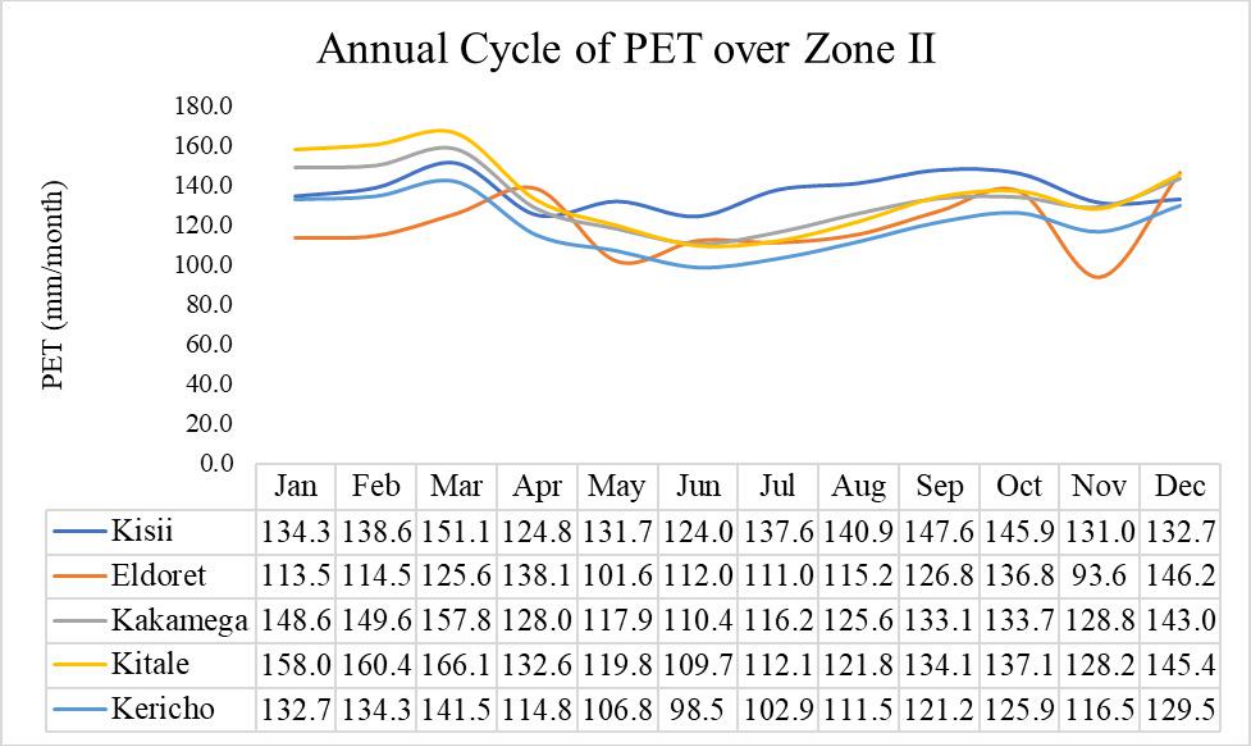

	Jan	Feb	Mar	Apr	May	Jun	Jul	Aug	Sep	Oct	Nov	Dec
Kisii	134.3	138.6	151.1	124.8	131.7	124.0	137.6	140.9	147.6	145.9	131.0	132.7
Eldoret	113.5	114.5	125.6	138.1	101.6	112.0	111.0	115.2	126.8	136.8	93.6	146.2
Kakamega	148.6	149.6	157.8	128.0	117.9	110.4	116.2	125.6	133.1	133.7	128.8	143.0
Kitale	158.0	160.4	166.1	132.6	119.8	109.7	112.1	121.8	134.1	137.1	128.2	145.4
Kericho	132.7	134.3	141.5	114.8	106.8	98.5	102.9	111.5	121.2	125.9	116.5	129.5

Figure 24: Climatology of Potential Evapotranspiration over Zone II

4.4.2 Moisture Regime Over Zone II

The annual cycle graphs show that the region has two rainfall seasons and hence the zone should have two complete crop growth cycles. However, temperature and rainfall changes alongside other factors such as evapotranspiration can lead to a shortening or break in one or both of the crop growing seasons. The LGP presented herein were computed using the Agrometshell model, and the onset was attached to the condition that the ratio of rainfall to evapotranspiration exceeded 0.5. The stations had more than two seasons in some years while other years had only one season.

The LGP over the zone varies from year to year and from one station to the other. Additionally, the number of seasons also vary with some stations having up to four seasons in a year. The temporal variations of both the LGP and number of seasons imply deleterious water requirement issues. Nonetheless, this study considers only the first and second seasons because of the bimodal patterns observed in rainfall and evapotranspiration data. However, the effects of the variations on the rest of the seasons were also considered in suitability analysis. The results of the LGP calculations are in Table 7.

Table 7: LGP Associated with Long and Short Rains over the Zone between 1985 and 2010

	Long Rains					Short Rains				
Station	Kisii	Eld*	Kaka*	Kit*	Ker*	Kisii	Els*	Kaka*	Kit*	Ker*
1985	82	120	305	140	283	0	2	0	21	55
1986	192	131	119	101	229	146	50	53	2	18
1987	244	116	185	129	365	0	51	0	50	0
1988	365	88	287	93	69	0	49	44	0	0
1989	173	112	329	124	192	81	97	0	0	0
1990	365	80	212	88	365	0	75	56	0	0
1991	225	116	365	192	177	113	36	0	51	111
1992	365	82	271	75	51	0	0	18	13	0
1993	365	146	91	177	189	0	37	38	43	0
1994	256	182	243	184	243	0	25	0	58	0
1995	200	180	205	197	182	64	66	0	0	0
1996	365	150	210	157	365	0	54	0	2	0
1997	138	96	133	100	114	117	79	107	84	77
1998	93	232	85	266	259	0	67	0	0	81
1999	156	105	150	78	347	0	74	0	0	0
2000	189	73	186	90	319	0	0	0	0	0
2001	143	88	283	206	92	134	46	46	0	0
2002	161	63	155	158	232	0	59	0	46	0
2003	158	125	232	189	291	0	0	34	0	0
2004	365	194	150	141	200	0	64	100	85	48
2005	200	75	222	84	283	0	21	14	75	48
2006	365	130	202	171	365	0	0	0	0	0
2007	365	105	130	213	89	0	51	0	46	0
2008	134	157	287	196	302	0	0	0	0	0
2009	158	63	143	153	136	0	53	0	77	0
2010	365	99	321	177	73	0	59	0	0	0
Note: Eld-Eldoret; Kit*-Kitale; Ker*-Kericho; and Kaka*-Kakamega*										

During the long rains LGP minima for Kisii, Eldoret, Kakamega, Kitale, and Kericho were 82, 63, 85, 75, and 51 respectively where the maxima were 365 days for Kisii, Kakamega, and Kericho. A trend assessment result established that the LGP in Eldoret, Kakamega, and Kericho decreased over the study period although it increased over Kitale and Kisii despite being the wettest among the five stations, did not show any trend in its LGP.

Table 8: Frequency Distribution of LGP Exceeding 300 days during the Long Rains

	Kisii	**Eldoret**	**Kakamega**	**Kitale**	**Kericho**
1985-90	2	0	2	0	2
1991-2000	3	0	1	0	3
2001-2014	4	0	0	0	2

The frequency distribution of the single LGP seasons shown in Table 8 suggests that Kisii and Kericho areas tend to receive rainfall throughout the year while Eldoret has the least number of completely wet years (LGP=365). Table 8 and Figure 25 summarize the trends and Sen's slopes for each of the station and the average LGP over the Zone.

Table 9: Sen's Slope indicating LGP trends over the Study Zone

Average LGP	Kericho	Kitale	Kakamega	Eldoret	Kisii
-0.0348	-1.6111	1.875	-1.9091	-0.7	0

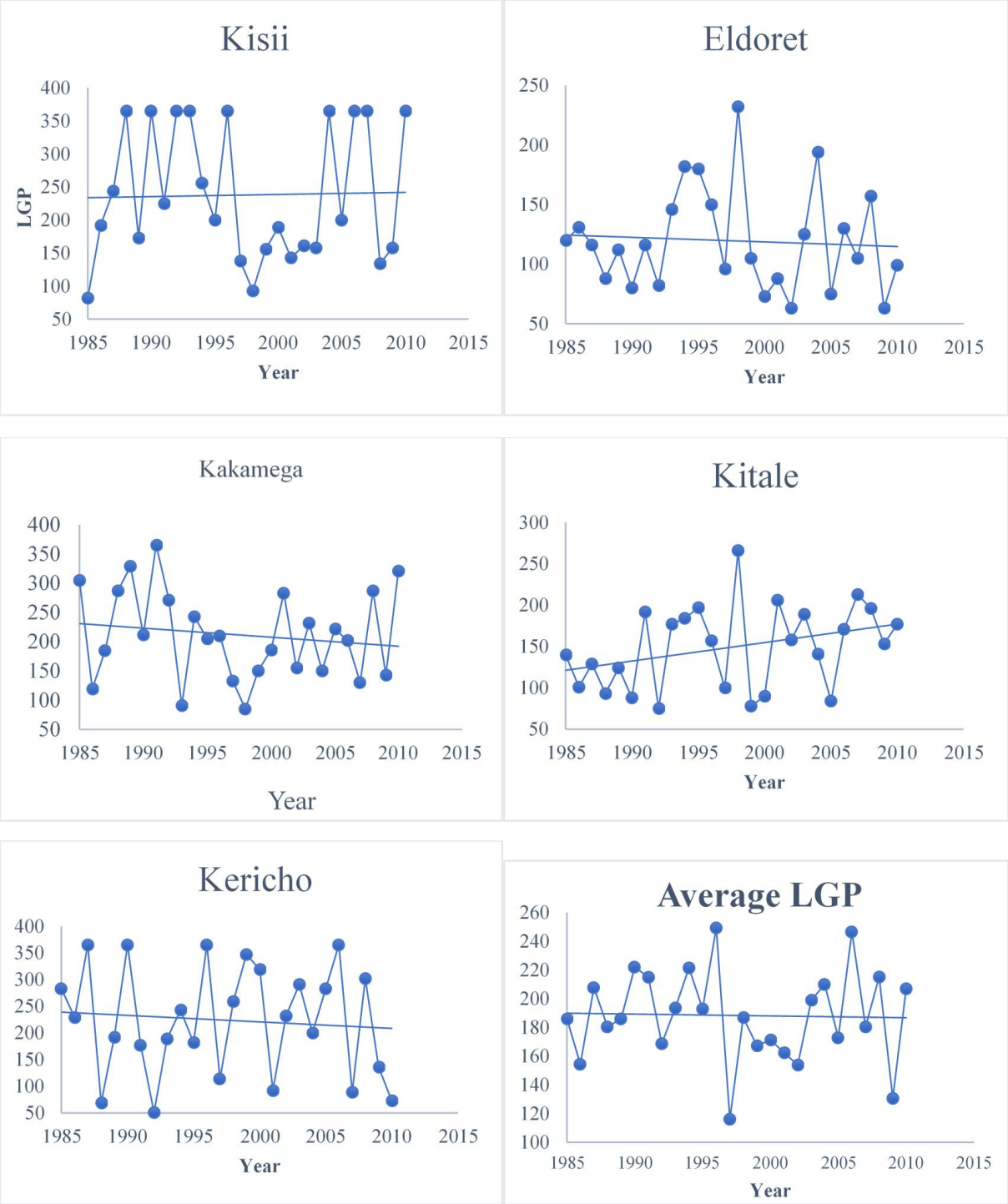

Figure 25: Trends of Length of Growing Period over the Zone from 1985 to 2014

The short rain LGP, their patterns and trends shed a more vivid picture on the effects of climate change on crop growth conditions. Over the study period, Kisii had six years with 365 LGP days and the rest of the years (14) had zero LGP days during the second season so that production is limited to one growth cycle or the persistent wetness affects the yield during such years. More

importantly, the number of over 300-LGP years are increasing over Kisii but decreasing Kakamega. Hence, there is likelihood of lengthening LGP over Kisii but shortening over Kakamega. Kitale and Eldoret do not have growth cycles with LGP exceeding 300 days.

The frequency distribution of Zero LGP days recorded over the period during the short rains was developed and is as shown in Table 10. The findings show that the frequency of LGP Zero days are increasing. The increase can be attributed to either lengthening of the LGP during the first season or shortening of the second season as response to either climate change or variability. Regarding the former, correcting for lengthened LGP (365 days) does not change the outcome of the analysis because years with LGP days for both long and short rain seasons have comparatively shorter growing periods than days with one season.

Table 10: Frequency Distribution of LGP with Zero Days during the Short Rains

	Kisii	Eldoret	Kakamega	Kitale	Kericho
1985-90	4	0	3	3	4
1991-2000	7	2	7	4	7
2001-2010	9	3	6	5	8

It is evident from Table 10 that the frequency of LGP zero days during the short rains are increasing and subsequently this season may not suit production because of high probability of moisture deficiency. More specifically, the zero days LGP were more frequent during the 2001-2010 period indicating shortening of the season.

A frequency distribution of Long Rains LGP suggests that Eldoret has sub-humid to semi-arid tendencies because it experiences the most frequent LGPs of less than 89 days during the long rains. Kisii, Kakamega, and Kericho tend to be hyper-humid (LGP >270 days) the average LGP ranges between 150 and 240 days during the long rain. However, occurrence of multiple LGPs per year affects this average with tendencies towards lower values when more than LGP season occurs in a year. Table 11 summaries the distribution of the long rain LGP for the five stations.

Table 11: Yearly Frequency Distribution of Long Rain LGP

LGP	Kisii	Eldoret	Kakamega	Kitale	Kericho
<89	1	8	1	4	3
90-119	1	7	2	4	3
120-149	3	5	3	4	1
150-179	5	2	3	6	1
180-209	4	3	4	6	4
209-239	1	1	4	1	2
240-369	2	0	1	1	2
270-299	0	0	4	0	3
300-329	0	0	3	0	2
330-364	0	0	0	0	1
365	9	0	1	0	4

In summary, the long rains LGP is shortening over Kericho (2 days/year), Kakamega (2days/year), and Eldoret (1 day/year) but lengthening over Kitale (2 days/year) and not changing over Kisii. The short rains LGP over Eldoret are shorter but persistent; at 95% confidence, the LGP over region lies between 32 and 55 days. Kisii only had 2-LGP seasons in six out of the 30 analysis years with a range of 64 to 146 days. The Short LGP over the region are becoming shorter and rare with most years having one season. The shortening or lengthening of the LGPs may be responses to changes and variabilities in temperature, rainfall, wind, and radiation parameters.

4.4.3 Thermal Regime Over the Zone

It is imperative to note that the study area is at the tropics so that using temperature intervals of either 5°C or 2.5°C could not clearly distinct its thermal differences. As a result, the LGPt and accumulative growing degree days (GDD) were used to assess the thermal resources over the zone. In this study area, it was possible to obtain a statistically significant change in the spatial and temporal trends of both the LGPt and GDD. The changes affect the thermal resources of the zone, especially vegetative performance based on underlying phenological influences. In the case of LGPt, the trend is positive although the study area being along the Equator limits the influence of this parameter on crop performance. Notably, the LGPt (the number of days taken to accumulate optimum heat units) was the only homogenous characteristics observed over the study area. The other variables were spatially and temporally variant. Nonetheless, the LGPt is a

proxy of the amount of heat that the zone receives annually, and it relates to thermal changes observed over the period of analysis.

The trend of thermal differentiation over the study area is strongly positive in Eldoret, Kakamega, Kitale, and Kericho but strongly negative in Kisii. The computation of the cumulated GDD used 0°C, 5°C, and 10°C as base temperatures to account for all the crops grown in the region. Specifically, cereals such as maize and wheat require base temperatures that range between 0°C and 4°C although there are strains that require up to 8°C (Salazar-Gutierrez *et al*., 2013). Despite the strong negative trends, Kisii area had the second highest cumulated GDD after Kakamega. Kericho and Kitale have equal cumulated GDD whereas Eldoret has the least (Table 12).

Table 12: Basic Characteristics of GDD over Eldoret, Kakamega, Kericho, Kitale, and Kisii

		Eldoret	Kakamega	Kericho	Kitale	Kisii
T_{base} 0°C	Mean	6291.4	7615.2	6470.1	6470.1	7408.5
	Minimum	6078.7	7251.3	6010.0	6010.0	6894.1
	Maximum	6553.3	7861.8	6749.3	6749.3	7714.3
	10-year Tendency	121.6	111.0	111.1	111.1	136.0
T_{base} 5°C	Mean	4465.3	5789.0	4644.0	5159.2	5582.3
	Minimum	4253.7	5426.3	4185.0	4915.3	5069.1
	Maximum	4728.3	6036.8	4924.3	5402.7	5889.3
	10-year Tendency	121.8	111.0	111.1	76.2	135.9
T_{base} 10°C	Mean	2639.1	3962.9	2817.8	3333.3	3756.6
	Minimum	2428.7	3601.3	2360.1	3090.3	3254.1
	Maximum	2903.3	4211.8	3099.3	3577.7	4064.5
	10-year Tendency	122.1	111.0	111.1	76.4	135.5

One can attribute the observed thermal differentiation to sub-zone features. In the analyzed regions, the cumulative GDD range from more than 4465 heat units in Eldoret to 5789 heat units in Kakamega and thermal classes can be created using the average cumulative GDD. In the case of 0°C base temperature, Kakamega and Kisii, as well as Kitale and Kericho, have similar thermal characteristics. Similarly, for the 5°C base temperature, Kakamega, Kitale, and Kisii have similar thermal features just as Eldoret and Kericho. The same differentiation holds for the 10°C base temperature. The variations (strong upward or downward trends) are critical for the evaluation of the characteristics of the study Zone because any spatial differentiation indicates inhomogeneity in the zone and it also has implications on production potential. Also, important temporal variations were observed with Eldoret, Kakamega, Kitale, and Kericho showing

increasing GDD per year and Kisii showing decreasing GDD. In general, cumulative GDD over the zone decreased sharply between 1987 and 1990 before increasing for the rest of the period in the case of Kitale, Kakamega, Eldoret, and Kericho (Figures 27, 28, 29, and 31).

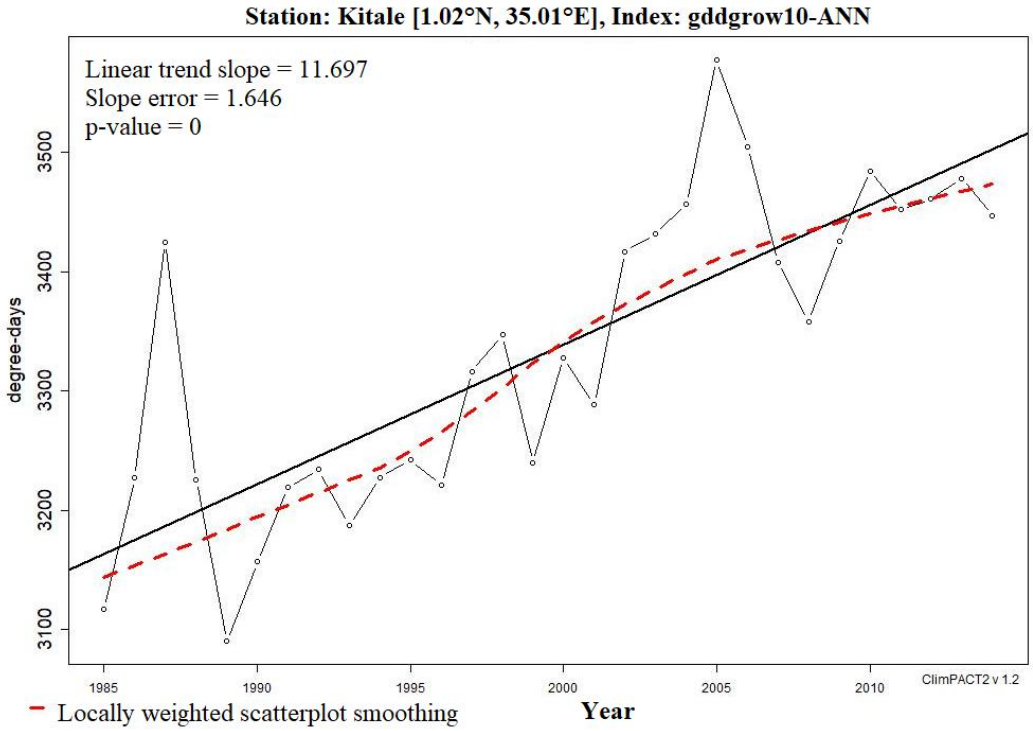

Figure 26: Trend of Growing Degree Days over Kitale between 1985 and 2014.

The linear trend in growing degree days is significant, and 1987 and 2005 had the best growing conditions while 1989, 1997, and 2007 had the worst growing conditions. Table 11 below summarizes the magnitude of the temporal changes of growing degree days over the study area.

Table 13: Linear GDD Trends for Eldoret, Kakamega, Kericho, Kitale, and Kisii

Base Temperature		Eldoret	Kakamega	Kericho	Kitale	Kisii
T_{base} 0°C	slope	5.407	10.357	10.289	11.721	-2.958
	p-value	0.06	0	0	0	0
T_{base} 5°C	slope	5.399	10.349	10.281	11.712	-2.966
	p-value	0.06	0	0	0	0
T_{base} 10°C	slope	5.39	10.341	10.273	11.697	-2.879
	p-value	0.061	0	0	0	0

From Table 13, cumulated GDD increased by over 5, 10, 10, and 11 units of cumulated heat per year over Eldoret, Kakamega, Kericho, and Kitale respectively. The trend is persistent for the three thermal base temperature classes. On the contrary, the cumulated GDD over Kisii region

reduced at a rate of about three heat units per year. The p-values ascertain statistically significant trends in Kakamega, Kericho, Kisii, and Kitale but the insignificant trend over Eldoret.

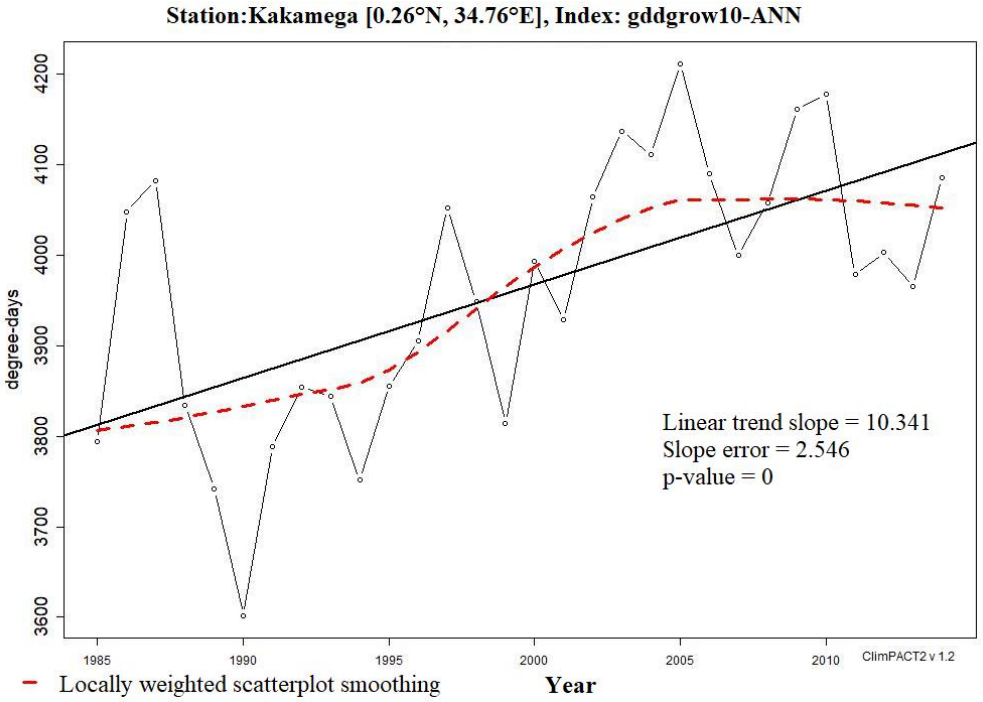

Figure 27: Trends of growing degree days over Kakamega between 1985 and 2014

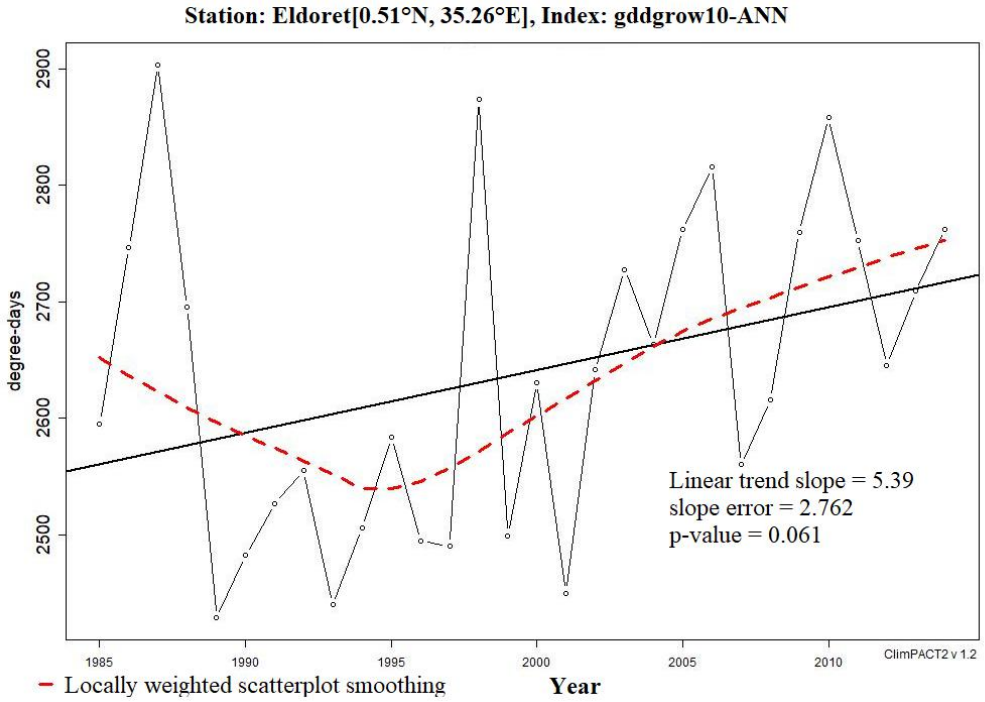

Figure 28: Trend of growing degree days over Eldoret between 1985 and 2014

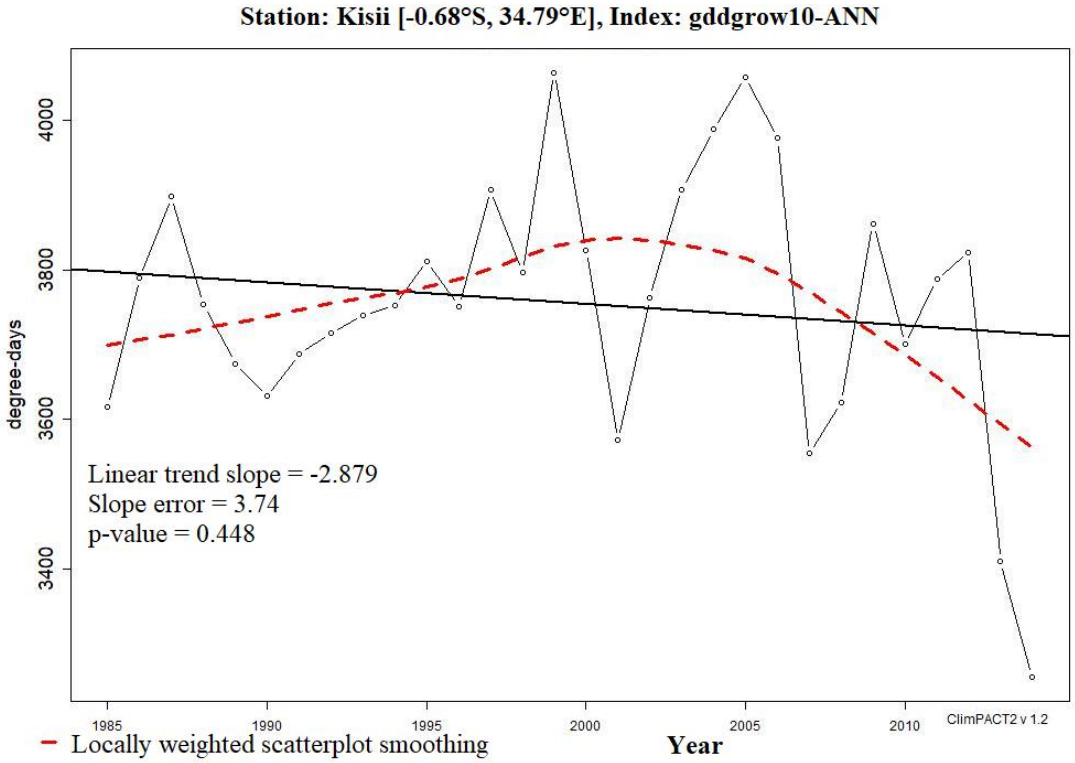

Figure 29:Trend of growing degree days over Kisii between 1985 and 2014

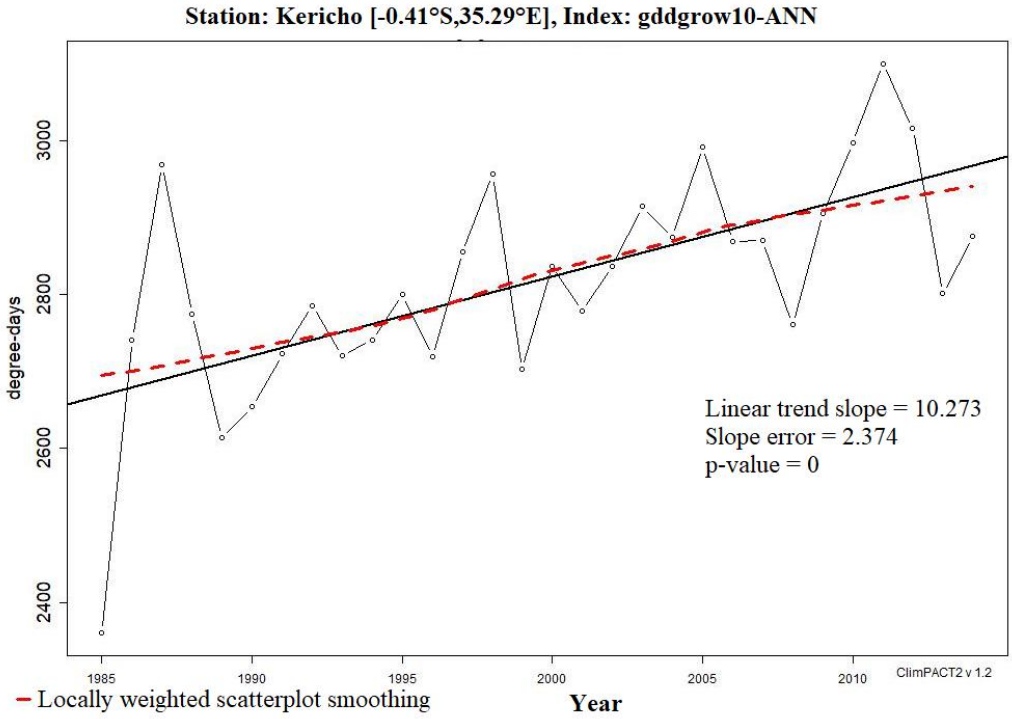

Figure 30:Trend of growing degree days over Kericho between 1985 and 2014

These findings agree with the observations that Hartfield (2016) made that warmer temperatures accelerate crop phenological stages and that the warming causes an increase in heat units.

However, using these observations for suitability assessments require GDD threshold for given crops as well as ecology.

4.5 Suitability of the Zone

The changes and variability in rainfall and temperatures besides wind speed and radiation explain the spatial and temporal differentiation observed in thermal and moisture characteristics of the zone. The spatial and temporal differentiation imply different suitability constraints and subsequent effects on the potential of crop farming in the region.

4.5.1 LGP Patterns and Moisture Constraints

(a) Annual Rainfall

Rainfed agriculture dominates the zone of study, and rainfall is the key determinant of soil moisture availability. According to the 1982 classification (Sombroek *et al.,* 1982), the Zone has an annual rainfall threshold that ranges between 1000 mm and 1600 mm. In this study, Eldoret received annual rainfall amounts that were below 1000 mm in 14 out of the 26 years while Kitale also received below normal rainfall in the mid-1980s (Figure 31).

The annual rainfall amounts received over Kitale were observed to be within the range defining the zone although some parts of the Kitale region are semi-humid. The rest of the stations (Kakamega, Kericho, and Kisii) are humid since they receive annual rainfall amounts that range from 1100 mm to 2700 mm. One can deduce that Eldoret and Kitale transition to semi-humid conditions from sub-humid conditions during some years. While Kakamega, Kericho, and Kisii exhibit tendencies of transitioning towards the sub-humid conditions.

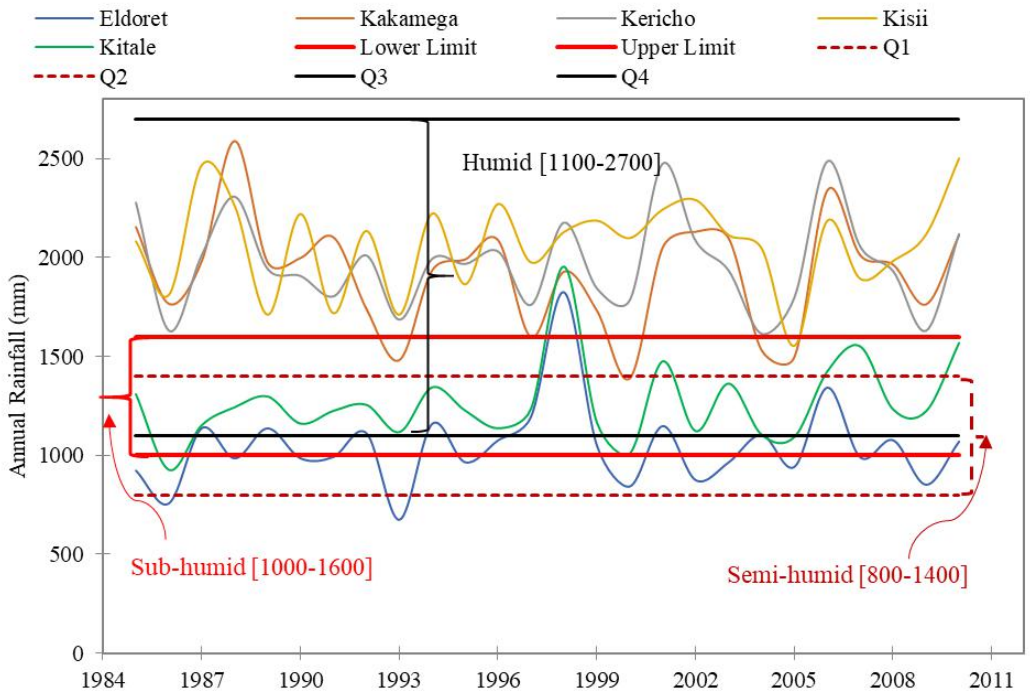

Figure 31: Evolution of Rainfall and Spatial Moisture Differentials over the Study Area

The inter-annual variability observed in annual rainfall can be associated with extreme weather events that result from global weather drivers such as the El Nino and La Nina. From this spatial aspect of rainfall distribution in the region, it is conclusive that moisture is not an agricultural production constraint although further investigation into its temporal distribution indicates plausible problems in future, particularly under the changing climate. The long-term annual rainfall over Eldoret, Kakamega, Kericho, Kisii, and Kitale over the study period were 1047 mm, 1921 mm, 1974 mm, 2068 mm, and 1266 mm respectively.

In regards to temporal distribution of the annual rainfall, the study established non-significant annual rainfall decrease over Kakamega $[s = -0.034, p = 0.5661]$ and Kericho $[s = -0.02, p = 0.964]$ but an equally statistically non-significant increment over Eldoret $[s = 0.021, p = 0.636]$, Kitale $[s = 0.053, p = 0.0227]$ and Kisii $[s = 0.02, p = 0.694]$ at 5% level of significance. The assessment of moisture regimes using annual rainfall trends is therefore inconclusive especially considering the non-significance of all the slopes. The ratio of annual rainfall to potential evapotranspiration and standard precipitation index were used for further moisture assessments.

(b) Moisture Indices (R/PET)

In the study, thermal-based equations were used to compute ET, and consequently, the change in daily minimum and maximum air temperatures served as the key determinants of PET rates. However, the altitude and geographical positioning of the stations also played a major role in radiation estimation. As a result, the ratio of rainfall to evapotranspiration gives a more comprehensive picture of the moisture condition over the zone. Figure 32 displays the temporal distribution of the ratio over the period of analysis and one can observe that the ratio transitions between semi-humid and sub-humid mostly over Eldoret and partly over Kitale. The rest of the stations exhibit sub-humid, humid and per humid moisture characteristics over the period and suits wheat, maize, beans, Irish potatoes and tea production besides dairy farming and forestry (Table 2). However, parts of the zone that experiences moisture characteristics observed over Eldoret are suitable for cotton and cassava production though they can still support wheat, beans, and maize growth under constrained moisture conditions.

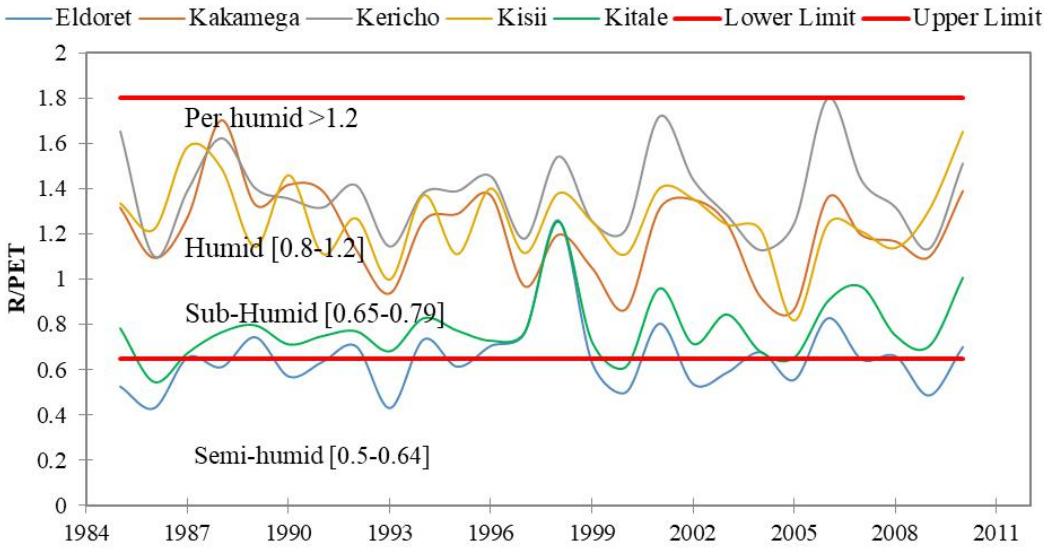

Figure 32: Evolution and Spatial Differentials of Moisture Index over the Zone

Using the long-term average of the R/PET ratio, one can conclude that R/PET was not a limiting factor over the region. Specifically, the R/PET ratio averaged 0.654, 1.211, 1.377, 1.268, and 0.782 over Eldoret, Kakamega, Kericho, Kisii, and Kitale respectively. The identified LGP constraints are derived from the frequency distribution in Table 11 and Maize and Cassava are used for demonstration of limiting conditions based on prevailing LGPs.

Table 14: Constraints that are associated with Long Rain LGPs over Zone II in Kenya

LGP	Maize	Cassava
75-89	Moisture stress	Moisture stress
90-119	Silk Drying	Dry/compact lifting conditions
120-149		
150-269		-
270-299	Borer	
300-330	Leaf spot/Leaf blight	
330-364	Streak Virus/ Wet produce	
365	Workability	

In humid ecologies, LGP that are less than 60 and 120 days represents extremely severe and severe moisture constraints respectively. However, LGP of less than 180 also poses some moderate constraints. In general, $LGP < 90$ are associated with rainfall variability constraints while LGPs between 90 and 120 days have frequent maize silk drying. From Table 11 (p.57), Kisii and Kericho regions are vulnerable to workability constraints during the long rains and single season LPGs. Kakamega and Kitale regions are susceptible to maize stalk borer, leaf spot and leaf blight during the long rains. However, all the regions are susceptible to rainfall variability, silk drying, and compact lifting conditions with Eldoret region as the most vulnerable. Additionally, some of short rains are associated with severe moisture deficit ($LGPs < 60\ days$).

4.5.2 Cumulative GDD Patterns and Thermal Constraints

The long-term average GDD sum over Eldoret, Kakamega, Kericho, Kitale, and Kisii are 2640, 3963, 2818, 3334, and 3757 heat units respectively. These values suit crop growth and development given that the minimum temperature is not less than 10°C and the maximum temperature does not exceed 30°Cfor maize growing areas. The average GDD sum suggests that the region is suitable for maize hybrid that matures in the range 140 to 250 days depending on the planting dates and the effects of other environmental constraints.

The increase in GDD sum is a sign of acceleration of mass accumulation during plant development and it comes with it challenges. Firstly, as GDD sum increases it becomes difficult to select crop variety and hybrids that suit the prevailing heat units. Secondly, increasing GDD

sum suggests faster mass accumulation which provide better conditions for pest and weed development. These challenges can undermine the potential of the zone if they are not addressed.

4.5.2 Climate Diagrams

The increase in GDD sum is suggestive of increasing temperatures whereas the shortening of the LGP indicates high likelihood of increasing moisture constraints in terms of water available in the soil. For agricultural application and overall assessment of vegetative growth under these changes and variabilities, climate diagrams and index of longest dry spell (Consecutive Dry Days) were included in the analysis. Consecutive Dry Days (CDD) indicates the number of days that an area has undergone when receiving rainfall amounts of less than 1 mm. The index is a predisposing factor to increasing moisture constraints. As Figure 33 shows, CDD is increasing over Eldoret region indicating that the number of days receiving rainfall amounts that are less than 1 mm are increasing.

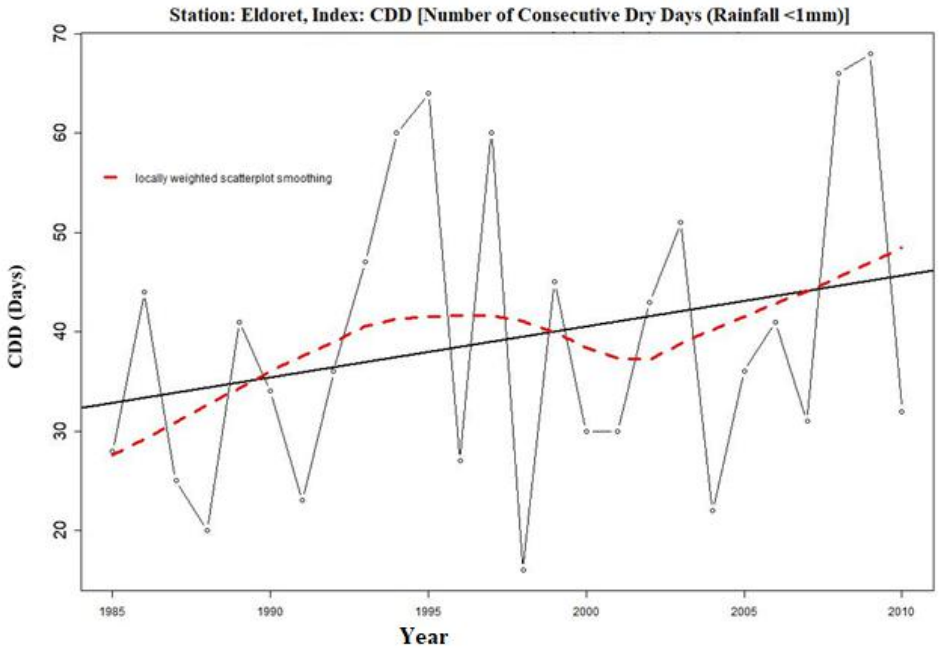

Figure 33: Trends in the Number of Consecutive Dry Days over Eldoret

Figures 34, 35, 36, and 37 also suggest that the number of consecutive dry days are increasing over Kakamega, Kericho, and Kisii respectively. However, the graphical model of this index is inconclusive over Kitale.

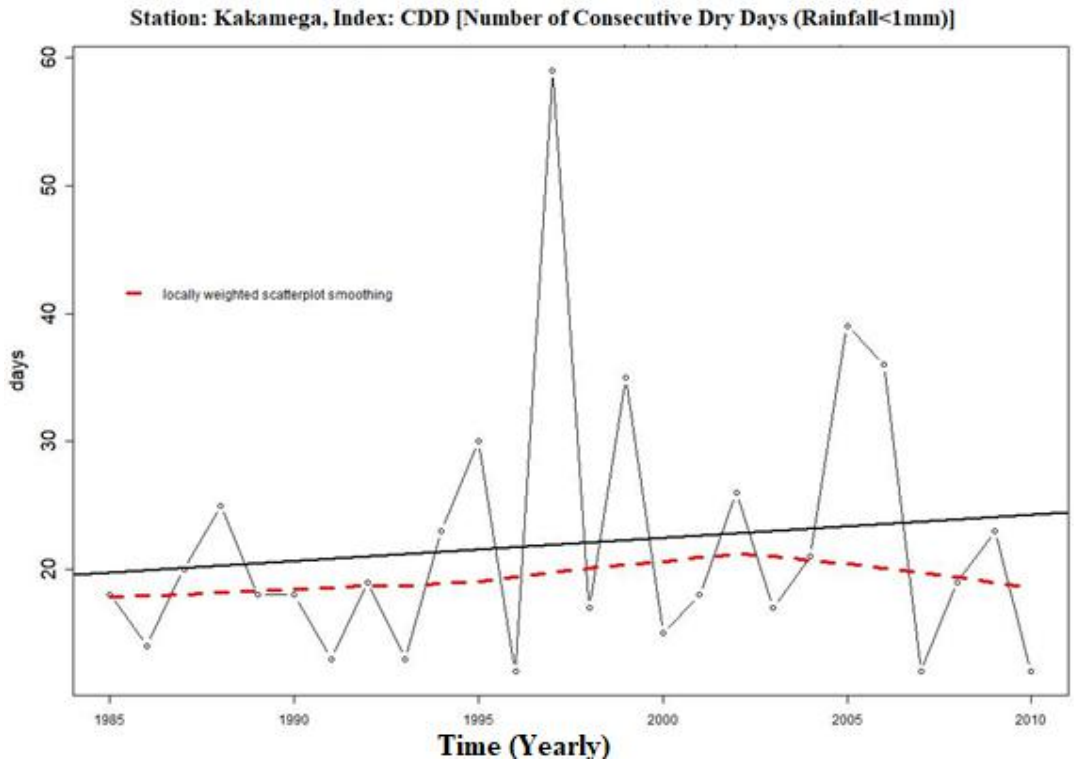

Figure 34: Graphical Representation of CDD Trends over Kakamega

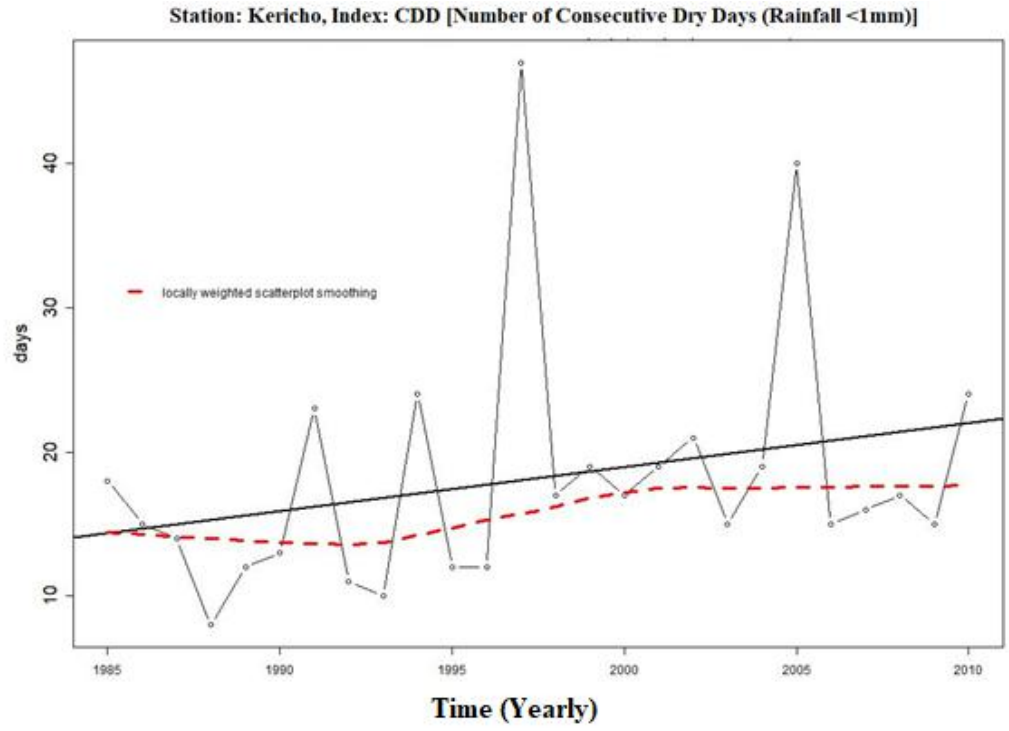

Figure 35:Graphical Representation of CDD Trends over Kericho

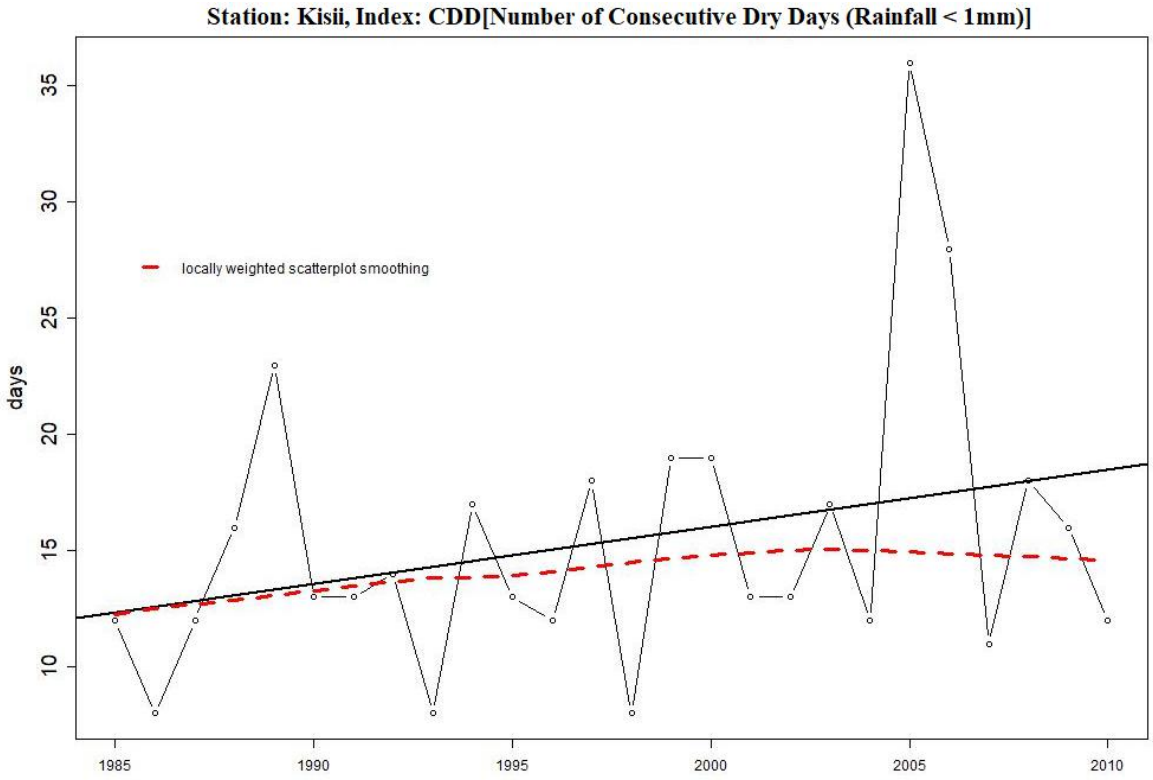

Figure 36:Graphical Representation of CDD Trends over Kisii

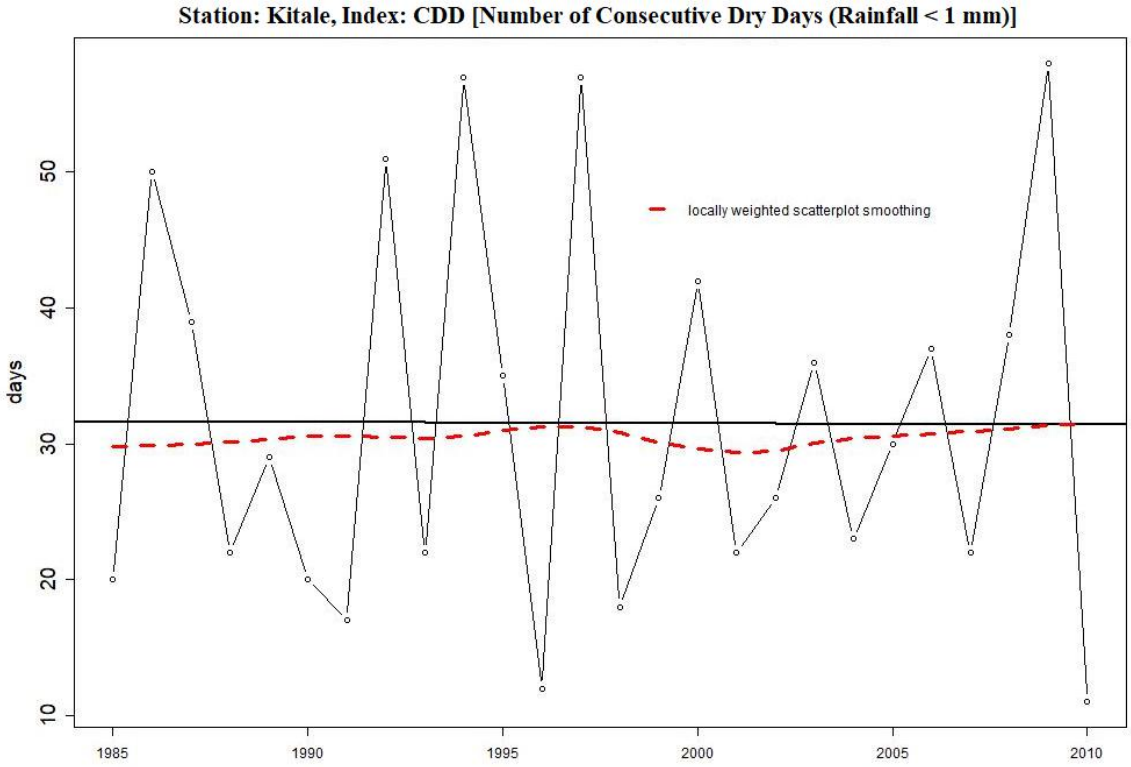

Figure 37:Graphical Representation of CDD Trends over Kitale

The identified increment in the number of consecutive dry days is indicative of increasing temperatures which results in suppressed rainfall amounts. Additionally, increased temperatures confounded with increased CDD may account for the shortening of the LGPs. Following the constraints in moisture and thermal resources over the zone, it became imperative to assess the monthly distribution of temperature and rainfall in a climatological sense using Walter & Leith Climate diagrams.

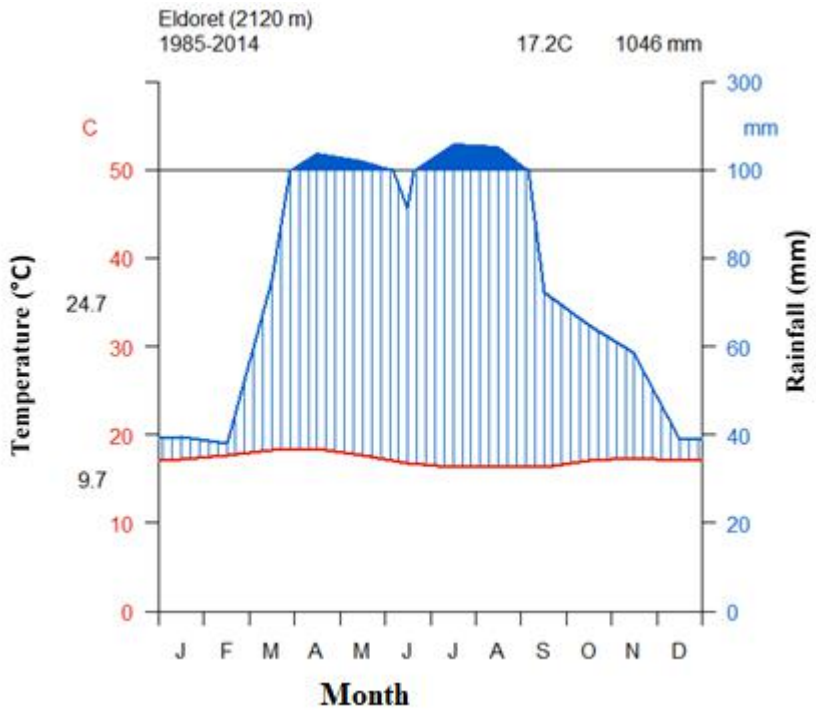

Figure 38: Climate Diagram Showing Moisture Deficit and Surplus and Temperature Limits for Eldoret Region

The diagrams suggest that Kitale has moisture deficit between January and February. However, it is wet between March and November, and it receives the least annual rainfall among the five areas (1266mm). The diagram also suggests that the maximum, optimum and minimum temperature limits over Kitale are 28.5°C, 19.1°C and 11.4°C (Figure 40). Similarly, Eldoret tends to be dry between February and March but wet between March and November with an annual rainfall of 1921 mm. The maximum, optimum and minimum temperature limits over Eldoret are 29.3°C, 20.8°C, and 13.7°C respectively (Figure 38). Kericho (Figure 41) and Kisii (Figure 42) are wet throughout the year with annual rainfall totals of 1974mm and 2068 mm although Kericho is comparatively cooler because of its maximum, optimum and minimum temperature limits of 25.9°C, 17.7°C and 10.9°C against 26.2°C, 20.3°C and 14.8°C limits

observed over Kisii. However, as temperatures increase over the zone, these limits are likely to rise making the region suitable for agricultural production and practices other than the current ones.

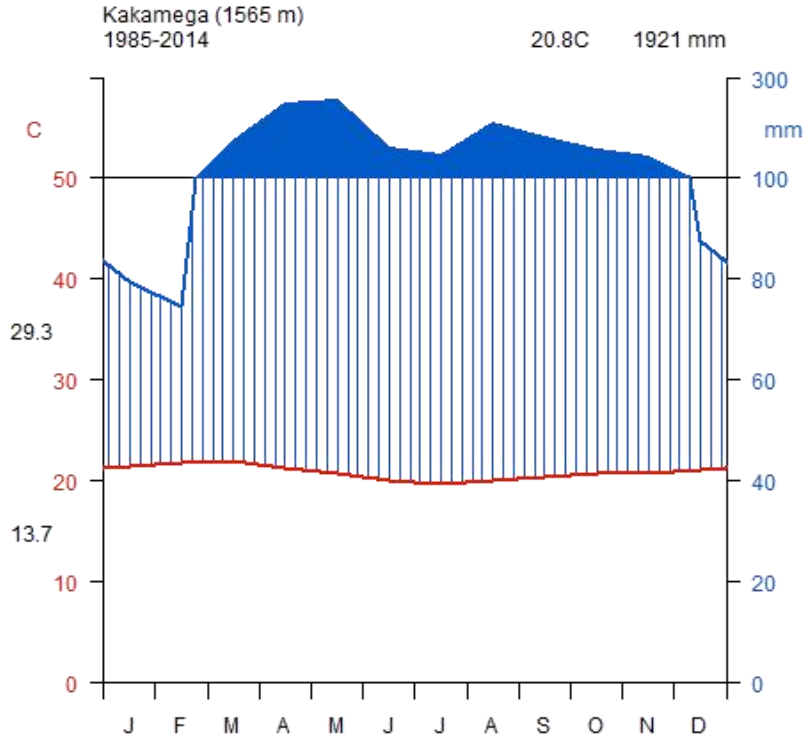

Figure 39: Climate Diagram Showing Moisture Deficit and Surplus and Temperature Limits for Kakamega Region

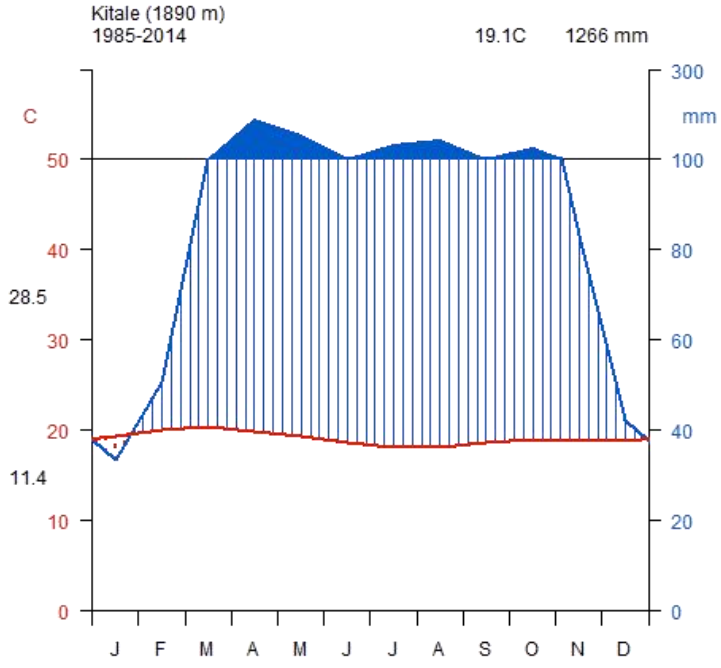

Figure 40: Climate Diagram Showing Moisture Deficit and Surplus and Temperature Limits for Kitale Region

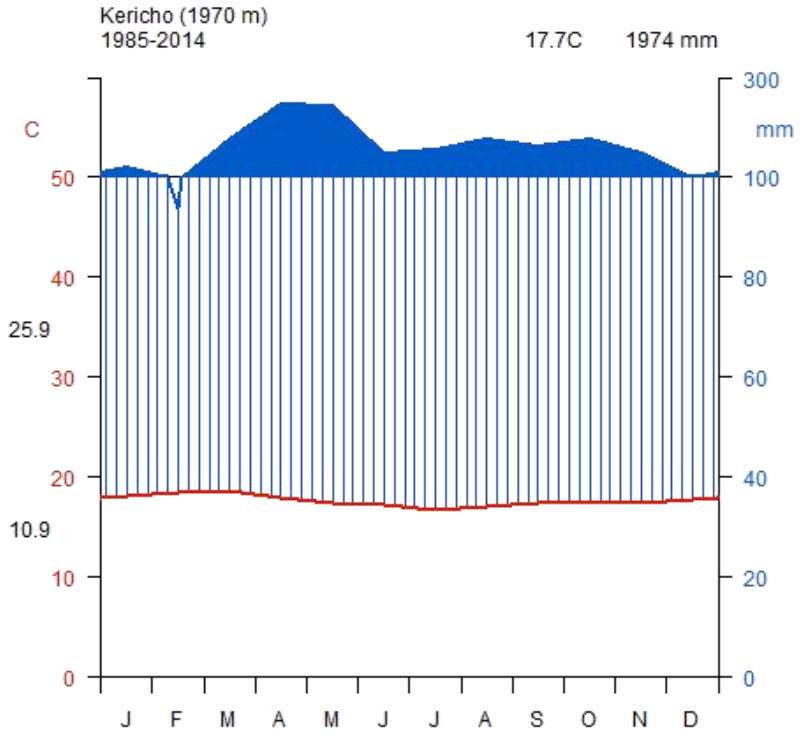

Figure 41: Climate Diagram Showing Moisture Deficit and Surplus and Temperature Limits for Kericho Region

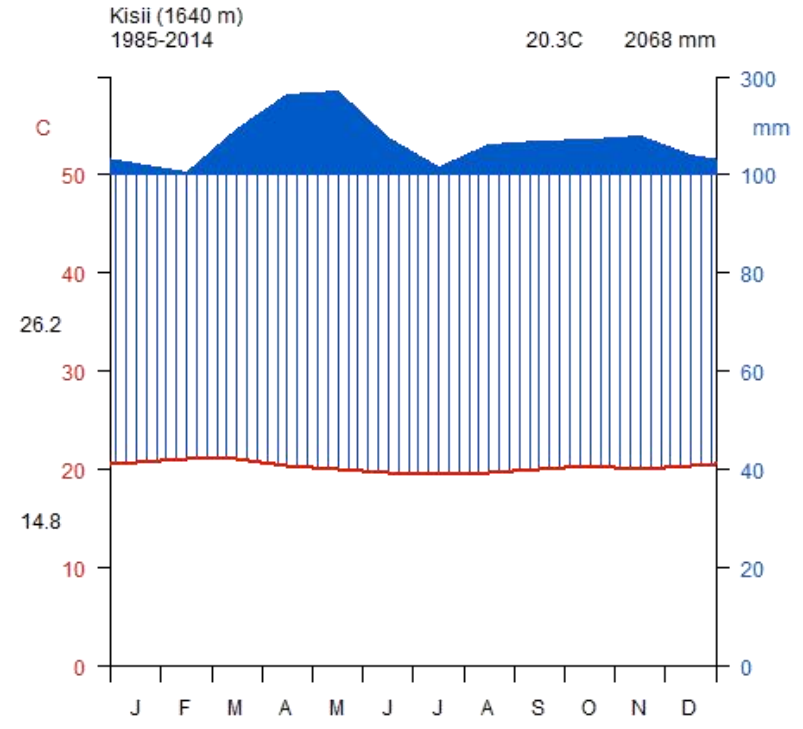

Figure 42: Climate Diagram Showing Moisture Deficit and Surplus and Temperature Limits for Kisii Region

CHAPTER FIVE: SUMMARY, CONCLUSIONS AND RECOMMENDATIONS

5.1 Introduction

The chapter summarizes and internalizes the findings of each specific objectives, draws inferences establishing climate change as a stressor, and presents recommendations based on the inferences and the findings. Hence, the chapter has summary, conclusion, and recommendation sections.

5.2 Summary of Study Findings

Temperatures (mean, maximum, and minimum) have significant monotonic upward trends over the study area suggesting that near surface temperatures are increasing. Additionally, trend components of the temperatures series revealed significant variations besides the random components. The change in trend and variability are the key climate loads that affect the thermal resources over the zone. Rainfall over Kitale showed a significant monotonic upward trend while rainfall over Kakamega and Kericho revealed significant downward trends. Kisii had no rainfall trends, and this could be ascribed to the tendencies of the region being wet because of its proximity to Lake Victoria and orographic advantages.

The variations and changes detected in both rainfall and temperature data reflected changes of moisture and thermal regimes over the zone. In specific terms, the GDD sum increased at the rate of 5 heat units per year, and it averaged 2639.1 heat units for a 10°C base temperature. The GDD sum increased at the rates of 10 heat units per year over Kakamega and Kericho, 12 heat units per year over Kitale and reduced at the rate of 3 heat units over Kisii. Spatial differentiation was clear as Eldoret and Kericho tended to have GDD sum averaging around 2700 heat units, while Kakamega, Kitale, and Kisii have GDD sum averaged about 3000 heat units. However, the temporal evolution suggested an upward increasing trend () in GDD sum over the region except Kisii for all the three base temperatures.

Indifference emerged while exploring rainfall because Kitale experienced increased rainfall over the study period while Kericho and Kakamega experienced reduced rainfall. However, the amounts received were highly variable across the five stations with Eldoret and Kitale receiving annual rainfall amounts that were less than 1000 mm during certain years and having moisture

characteristics of Zone III. Kisii, Kitale, and Kericho received annual rainfall amounts that exceeded the 1600 mm limit and as a result had Zone I moisture characteristics. The moisture index also confirmed that the Zone transitions between semi-humid (over Eldoret and Kitale) and per-humid (over Kisii, Kakamega, and Kericho). Furthermore, using a number of consecutive dry days and the length of the growing period revealed significant trends in the moisture regime. The CDD index suggested that dry spells tend to lengthen over the region and this is likely to affect the potential of the area. Conversely, the LGP results suggest that the Zone tends to have two distinct seasons although Kisii tends to have one season in most years. Eldoret and Kitale have a more persistent second season although the average LGPs suggest moisture constraints. The temperature limits (maximum, optimum, and minimum) for vegetative growth that the climate diagrams revealed confirmed that the zone has thermal and moisture homogeneity. The diagrams suggest that Eldoret and Kitale transitions to semi-arid conditions between January and March during some years. Additionally, the diagrams indicate that the region support crop growth cycles that lie between March and November. However, any increase in temperature will affect the limits and change the production characteristics of the zone. Moreover, the resultant variations in both moisture and thermal resources can impose pest and diseases and workability constraints. Specifically, increasing GDD sum can result in hybrid and crop variety selection challenges.

5.3 Conclusion

Rainfall and temperatures over the zone are highly variable with mean, maximum, and minimum temperatures increasing and rainfall increasing over Kitale and Eldoret but decreasing over Kakamega and Kericho. More so, the changes and variations in maximum temperatures influence changes and variations in rainfall while aggregated changes and variations in both affect thermal (GDD sum) and moisture resources (MI, LGP, CDD). Increasing temperatures results in increases in cumulated GDD that induce abiotic suitability and disease challenges. Specifically, increased GDD sum implies accelerated plant growth and development so that the findings of this study suggest that the zone has likely weed challenges. Besides, the increasing GDD sum also suggest accelerated rates development of pests and diseases. Finally, the GDD sum variations results in variations in the length of growing season, which can be problematic when it comes to selecting hybrid and crop varieties suitable for the zone. Selection of poor hybrid and crop varieties can also account for harvest failures over the zone. Furthermore,

increasing CDD, shortening of LGPs alongside decreasing rainfall are indicative of moisture stress, silk drying in maize growing areas, and dry/ compaction in cassava growing areas.
However, increased rainfall can also cause abiotic suitability challenges such as stem borer infestations, leaf spot, leaf blight, steak virus infestations as well as wet produce. These suitability issues suppress crops performance, reduce land potentials, and are consequence of climate loads (climate change and variability). Such consequences cause stress in a high potential agriculture zone in Kenya because of the constraints that they bring along. The stress in the high potential zone can account for the rampant food insecurity and food crisis in Kenya since the zone accounts for a larger percentage of food and cash crops in the country.

5.4 Recommendations

The area studied accounts for most of the food and cash production in Kenya, and therefore plays an important role in ensuring food availability and guaranteeing food access. However, the recent food insecurity and crisis that Kenya faces confirms the country's vulnerability to climate change. As this study has shown, climate change is a stress factor in the zone and it is prudent that some measures are taken to reduce overdependence on natural-resource based livelihood income sources, to plan for limited resources and use them effectively in adapting and mitigating climate change, to develop national level planning tools for preparation, management and recovery from weather-related crises and hazards. Regarding these concerns, the following are recommended.

Firstly, farm level adjusted responses to changes in thermal and moisture resources can help in managing production within the zone and assuring against food unavailibilty and inacessbility. Specifically, farmers can use information on GDD sum and LGP to switch to crops that match the prevailing crop growth conditions.

Secondly, there is a need for semi-empirical weather-based financial derivates to help protect agricultural producers and consumers against exteme price fluactuations. The government can include a pricepolicy for agricultural harvest in its risk management framework to protect both farmers and the common citizen from extreme prices.

Finally, the Ministry of Agriculture, Kenya Meteorological Service office, and other bodies such as the National Drought Management Authority should collobarate and develop an agriculture-

based resource management domain for national planning and resource allocation for both climate change mitigation and food production improvement.

References

Adler P.B., Leiker J., & Levine J.M. 2009. Direct and Indirect Effects of Climate Change on a Prairie Plant Community. *PLoS ONE 4*(9): e6887. doi: 10.1371/journal.pone.0006887

Ainsworth, E.A. & Ort, D.R. 2010. How Do We Improve Crop Production in a Warming World? *Plant Physiology, 154*(2), 526-30.

Alexander, L., Yang, H. & Perkins, S. 2013. Background Material to ClimPACT: Indices and Software. *World Climate Programme*.

Aldrian, E., & Susanto, R. 2003. Identification of three Dominant Rainfall Regions within Indonesia and their Relationship to Sea Surface Temperature. *International Journal of Climatology*, *23*(12), 1435-1452.

Amaechi, C. F., & Ekene, B. 2016. Gas flaring: Carbon dioxide contribution to global warming. *Journal of Applied Science & Environmental Management,20*(2), 309-317. doi: http://dx.doi.org/10.4314/jasem.v20i2.11

Awuor, V.O. & Ogola, J.S., 1997. Effects of climate change on agriculture. In *Potential impacts of climate change in Kenya*.

Azur, M.J., Stuart, E.A., Frangakis, C. & Leaf, P.J. 2011. Multiple Imputation by Chained Equations: What is it and How does it Work? *International Journal of Methods in Psychiatric Research*, *20*(1), 40-49.

Back, L., Russ, K., Liu, Z., Inoue, K., Zhang, J., & Otto-Bliesner, B. (2013). Global hydrological cycle response to rapid and slow global warming. *Journal of Climate*, *26*(22), 8781-8786

Bandoc, G. 2012. Estimation of the Annual and Inter-Annual Variation of Potential Evapotranspiration. In *Evapotranspiration-Remote Sensing and Modeling*. Intech.

Boitt, M.K. & Pellikka, P. 2014. Modelling the Impacts of Climate Change on Agro-Ecological Zones–a Case Study of Taita Hills, Kenya. *Universal Journal of Geoscience*, *2*(6), 172-179.

Black, E. 2005. The relationship between Indian Ocean sea–surface temperature and East African rainfall. *Philosophical Transactions of the Royal Society of London A: Mathematical, Physical and Engineering Sciences*, *363*(1826), 43-47.

Bryan, E., Ringler, C., Okoba, B., Roncoli, C., Silvestri, S. and Herrero, M., 2013. Adapting agriculture to climate change in Kenya: Household strategies and determinants. *Journal of environmental management, 114*, 26-35.

Bunn, C., Läderach, P., Jimenez, J.G., Montagnon, C. & Schilling, T. 2015, Multiclass Classification of Agro-Ecological Zones for Arabica Coffee: An Improved Understanding of the Impacts of Climate Change, *PLoS One, (10)* 10. 36-43.

Durre, I., Menne, M. J., Gleason, B. E., Houston, T. G., & Vose, R. S. 2010. Comprehensive Automated Quality Assurance of Daily Surface Observations. *Journal of Applied Meteorology and Climatology*, *49*(8), 1615-1633.

Cao, L., Bala, G., Zheng, M. & Caldeira, K. 2015. Fast and slow climate responses to CO2 and solar forcing: A linear multivariate regression model characterizing transient climate change, *Journal of Geophysical Research Atmospheres, 120*(23), 12,037-12,053.

Chavance, M., 2002. Handling of Missing Data. In *Statistical Methods for Quality of Life Studies*. Springer: US, 303-305.

Clavero, M., Villero, D. & Brotons, L. 2011. Climate Change or Land Use Dynamics: Do We Know What Climate Change Indicators Indicate? *PLoS One,* 6(4).

Cong, R.G. and Brady, M., 2012. The interdependence between rainfall and temperature: copula analyses. *The Scientific World Journal*, *2012*.

Dobrynin, M., Murawski, J., Baehr, J. & Ilyina, T. 2015. Detection and Attribution of Climate Change Signal in Ocean Wind Waves, *Journal of Climate, 28*(4), 1578-1591.

Fan, S.A. and Rosegrant, M.W., 2016. *Investing in agriculture to overcome the world food crisis and reduce poverty and hunger*. Washington, DC: IFPRI (International Food Policy Research Institute).

Fangfang, Z., Zongxue, X. & Junxiong, H., 2007. Long-term trend and abrupt change for major climate variables in the upper Yellow River Basin. *Acta Meteorologica Sinica*, *21*(2), 204-210.

Fay, P.A., Carlisle, J.D., Knapp, A.K., Blair, J.M. & Collins, S.L. 2003. Productivity responses to altered rainfall patterns in a C4-dominated grassland, *Oecologia, 137*(2), pp. 245-51.

Fischer, G., Frohberg, K., Parry, M.L. & Rosenzweig, C., 1996. Impacts of potential climate change on global and regional food production and vulnerability. In *Climate change and world food security* (pp. 115-159). Springer Berlin Heidelberg.

Fischer, G., Van Velthuizen, H.T. and Prieler, S., 2001. Assessment of potential productivity of tree species in China, Mongolia and the Former Soviet Union: Methodology and Results. *IIASA Research Report*. IIASA, Laxenburg, Austria: R-01-015.

Fischer, G., Shah, M.M. and Van Velthuizen, H.T., 2002(a). Climate Change and Agricultural Vulnerability.

Fischer, G., Velthuizen, H.T., Shah, M.M. & Nachtergaele, F.O., 2002(b). Global agro-ecological assessment for agriculture in the 21st century: Methodology and Results. *IIASA Research Report*. IIASA, Laxenburg, Austria: RR-02-02.

Fischer, G., Mahendra, S., Francesco N. T, & Harrij V. 2005. Socio-Economic and Climate Change Impacts on Agriculture: An Integrated Assessment, 1990–2080. *Philosophical Transactions of the Royal Society of London B: Biological Sciences* 360(1463), 2067-2083.

Fischer, G., Shah, M., van Velthuizen, H., & Nachtergaele, F. 2006. *Agro-ecological zones assessments*. IIASA, Laxenburg, Austria: RP-06-03.

Fischer, G., Nachtergaele, F.O., Prieler, S., Teixeira, E., Tóth, G., Van Velthuizen, H., Verelst, L. and Wiberg, D., 2012. Global Agro-ecological Zones (GAEZ v3. 0)-Model Documentation.

Gommes, R., 2007. Non-Parametric Crop Yield Forecasting. In *Proceedings of the 2nd International Workshop on Crop and Rangeland Monitoring in Eastern Africa*.

Goossens, C. & Berger, A., 1987. How to recognize an abrupt climatic change? In *Abrupt Climatic Change* (pp. 31-45). Springer Netherlands.

Guijarro, J. A., & Maintainer, J. A. 2016. Package 'Climatol'

Guijarro, J. A. 2011. User's Guide to Climatol. An R Contributed Package for Homogenization of Climatological Series. *Report; State Meteorological Agency.* Balearic Islands Office, Spain.

Guolin, F.E., Zhiqiang, G.O. & Rong, Z.H.I., 2010. Latest advances in climate change detection techniques. *Journal of Meteorological Research, 24*(1), 1-16.

Guhathakurta, P. & Saji, E. 2013. Detecting changes in rainfall pattern and seasonality index vis-à-vis increasing water scarcity in Maharashtra, *Journal of Earth System Science, 122*(3), 639-649.

Habeeb, D., Vargo, J. & Stone, B. 2015. Rising Heat Wave Trends in large US Cities. *Natural Hazards, 76*(3), 1651-1665.

Habtemariam, L.T., Gandorfer, M., Kassa, G.A. & Heissenhuber, A. 2016. Factors Influencing Smallholder Farmers' Climate Change Perceptions: A Study from Farmers in Ethiopia, *Environmental management, 58*(2), 343-358.

Hasselmann, K. 1997. Multi-pattern fingerprint method for detection and attribution of climate change, *Climate Dynamics, 13*(9), 601-611.

He, W., Wan, S., Jiang, Y., Jin, H., Zhang, W., Wu, Q. and He, T., 2013. Detecting abrupt change on the basis of skewness: numerical tests and applications. *International journal of climatology, 33*(12), 2713-2727.

Hegerl, G.C., Karl, T.R., Allen, M., & Bindoff, N.L. 2006. Climate Change Detection and Attribution: Beyond Mean Temperature Signals*, Journal of Climate, 19*(20), 5058-5077.

Herold, N., & Alexander, L. 2017. Heatwave and Drought Indices Recommended by the ET-SCI.

Herrero, M., Ringler, C., van de Steeg, J.A., Thornton, P.K., Zhu, T., Bryan, E., Omolo, A., Koo, J. and Notenbaert, A.M.O., 2010. Climate variability and climate change and their impacts on Kenya's agricultural sector.

Huho, J.M., Ngaira, J.K.W., Ogindo, H.O. & Masayi, N. 2012. The Changing Rainfall Pattern and the Associated Impacts on Subsistence Agriculture in Laikipia East District, Kenya, *Journal of Geography and Regional Planning, 5*(7), 198-206.

Hulme, M. 2014. Attributing Weather Extremes to 'Climate Change': A Review Progress in *Physical Geography, 38*(4), 499-511.

Ibrahim, S.B., Ayinde, I.A. & Arowolo, A.O. 2015. Analysis of arable crop farmers' awareness to causes and effects of climate change in south western Nigeria, *International Journal of Social Economics, 42* (7), 614-628.

Imbers, J., Lopez, A., Huntingford, C. & Allen, M. 2014. Sensitivity of Climate Change Detection and Attribution to the Characterization of Internal Climate Variability, *Journal of Climate, 27*(10), 3477-3491.

Inbar, M., Doostdar, H., & Mayer, R. T. 2001. Suitability of Stressed and Vigorous Plants to Various Insect Herbivores. *Oikos*, *94*(2), 228-235.

Jabloun, M. D., & Sahli, A. 2008. Evaluation of FAO-56 Methodology for Estimating Reference Evapotranspiration Using Limited Climatic Data: Application to Tunisia. *Agricultural water management*, *95*(6), 707-715.

Jätzold, R. & Kutsch, H., 1982. Agro-ecological zones of the tropics, with a sample from Kenya. *Der Tropenlandwirt-Journal of Agriculture in the Tropics and Subtropics*, *83*(1), 15-34.

Laswai, H., 2010. Food crisis in Africa. *African Journal of Food, Agriculture, Nutrition and Development*, *10*(1).

Kabubo-Mariara, J, & Kabara, M. 2015. Climate Change and Food Security in Kenya. *The environment for Development Centers: Discussion Paper Series.*

Kala, N., Kurukulasuriya, P., & Mendelsohn, R., 2012. The impact of climate change on agro-ecological zones: evidence from Africa. *Environment and Development Economics 17*(6), 663-687. doi:10.1017/S1355770X12000241

Kang, S., Xu, Y., You, Q., Flügel, W.A., Pepin, N. & Yao, T., 2010. Review of climate and cryospheric Change in the Tibetan Plateau. *Environmental Research Letters, 5*(1), 015101.

Karl, T.R. & Easterling, D.R. 1999. Climate extremes: Selected Review and Future Research Directions. *Climatic Change, 42*(1), 309-325.

Kato, T., Ito, A. & Kawamiya, M. 2009. Multiple temporal scale variability during the twentieth century in global carbon dynamics simulated by a coupled climate-terrestrial carbon cycle model, *Climate Dynamics, 32*(7-8), 901-923.

Katz, R. W., & Brown, B. G. 1992. Extreme events in a changing climate: variability is more important than averages. *Climatic change*, *21*(3), 289-302.

Kerr, R.A. 2001. Rising global temperature, rising uncertainty, *Science, 292*(5515), 192-194.

Kirschbaum, M.U. 2004. Soil respiration under prolonged soil warming: are rate reductions caused by acclimation or substrate loss? *Global Change Biology*, *10*(11), pp.1870-1877.

Koster, R. D., Schubert, S., Pozzi, W., Mo, K., Wood, E. F., Stahl, K. & Pulwarty, R. 2015.

Körner, C. & Basler, D., 2010. Phenology under global warming. *Science*, *327*(5972), pp.1461-1462. Technical Report Series on Global Modeling and Data Assimilation. *GDIS Workshop Report (41).*

Kotir, J.H., 2011. Climate change and variability in Sub-Saharan Africa: a review of current and future trends and impacts on agriculture and food security. *Environment, Development and Sustainability, 13*(3), 587-605.

Kreyling, J., Wenigmann, M., Beierkuhnlein, C. & Jentsch, A. 2008. Effects of Extreme Weather Events on Plant Productivity and Tissue Die-Back are Modified by Community Composition, *Ecosystems, 11*(5), 752-763.

Kurukulasuriya, P. & Mendelsohn, R.O., 2008. How will climate change shift agro-ecological zones and impact African Agriculture? *World Bank Policy Research Working Paper Series.*

Lackner, B.C., Steiner, A.K., Kirchengast, G. & Hegerl, G.C. 2011. Atmospheric Climate Change Detection by Radio Occultation Data Using a Fingerprinting Method*, Journal of Climate, 24*(20), 5275-5291.

Lean, J. L., & Rind, D. H. 2009. How will earth's surface temperature change in future decades? *Geophysical Research Letters, 36*(15) doi: http://dx.doi.org/10.1029/2009GL038932

Leclère, D., Havlík, P., Fuss, S., Schmid, E., Mosnier, A., Walsh, B., Valin, H., Herrero, M., Khabarov, N. and Obersteiner, M., 2014. Climate change induced transformations of agricultural systems: insights from a global model. *Environmental Research Letters, 9*(12), p.124018.

Lee, T.C.K., Zwiers, F.W., Hegerl, G.C., Zhang, X. & Tsao, M. 2005. A Bayesian Climate Change Detection and Attribution Assessment, *Journal of Climate, 18*(13), 2429-2440.

Leroy, S.S. & Anderson, J.G. 2010. Optimal Detection of Regional Trends Using Global Data, *Journal of Climate*, *23*(16), 4438-4446.

Li, Y., Ding, Y., & Li, W. (2017). Interdecadal variability of the Afro-Asian summer monsoon system. *Advances in Atmospheric Sciences, 34*(7), 833-846. doi: http://dx.doi.org/10.1007/s00376-017-6247-7

Lin, T.H., 2010. A Comparison of Multiple Imputation with EM Algorithm and MCMC Method for Quality of Life Missing Data. *Quality & Quantity*, *44*(2), 277-287.

Lin, Y., Liu, A., Ma, E. & Zhang, F. 2013. Impacts of Future Climate Changes on Shifting Patterns of the Agro-Ecological Zones in China. *Advances in Meteorology*, 1-9.

Liu, Q., Wan, S. & Gu, B. 2016. A Review of the Detection Methods for Climate Regime Shifts. *Discrete Dynamics in Nature and Society*, doi: http://dx.doi.org/10.1155/2016/3536183

Li, Y., Wang, a., & Zhang, C. (2014). An abrupt centennial-scale drought event and mid-Holocene climate change patterns in monsoon marginal zones of east Asia. *PLoS One*, *9*(3) doi: http://dx.doi.org/10.1371/journal.pone.0090241

Luo, Q. 2016. Necessity for post-processing dynamically downscaled climate projections for impact and adaptation studies. *Stochastic Environmental Research and Risk Assessment, 30*(7), pp. 1835-1850.

Luo, Q. & Yu, Q. 2012. Developing higher resolution climate change scenarios for agricultural risk assessment: progress, challenges and prospects, *International journal of biometeorology*, *56*(4), 557-68.

Matsui, T., Omasa, K., & Horie, T. 1997. High temperature-induced Spikelet Sterility of Japonica Rice at Flowering in Relation to Air Temperature, Humidity and Wind Velocity Conditions. *Japanese journal of crop science*, *66*(3), 449-455.

Mattson, W. J., & Haack, R. A. (1987). The role of drought in outbreaks of plant-eating insects. *Bioscience*, *37*(2), 110-118.

Mendelsohn, R. & Dinar, A., 2009. Land use and climate change interactions. *Annual Review Resource Economics 1*(1), 309-332.

Mayowa, O.O., Pour, S.H., Shahid, S., Mohsenipour, M., Harun, S.B., Heryansyah, A. & Ismail, T. 2015. Trends in rainfall and rainfall-related extremes in the east coast of peninsular Malaysia, *Journal of Earth System Science, 124*(8), 1609-1622.

Milfont, T.L., Evans, L., Sibley, C.G., Ries, J. & Cunningham, A. 2014. Proximity to Coast Is Linked to Climate Change Belief, *PLoS One, (9)*7, 103180-103-188.

Mika, J. 2012, Weather and Climate Extremes in Light of the IPCC SREX (2011) and Beyond, *Aerul si Apa.Componente ale Mediului*, 25-32.

Min, S., Zhang, X., Zwiers, F., Shiogama, H., Tung, Y. & Wehner, M. 2013. Multimodal Detection and Attribution of Extreme Temperature Changes, *Journal of Climate, 26*(19), 7430-7451.

Montzka, S. A., Dlugokencky, E. J., & Butler, J. H. (2011). Non-CO_2 greenhouse gases and climate change. *Nature, 476*(7358), 43-50.

Mukhala, E. & Hoefsloot, P. 2004. *Agrometshell Manual*. FAO, Rome.

Paeth, H. & Mannig, B. 2013. On the added value of regional climate modeling in climate change assessment, *Climate Dynamics, 41*(3-4), 1057-1066.

Parry, M.L., Rosenzweig, C., Iglesias, A., Livermore, M. & Fischer, G., 2004. Effects of climate change on global food production under SRES emissions and socio-economic scenarios. *Global Environmental Change,14*(1), 53-67.

Pigott, T.D. 2001. A Review of Methods for Missing Data. *Educational Research and Evaluation*, *7*(4), 353-383.

Pingale, S., Adamowski, J., Jat, M. & Khare, D. 2015. Implications of spatial scale on climate change assessments, *Journal of Water and Land Development, 26* (1), 37-55.

Pohlert, T. (2016). Non-parametric trend tests and change-point detection. *CC BY-ND*, *4*.

Potopová, V., Zahradníček, P., Türkott, L., Štěpánek, P., & Soukup, J. 2015. The effects of climate change on variability of the growing seasons in the Elbe River Lowland, Czech Republic. *Advances in Meteorology*, *2015*.

Pretty, J. and Bharucha, Z.P., 2015. Integrated pest management for sustainable intensification of agriculture in Asia and Africa. *Insects*, *6*(1), pp.152-182.

Ranjitkar, S., Sujakhu, N.M., Merz, J., Kindt, R., Xu, J., Matin, M.A., Ali, M. & Zomer, R.J. 2016. Suitability Analysis and Projected Climate Change Impact on Banana and Coffee Production Zones in Nepal, *PLoS One, 11*(9), 172-181.

Rajeevan, M., Pai, D. S., & Thapliyal, V. 1998. Spatial and temporal relationships between global land surface air temperature anomalies and Indian summer monsoon rainfall. *Meteorology and Atmospheric Physics*, *66*(3), 157-171.

Raut, B.A., Jakob, C. & Reeder, M.J. 2014. Rainfall Changes Over Southwestern Australia and Their Relationship to the Southern Annular Mode and ENSO, *Journal of Climate, 27*(15), 5801-5814.

Ribes, A., Azaïs, J. & Planton, S. 2010. A method for regional climate change detection using smooth temporal patterns, *Climate Dynamics, 35*(2-3), 391-406.

Ripley, E. A. 1987. Plotting Climate Diagrams with a Microcomputer. *Bull. Climatology. URL http://www. cmos. ca/CB/cb210303. pdf*.

Rosenzweig, C. & Parry, M.L., 1994. Potential impact of climate change on world food supply. *Nature*, *367*(6459), 133-138.

Sachs, J., Remans, R., Smukler, S., Winowiecki, L., Andelman, S.J., Cassman, K.G., Castle, D., DeFries, R., Denning, G., Fanzo, J. & Jackson, L.E., 2010. Monitoring the world's agriculture. *Nature, 466*(7306), 558-560.

Samways, M. J. (1989). Climate Diagrams and Biological Control: An Example from the Aerography of the Ladybird. *Journal of Biogeography*, 345-351.

Seo, S.N. & Mendelsohn, R., 2008. A Ricardian analysis of the impact of climate change on South American farms. *Agricultura técnica*, *68*(1), 69-79.

Seo, S.N., Mendelsohn, R., Dinar, A., Hassan, R. & Kurukulasuriya, P. 2009, A Ricardian Analysis of the Distribution of Climate Change Impacts on Agriculture across Agro-Ecological Zones in Africa. *Environmental and Resource Economics, 43*(3), 313-332.

Seo, S.N., 2014. Evaluation of the Agro-Ecological Zone methods for the study of climate change with micro farming decisions in sub-Saharan Africa. *European Journal of Agronomy, 52*, 157-165.

Shi, P., Sun, S., Gong, D. & Zhou, T. 2016. World Regionalization of Climate Change (1961-2010), *International Journal of Disaster Risk Science, 7*(3), 216-226.

Shukla, R., Chakraborty, A. & Joshi, P.K. 2017. Vulnerability of Agro-Ecological Zones in India Under the Earth System Climate Model Scenarios. *Mitigation and Adaptation Strategies for Global Change*, *(22)*3, 399-425.

Stott, P. A., & Jones, G. S. 2009. Variability of high latitude amplification of anthropogenic warming. *Geophysical Research Letters, 36*(1) doi: http://dx.doi.org/10.1029/2009GL037698

Sombroek, W.G., Braun, H.M., & Van der Pouw, B.J.A., 1982. *Exploratory soil map and agro-climatic zone map of Kenya, 1980. Scale 1: 1,000,000*. Kenya Soil Survey.

Subedi, A. & Chávez, J.L., 2015. Crop Evapotranspiration (ET) Estimation Models: A Review and Discussion of the Applicability and Limitations of ET Methods. *Journal of Agricultural Science, 7*(6), 50-57.

Tait, L.W. & Schiel, D.R. 2013. Impacts of Temperature on Primary Productivity and Respiration in Naturally Structured Macroalgal Assemblages, *PLoS One, 8* (9).

Tol R.S.J., 2002. Estimates of the damage cost of climate change. *Environment and Resource Economics 21,* 47–73.

Trnka, M., Eitzinger, J., Hlavinka, P., Dubrovsky, M., Semerádová, D., Stepanek, P., ... & Formayer, H. 2009. Climate-driven Changes of Production Regions in Central Europe. *Plant and Soil*, *521*, 257-266.

Vasseur, D.A., DeLong, J.P., Gilbert, B., Greig, H.S., Harley, C.D., McCann, K.S., Savage, V., Tunney, T.D. and O'Connor, M.I., 2014. Increased temperature variation poses a greater risk to species than climate warming. *Proceedings of the Royal Society of London B: Biological Sciences*, *281*(1779), p.20132612.

Verpoorten, M., Arora, A., Stoop, N. and Swinnen, J., 2013. Self-reported food insecurity in Africa during the food price crisis. *Food Policy*, *39*, pp.51-63.

Waha, K., Zipf, B., Kurukulasuriya, P., & Hassan, R. M. (2016). An agricultural survey for more than 9,500 African households. *Scientific Data, 3*, 160020. doi: http://dx.doi.org/10.1038/sdata.2016.20

Wang, X.L. 2008. Penalized Maximal F Test for Detecting Undocumented Mean Shift Without Trend Change. *Journal of Atmospheric and Oceanic Technology*, *25*(3), 368-384.

Xu, C.Y. & Singh, V.P., 2001. Evaluation and generalization of temperature-based methods for calculating evaporation. *Hydrological processes*, *15*(2), pp.305-319.

Yildiz, H., Mermer, A., Aydoğdu, M., & Şimşek, O. 2015. Forecasting of Winter Wheat Yield for Turkey using Water Balance Model. In *Agro-Geoinformatics, 2015 Fourth International Conference*, 352-356, IEEE.

Yuan, Y.C., 2010. Multiple Imputation for Missing Data: Concepts and New Development (Version 9.0). *SAS Institute Inc, Rockville, MD*, *49*, 1-11.

Yu, R. & Li, J. 2012. Hourly Rainfall Changes in Response to Surface Air Temperature Over Eastern Contiguous China. *Journal of Climate, 25*(19), 6851-6861.

Yu, G., Schwartz, Z. & Walsh, J.E., 2009. Effects of Climate Change on the Seasonality of Weather for Tourism in Alaska. *Arctic, 62*(4), 443-457.

Zhang, Z. 2016. Missing data imputation: focusing on single imputation. *Annals of Translational Medicine*, *4*(1), 9. http://doi.org/10.3978/j.issn.2305-5839.2015.12.38

Zhang, X., Alexander, L., Hegerl, G.C., Jones, P., Klein, T.A, Peterson, T.C., Trewin, B., Zwiers F.W. 2011. Indices for Monitoring Changes in Extremes Based on Daily Temperature and Precipitation data. *WIREs Climate Change*, doi:10.1002/wcc.147.

Zhou, J., & Tung, K. 2013. Deducing multidecadal anthropogenic global warming trends using multiple regression analysis. *Journal of the Atmospheric Sciences, 70*(1), 3-8.

Ziska, L.H. 2014. Increasing Minimum Daily Temperatures Are Associated with Enhanced Pesticide Use in Cultivated Soybean along a Latitudinal Gradient in the Mid-Western United States, *PLoS One, 9*(6).

Appendices

Appendix 1: Pearl Script for Data Download

```
#!/usr/bin/perl -w
#############################################################################
# Perl Script to retrieve 3 online Data files of 'ds564.0',  #total 51.2M. This script uses 'wget' to
download data. #Highlight this script by Select All, Copy and Paste it into a file;
# make the file executable and run it on command line.
# You need pass in your password as a parameter to execute
# this script; or you can set an environment variable RDAPSWD
# if your Operating System supports it.
#############################################################################
Use strict;
my($syscmd,$vn,$opt,$i,@filelist); my$pswd=(@ARGV?$ARGV[0]:$ENV{RDAPSWD});
if(!$pswd){
print"\n Usage: $0 YourPassword\n\n"; exit1;
}
 openVN,"wget -V |"ordie'cannot find wget';
$vn=(<VN>=~/^GNU Wget (\d+)\.(\d+)/)?(100*$1+$2):109;
close(VN);
$syscmd=($vn>109?'wget --no-check-certificate':'wget'); $syscmd.=' -O Authentication.log --
save-cookies auth.rda_ucar_edu --post-data'
"=\"email=ouma.antony\@gmail.com&passwd=$pswd&action=login\" ".
'https://rda.ucar.edu/cgi-bin/login';
system($syscmd);
$opt='wget -N';
$opt.=' --no-check-certificate'if($vn>109);
 $opt.=' --load-cookies auth.rda_ucar_edu '. 'http://rda.ucar.edu/data/ds564.0/';
 @filelist=(
"v2.prcp-sprd.gz",
"v2.max-sprd.gz",
"v2.mean-sprd.gz", );
 for($i=0;$i<@filelist;$i++){
$syscmd=$opt.$filelist[$i];
print"$syscmd...\n"; system($syscmd);
}
system('rm -f auth.rda_ucar_edu Authentication.log');
exit0;
```

Appendix 2: Source Code for Decomposing the Time Series

```
#Timeseries Decomposition using STL
EldTm<-read.csv(file.choose(), header = TRUE, sep = ",")
EldTmts<- ts(EldTm, start = c(1985, 1, 1), end = c(2014, 12, 31),
frequency = 365)
EldTmts.stl<-stl(EldTmts, s.window="periodic")
EldTmTrend<-KakTmts.stl$time.series[, "trend"]
plot(EldTmts.stl)
dev.copy(png,'Timeseries Components of Mean Temperature over Eldoret.png')
dev.off()
KitTm<-read.csv(file.choose(), header = TRUE, sep = ",")
KitTmts<- ts(KitTm, start = c(1985, 1, 1), end = c(2014, 12, 31),
frequency = 365)
KitTmts.stl<-(KitTmts, s.window="periodic")
KitTmTrend<-KakTmts.stl$time.series[, "trend"]
plot(KitTmts.stl)
dev.copy(png,'Timeseries Components of Mean Temperature over Kitale.png')
dev.off()
KakTm<-read.csv(file.choose(), header = TRUE, sep = ",")
KakTmts<- ts(KakTm, start = c(1985, 1, 1), end = c(2014, 12, 31),
frequency = 365)
KakTmts.stl<-(KakTmts, s.window="periodic")
KakTmtsTrend<-KakTmts.stl$time.series[, "trend"]
plot(KakTmts.stl)
dev.copy(png,'Timeseries Components of Mean Temperature over Kakamega.png')
dev.off()
KisTm<-read.csv(file.choose(), header = TRUE, sep = ",")
KisTmts<- ts(KisTm, start = c(1985, 1, 1), end = c(2014, 12, 31),
frequency = 365)
KisTmts.stl<-(KisTmts, s.window="periodic")
KisTmTrendTrend<-KisTmts.stl$time.series[, "trend"]
plot(KisTmts.stl)
dev.copy(png,'Timeseries Components of Mean Temperature over Kisii.png')
dev.off()
KerTm<-read.csv(file.choose(), header = TRUE, sep = ",")
KerTmts<- ts(KerTm, start = c(1985, 1, 1), end = c(2014, 12, 31),
frequency = 365)
KerTmts.stl<-(KerTmts, s.window="periodic")
KerTmTrend<-KerTmtsTxts.stl$time.series[, "trend"]
plot(KerTmts.stl)
dev.copy(png,'Timeseries Components of Mean Temperature over Kerichp.png')
dev.off()
#Eldoret Tx
EldTx<-read.csv(file.choose(), header = TRUE, sep = ",")
EldTxts<- ts(EldTx, start = c(1985, 1, 1), end = c(2014, 12, 31),
frequency = 365)
EldTxts.stl<-stl(EldTxts, s.window="periodic")
#Eldoret Tn
```

```
EldTn<-read.csv(file.choose(), header = TRUE, sep = ",")
EldTnts<- ts(EldTn, start = c(1985, 1, 1), end = c(2014, 12, 31),
frequency = 365)
EldTnts.stl<-stl(EldTnts, s.window="periodic")
EldTxTrend<-EldTxts.stl$time.series[, "trend"]
EldTnTrend<-EldTnts.stl$time.series[, "trend"]
EldTxTrendts<-ts(EldTxTrend, start = c(1985, 1, 1), end = c (2014, 12, 31),
frequency =365)
EldTnTrendts<-ts(EldTnTrend, start = c(1985, 1, 1), end = c (2014, 12, 31),
frequency =365)
write.csv(EldTnTrendts, file = "EldoretMinimum.csv")
write.csv(EldTxTrendts, file = "EldoretMaximum.csv")
op <- par(mar = c(0, 4, 0, 3), oma = c(5, 0, 4, 0), mfcol = c(4, 2))
plot(EldTxts.stl, set.pars =NULL, labels= NULL, main= "Trend, Seasonal &
Random Components of Maximum and Minimum Temperature over Eldoret")
plot(EldTnts.stl, set.pars = NULL)
par(op)
dev.copy(bmp,'Eldoret Tn and Tx.bmp')
dev.off()
#Kitale Tx
KitTx<-read.csv(file.choose(), header = TRUE, sep = ",")
KitTxts<- ts(KitTx, start = c(1985, 1, 1), end = c(2014, 12, 31),
frequency = 365)
KitTxts.stl<-stl(KitTxts, s.window="periodic")
KitaleTn
KitTn<-read.csv(file.choose(), header = TRUE, sep = ",")
KitTnts<- ts(KitTn, start = c(1985, 1, 1), end = c(2014, 12, 31),
frequency = 365)
KitTnts.stl<-stl(KitTnts, s.window="periodic")
KitTxTrend<-KitTxts.stl$time.series[, "trend"]
KitTnTrend<-KitTnts.stl$time.series[, "trend"]
KitTxTrendts<-ts(KitTxTrend, start = c(1985, 1, 1), end = c (2014, 12, 31),
frequency =365)
KitTnTrendts<-ts(KitTnTrend, start = c(1985, 1, 1), end = c (2014, 12, 31),
frequency =365)
write.csv(KitTxTrendts, file = "KitaleMaximum.csv")
write.csv(KitTnTrendts, file = "KitaleMinimum.csv")
op <- par(mar = c(0, 4, 0, 3), oma = c(5, 0, 4, 0), mfcol = c(4, 2))
plot(KitTxts.stl,set.pars =NULL, labels= NULL, main= "Trend, Seasonal &
Random Components of Maximum and Minimum Temperature over Kitale")
plot(KitTnts.stl, set.pars = NULL)
par(op)
dev.copy(bmp,'Kitale Tn and Tm.bmp')
dev.off()
#Kakamega Tx
KakTx<-read.csv(file.choose(), header = TRUE, sep = ",")
KakTxts<- ts(KakTx, start = c(1985, 1, 1), end = c(2014, 12, 31),
frequency = 365)
KakTxts.stl<-stl(KakTxts, s.window="periodic")
#Kakamega Tn
KakTn<-read.csv(file.choose(), header = TRUE, sep = ",")
KakTnts<- ts(KakTn, start = c(1985, 1, 1), end = c(2014,12, 31), frequency
= 365)
KakTnts.stl<-stl(KakTnts, s.window="periodic")
KakTxTrend<-KakTxts.stl$time.series[, "trend"]
KakTnTrend<-KakTnts.stl$time.series[, "trend"]
```

```
KakTxTrendts<-ts(KakTxTrend, start = c(1985, 1, 1), end = c (2014, 12, 31),
frequency =365)
KakTnTrendts<-ts(KakTnTrend, start = c(1985, 1, 1), end = c (2014, 12, 31),
frequency =365)
write.csv(KakTxTrendts, file = "KakamegaMaximum.csv")
write.csv(KakTnTrendts, file = "KakamegaMinimum.csv")
op <- par(mar = c(0, 4, 0, 3), oma = c(5, 0, 4, 0), mfcol = c(4, 2))
plot(KakTxts.stl,set.pars =NULL, labels= NULL, main= "Trend, Seasonal &
Random Components of Maximum and Minimum Temperature over Kakamega")
plot(KakTnts.stl, set.pars = NULL)
par(op)
dev.copy(bmp,'Kakamega Tn and Tm.bmp')
dev.off()
#Kisii Tx
KisTx<-read.csv(file.choose(), header = TRUE, sep = ",")
KisTxts<- ts(KisTx, start = c(1985, 1, 1), end = c(2014, 12, 31),
frequency = 365)
KisTxts.stl<-stl(KisTxts, s.window="periodic")
#Kisii Tn
KisTn<-read.csv(file.choose(), header = TRUE, sep = ",")
KisTnts<- ts(KisTn, start = c(1985, 1, 1), end = c(2014, 12, 31),
frequency = 365)
KisTnts.stl<-stl(KisTnts, s.window="periodic")
KisTxTrend<-KisTxts.stl$time.series[, "trend"]
KisTnTrend<-KisTnts.stl$time.series[, "trend"]
KisTxTrendts<-ts(KisTxTrend, start = c(1985, 1, 1), end = c (2014, 12, 31),
frequency =365)
KisTnTrendts<-ts(KisTnTrend, start = c(1985, 1, 1), end = c (2014, 12, 31),
frequency =365)
write.csv(KakTxTrendts, file = "KisiiMaximum.csv")
write.csv(KakTnTrendts, file = "KisiiMinimum.csv")
op <- par(mar = c(0, 4, 0, 3), oma = c(5, 0, 4, 0), mfcol = c(4, 2))
plot(KisTxts.stl,set.pars =NULL, labels= NULL, main= "Trend, Seasonal &
Random Components of Maximum and Minimum Temperature over Kisii")
plot(KisTnts.stl, set.pars = NULL)
par(op)
dev.copy(bmp,'Kisii Tx and Tn.bmp')
#Kericho Tx
KerTx<-read.csv(file.choose(), header = TRUE, sep = ",")
KerTxts<- ts(KerTx, start = c(1985, 1, 1), end = c(2014, 12, 31),
frequency = 365)
KerTxts.stl<-stl(KerTxts, s.window="periodic")
#Kericho Tn
KerTn<-read.csv(file.choose(), header = TRUE, sep = ",")
KerTnts<- ts(KerTn, start = c(1985, 1,1), end = c(2014, 12, 31), frequency
= 365)
KerTnts.stl<-stl(KisTnts, s.window="periodic")
KerTxTrend<-KerTxts.stl$time.series[, "trend"]
KerTnTrend<-KerTnts.stl$time.series[, "trend"]
KerTxTrendts<-ts(KerTxTrend, start = c(1985, 1, 1), end = c (2014, 12, 31),
frequency =365)
KerTnTrendts<-ts(KerTnTrend, start = c(1985, 1, 1), end = c (2014, 12, 31),
frequency =365)
write.csv(KerTnTrendts, file = "KerichoMinimum.csv")
write.csv(KerTxTrendts, file = "KerichoMaximum.csv")
op <- par(mar = c(0, 4, 0, 3), oma = c(5, 0, 4, 0), mfcol = c(4, 2))
```

```
plot(KerTxts.stl,set.pars =NULL, labels= NULL, main= "Trend, Seasonal &
Random Components of Maximum and Minimum Temperature over Kericho")
plot(KerTnts.stl, set.pars = NULL)
par(op)
dev.copy(bmp,'Kericho Tx and Tn.bmp')
dev.off()
```

Appendix 3: Source Code for Plotting the Climate Diagrams

```
#Climate Diagram
#Climatol package~diagwl function
#-------------------------------------------------------------------------
------
library(climatol)#loads climatol package
Kakamega<-read.csv(file.choose(), header=FALSE, sep=",")
diagwl(Kakamega, est="Kakamega", alt=1565, per="1985-2014",
mlab="en",pcol="#005ac8", tcol="#e81800",sfcol="#09a0d1")
dev.copy(png,'Kakamega W&L.png')
dev.off()
Kericho<-read.csv(file.choose(), header=FALSE, sep=",")
diagwl(Kericho, est="Kericho", alt=1970, per="1985-2014",
mlab="en",pcol="#005ac8", tcol="#e81800",sfcol="#09a0d1")
dev.copy(png,'Kericho W&L.png')
dev.off()
op <- par(mar = c(0, 4, 0, 3), oma = c(5, 0, 4, 0), mfcol = c(4, 2))
Kitale<-read.csv(file.choose(), header=FALSE, sep=",")
diagwl(Kitale, est="Kitale", alt=1890, per="1985-2014",
mlab="en",pcol="#005ac8", tcol="#e81800",sfcol="#09a0d1")
dev.copy(png,'Kitale W&L.png')
dev.off()
Kisii<-read.csv(file.choose(), header=FALSE, sep=",")
diagwl(Kisii, est="Kisii", alt=1640, per="1985-2014",
mlab="en",pcol="#005ac8", tcol="#e81800",sfcol="#09a0d1")
dev.copy(png,'Kisii W&L.png')
dev.off()
```